

5-2013

Design and Implementation of Wireless Point-Of-Care Health Monitoring Systems: Diagnosis For Sleep Disorders and Cardiovascular Diseases

Se Chang Oh

University of Arkansas, Fayetteville

Follow this and additional works at: <http://scholarworks.uark.edu/etd>

 Part of the [Biomedical Devices and Instrumentation Commons](#), [Cardiovascular Diseases Commons](#), and the [Electrical and Electronics Commons](#)

Recommended Citation

Oh, Se Chang, "Design and Implementation of Wireless Point-Of-Care Health Monitoring Systems: Diagnosis For Sleep Disorders and Cardiovascular Diseases" (2013). *Theses and Dissertations*. 790.
<http://scholarworks.uark.edu/etd/790>

This Dissertation is brought to you for free and open access by ScholarWorks@UARK. It has been accepted for inclusion in Theses and Dissertations by an authorized administrator of ScholarWorks@UARK. For more information, please contact scholar@uark.edu, ccmiddle@uark.edu.

**DESIGN AND IMPLEMENTATION OF WIRELESS POINT-OF-CARE HEALTH
MONITORING SYSTEMS: DIAGNOSIS FOR SLEEP DISORDERS AND
CARDIOVASCULAR DISEASES**

DESIGN AND IMPLEMENTATION OF WIRELESS POINT-OF-CARE HEALTH
MONITORING SYSTEMS: DIAGNOSIS FOR SLEEP DISORDER AND
CARDIOVASCULAR DISEASES

A dissertation submitted in partial fulfillment
of the requirements for the degree of
Doctor of Philosophy in Electrical Engineering

By

Se Chang Oh
Kyungpook National University
Bachelor of Engineering in Electronics Engineering, 1996
Pohang University of Science and Technology
Master of Science in Electronic & Electrical Engineering, 1999

May 2013
University of Arkansas

ABSTRACT

Chronic sleep disorders are present in 40 million people in the United States. More than 25 million people remain undiagnosed and untreated, which accounts for over \$22 billion in unnecessary healthcare costs. In addition, another major chronic disease is the heart diseases which cause 23.8% of the deaths in the United States. Thus, there is a need for a low cost, reliable, and ubiquitous patient monitoring system. A remote point-of-care system can satisfy this need by providing real time monitoring of the patient's health condition at remote places. However, the currently available POC systems have some drawbacks; the fixed number of physiological channels and lack of real time monitoring.

In this dissertation, several remote POC systems are reported to diagnose sleep disorders and cardiovascular diseases to overcome the drawbacks of the current systems. First, two types of remote POC systems were developed for sleep disorders. One was designed with ZigBee and Wi-Fi network, which provides increase/decrease the number of physiological channels flexibly by using ZigBee star network. It also supports the remote real-time monitoring by extending WPAN to WLAN with combination of two wireless communication topologies, ZigBee and Wi-Fi. The other system was designed with GSM/WCDMA network, which removes the restriction of testing places and provides remote real-time monitoring in the true sense of the word. Second, a fully wearable textile integrated real-time ECG acquisition system for football players was developed to prevent sudden cardiac death. To reduce power consumption, adaptive RF output power control was implemented based on RSSI and the power consumption was reduced up to 20%. Third, as an application of measuring physiological signals, a wireless brain machine interface by using the extracted features of EOG and EEG was implemented to control the

movement of a robot. The acceleration/deceleration of the robot is controlled based on the attention level from EEG. The left/right motion of eyeballs of EOG is used to control the direction of the robot. The accuracy rate was about 95%.

These kinds of health monitoring systems can reduce the exponentially increasing healthcare costs and cater the most important healthcare needs of the society.

This dissertation is approved for recommendation
to the Graduate Council

Dissertation Director:

Dr. Vijay K. Varadan

Dissertation Committee:

Dr. Randy L. Brown

Dr. Roy A. McCann

Dr. Ryan Z. Tian

DISSERTATION DUPLICATION RELEASE

I hereby authorize the University of Arkansas Libraries to duplicate this thesis when needed for research and/or scholarship.

Agreed

(Se Chang Oh)

Refused

(Se Chang Oh)

ACKNOWLEDGEMENTS

I would like to take this opportunity to express my deepest gratitude to Dr. Vijay K. Varadan, my major advisor and the graduate committee chair, for giving me an opportunity to work under him. He was a fabulous advisor: sharp, cheery, perceptive, and mindful of the things that truly matter.

Dr. Randy L. Brown, for his patience, support and guidance in my research and coursework.

Dr. Ryan Z. Tian, for his critical reviews, suggestions, constant encouragement and his time.

Dr. Roy A. McCann, for his enthusiasm and making me ponder over engineering applications with civic sense and societal cause.

I would like to extend my thanks to my research group members – Dr. Gyanesh Mathur, Prashanth Shyamkumar, Pratyush Rai, Hyeokjun Kwon, Dr. Linfeng Chen, Phillip Hankins, Andrea Summers, and Mouli Ramasamy.

I was fortunate to have In Kwang Kim, Sameer Thalappil and Yongtae Park as my friends. My sincere thanks to them for their friendship and support.

I offer my sincerest thanks to my parents, sisters, brothers-in-law for their support. A nephew and nieces make me happy and especially, my precious niece, Hyunju Lee, for her affection. I am also grateful to Myeonghui's parents, her sisters for their encouragement.

Last but not the least, I would like extend my sincere thanks to my family, Myeonghui and Hoonseok. It would have been very difficult for me to concentrate on my research without their love, affection, and support.

TABLE OF CONTENTS

Chapter 1: Introduction	1
1.1 Introduction	1
1.2 Sleep Disorders	3
1.2.1 Types of Sleep Disorders	3
1.2.1 Risk Factors of Sleep Disorders	5
1.2.2 Symptoms of Sleep Disorders	6
1.2.3 Test Method for Diagnosing Sleep Disorders	6
1.3 Remote Monitoring of Physiological Signals for Point-Of-Care	7
1.4 Configuration of the Remote Patient Monitoring System	8
1.4 Current State of Art in Wireless Health Monitoring Systems	10
1.5 Objectives and Organization	13
Chapter 2: Biopotentials for Sleep Disorders Diagnosis	15
2.1 Electroencephalogram	15
2.1.1 EEG Measurement	15
2.1.2 Classification of EEG waveforms	16
2.2 Electrooculogram	18
2.3 Electromyogram	20
2.4 Electrocardiogram	21
2.4.1 ECG Measurements	22
2.4.2 ECG Waveform	24
2.5 Scoring Sleep Stages Using Biopotentials	25
2.5.1 Electrodes Placement for Scoring Sleep Stages	26
2.5.2 Scoring Criteria for Sleep Stages	27
Chapter 3: Wireless Communication	30
3.1 Introduction	30
3.2 Bluetooth	32
3.3 Wi-Fi	34
3.4 ZigBee	37

3.5 GSM/WCDMA	40
Chapter 4: Wireless Health Monitoring Systems for Sleep Disorders	43
4.1 Introduction	43
4.2 System Design and Implementation	49
4.2.1 Sensors	50
4.2.2 Amplifier Module	51
4.2.3 Data Acquisition and Wireless Unit	53
4.2.3.1 Devices with ZigBee and Wi-Fi	53
4.2.3.2 Device with GSM/WCDMA	59
4.3 System Evaluation	64
4.4 Conclusion	72
Chapter 5: Real-time Wireless Cardiac Monitoring of Football Players on the Field	74
5.1 Introduction	74
5. 2 Research Objectives	77
5. 3 System Implementation	80
5.3.1 Sensor Platform	81
5.3.2 Wireless Module	82
5.3.2.1 Amplifier and Microcontroller	83
5.3.2.2 Wireless Module - ZigBee	84
5.3.3 Software Implementation	84
5.4. Adaptive RF Output Power Control	85
5.5 Results	88
5.6 Discussion and Conclusions	89
Chapter 6: Application - Wireless Brain-Machine Interface Using EEG and EOG	91
6.1 Introduction	91
6.2 System Design	93
6.2.1 Sensor	94
6.2.2 Amplifier	95
6.2.3 Microprocessor	95
6.3 Feature extraction and Classification	96

6.4 Experimental Test	100
6.5 Results	101
6.6 Conclusion	103
Chapter 7: Conclusions	104
References	107
Appendices	114

LIST OF FIGURES

Figure 1.1 Healthcare Spending in the United States [2]	1
Figure 1.2 Causes of death in the United States in 2011	3
Figure 1.3 Data flow of the remote point-of-care system	9
Figure 2.1 Labels for points according to the 10-20 system of electrodes placement [32]	16
Figure 2.2 EEG waveforms at different frequencies [32]	18
Figure 2.3 EOG waveforms generated by movement of the eyes [32]	19
Figure 2.4 Electrodes placement for EOG measurement	19
Figure 2.5 Measurement and waveforms of EMG [35]	21
Figure 2.6 Lead system for ECG measurement; (a) limb leads, (b) precordial leads and (c) augmented limb leads [32]	23
Figure 2.7 One cycle ECG waveform and its components	25
Figure 2.8 The placement of electrodes for EEG, EOG, and EMG recording	27
Figure 3.1 Network configuration of Bluetooth; (a) piconet and (b) scatternet	33
Figure 3.2 Network configuration of Wi-Fi; (a) ad-hoc, (b) infrastructure and (c) extended service set	35
Figure 3.3 Network configuration of ZigBee; (a) star, (b) cluster-tree and (c) mesh	38
Figure 3.4 Data transmission in IEEE 802.15.4	39
Figure 3.5 Evaluation of mobile communication	41
Figure 4.1 Comparison of wireless communication standards	46
Figure 4.2 Data flow of the system to diagnose sleep disorders with ZigBee and Wi-Fi	48

Figure 4.3 Data flow of the system to evaluate sleep stages with GSM/WCDMA	49
Figure 4.4 Sensors to diagnose sleep disorders	51
Figure 4.5 Schematic diagram of the amplification circuit for biopotential signals	53
Figure 4.6 Data flow in the microcontroller of the HST transmitters	55
Figure 4.7 Wireless HST device: (a) block diagram and (b) image	56
Figure 4.8 Data flow in the wireless receiver	58
Figure 4.9 Wireless HST receiver; (a) block diagram and (b) image	58
Figure 4.10 Block diagram of the data acquisition/wireless device with GSM/WCDMA	59
Figure 4.11 Schematic diagram of the GSM/WCDMA circuitry	63
Figure 4.12 Images of the wireless HST system with GSM/WCDMA; (a) top and (b) bottom side of the system	64
Figure 4.13 Experimental test set-up for the system with Zigbee and Wi-Fi; (a) image of a subject under experiment and (b) GUI of the monitoring utility program [86]	66
Figure 4.14 Experimental test set up for the system with GSM/CDMA [88]	67
Figure 4.15 Monitored physiological signals from the wireless type III HST device	68
Figure 4.16 Monitored physiological signals from the wireless supplement HST device	70
Figure 4.17 Monitored physiological signals from the system with GSM/WCDMA	71
Figure 5.1 Schematic of the overall implementation of the football player monitoring system	80
Figure 5.2 (a) Compression base layer vest with sensor electrodes and printed traces, (b) protective shoulder pad with snap on connection cables to connect sensors to wireless module, (c) wireless module with 5 channel amplifier and ZigBee module and (d) wireless communication module placed in a pocket on the interior of the shoulder pad	82

Figure 5.3 Schematic of the wireless module	83
Figure 5.4 Schematic of (a) the 3 stage amplifier and (b) the WCT generation circuit	84
Figure 5.5 Data flow between the transmitter and the receiver with adaptive RF output power control	86
Figure 5.6 Experimental results; (a) relation between communication distance and RSSI with different RF output power values and (b) current consumption with different RF output power values	87
Figure 5.7 (a) ECG signals acquired using the system and (b) derived ECG signals	88
Figure 5.8 Schematic for WPAN implementation for multiple sensors spanning the full body of the athlete	90
Figure 6.1 Data flow of the wireless brain machine interface	93
Figure 6.2 Image of the wearable wireless sensing transmitter	94
Figure 6.3 Block diagram of the wireless sensing transmitter	96
Figure 6.4 Measured EOG signals with the system	97
Figure 6.5 Classification process of EOG signals; (a) raw left and right EOG signals, (b) integrated signals, (c) filtered signals, (d) noise removed signals and (e) classified signals	98
Figure 6.6 Plot of AR PSD of EEG signals	99
Figure 6.7 Flow chart for feature extraction and classification	100
Figure 6.8 Results of attention level based on different ratio	101
Figure 6.9 Results of ratio the peak of the AR PSD value of low beta and alpha waves	102

LIST OF TABLES

Table 1.1 Definitions of the types of sleep studies devices	7
Table 1.2 Comparison of the wireless health monitoring systems from research institutes	11
Table 1.3 Features of the commercially available home sleep test devices	13
Table 2.1 Summary of sleep-wake scoring criteria	29
Table 3.1 Comparison of the Bluetooth, Wi-Fi and ZigBee	42
Table 4.1 Specification of the amplifiers for physiological signals	53
Table 5.1 Summarization of 12 lead ECG prescreening parameters	80

Chapter 1: Introduction

1.1 Introduction

Rapid economic growth in this decade improves the quality of life, but people have been getting stresses to survive in a competitive society. Most of the people may have experienced sleep disturbance due to stresses. Sleep disorders or sleep deprivation itself may be considered as an insignificant disease. However, cumulative-long term effects of sleep disorders are associated with serious health consequences and they lead to chronic diseases [1].

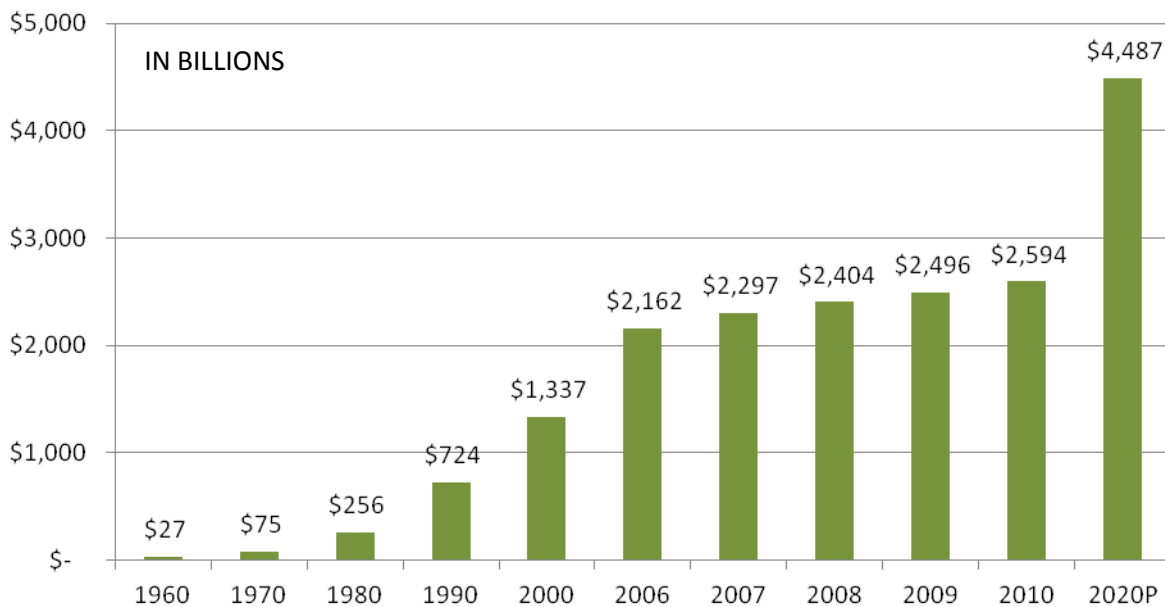


Figure 1.1 Healthcare Spending in the United States [2]

As shown in Figure 1.1, the healthcare cost for the chronic diseases is on an increasing trend. The healthcare cost increased by 94% from \$1,337 billion in 2000 to \$2,594 billion in 2010. They projected the cost will be \$4,487 billion in 2020 [2]. This exponential increase in the healthcare costs is an important fact to the states whose budgets constitute an average of 20%

from Medicaid [3]. Therefore, the ever increasing costs affect health insurance, mental health problems, and other healthcare problems [4-9]. The potential methods to control the healthcare costs include improved prevention, early detection/identification of the causes of chronic diseases. Improved prevention methods can be introduced by educating people about healthy lifestyle, origin of various chronic diseases and their ill effects. Because preventive effort and improving care for a smaller group of people will be more effective in terms of quality than implementing it on a larger population. Early detection/identification of the causes of chronic diseases leads to a substantial reduction in the cost of treatments. Constant monitoring is one of the significant factors in early detection of chronic diseases, but repetitive visits to the hospital may involve large expenses. As a solution for this, remote Point-of-Care (POC) systems can be introduced. The remote POC systems allow monitoring the physiological signals of the patient and diagnosing the diseases with his/her daily routine instead of visiting a hospital or a physician. Cost of hospitalization and lab tests can be reduced by implementing POC. Identification of causes leading to chronic diseases can also reduce the cost of treatment to a great extent. One of the causes of chronic diseases is sleep disorders. Undiagnosed and untreated sleep disorders can be associated with cardiac problems, hypertension, stroke, and memory loss, to name a few [10, 11]. Various studies have shown the prevalence of the sleep disorders with chronic diseases. The sleep disorders are associated with heart failure by 60% [12], stroke/transient ischemic attack (TIA) by 70% [13, 14], type 2 diabetes by 65 % [15], and hypertension by 37% [16]. According to the report from Centers for Disease Control and Prevention, diseases of heart were a top-ranked chronic disease among leading causes of death in 2011, by comprising 23.8% of cause of death [17]. For this reason the expenditure for the heart diseases is the biggest part of healthcare cost. Sleep disorders, causing the chronic disease, and heart diseases, a major leading cause of

death, should be monitored/diagnosed in the early stages in both the personal and social viewpoint.

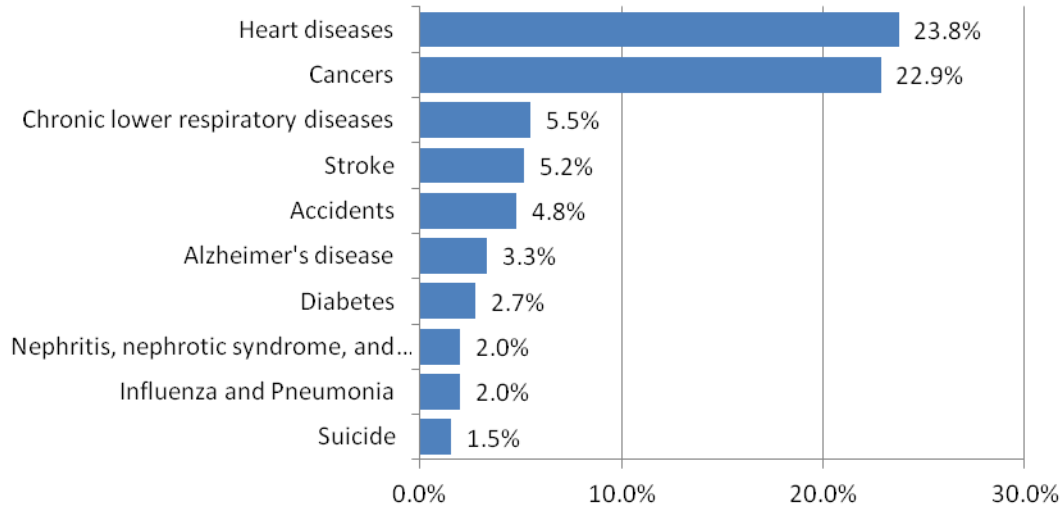


Figure 1.2 Causes of death in the United States in 2011

1.2 Sleep Disorders

1.2.1 Types of Sleep Disorders

Sleep disorders are related to sleep patterns and characterized by disturbance in the amount, quality or timing of sleep. There are about 88 recognized sleep disorders. The International Classification of Sleep Disorders (ICSD) classified the sleep disorders as four categories; dyssomnias, parasomnias, sleep disorders associated with other disorders, proposed sleep disorders [18].

Dyssomnias - Dyssomnias are one of the primary sleep disorders mentioned in Diagnostic Classification of Sleep and Arousal Disorders (DCSAD). These disorders cause excessive sleep, or sleep deprivation in the form of difficulty in sleep initiation or maintaining a constant sleep.

Dyssomnias are the primary factors behind disturbed sleep and insomnia. Dyssomnias originate from a cluster of sleep related disorders from various systems in the body. For instance, narcolepsy is caused by the central nervous system and obstructive sleep apnea syndrome is caused by a physical obstruction in the upper airway.

Parasomnias - Parasomnias are another group of sleep disorders which are related to the undesirable physical phenomena that occur during sleep. These disorders are mainly caused by the central nervous system. These disorders do not cause complications like insomnia or excessive sleep which leads to dyssomnias. Parasomnias may include arousal, partial arousal, sleep-wake transition and parasomnias are related with REM sleep and other parasomnias. Partial arousal and arousal consist of nightmares, somnambulism, and so on. The sleep wake transition disorders include the disorders which arise during the sleep-wake cycle and wake-sleep cycle. However, this does not include the disorders related to the REM sleep. Even though the disorders include both the transition cycles, most of the disorders are associated with the wake-sleep cycle. One exception is the restless legs syndrome which occurs during the sleep-wake cycle. However, it is considered to be dyssomnia as it is associated with insomnia.

Sleep disorders associated with other disorders - Sleep disorders are not limited only to medical problems, but also related to mental disorders which are associated with disturbances in sleep. Mental disorders have proved to be a very common cause of sleep disturbance in these days. The general classification of sleep disorders include mental disorders, neurologic disorders and other disorders which are placed under special medical areas because of their low prominence and occurrence.

Proposed sleep disorders - Some sleep disorders like laryngospasm, which are lesser studied or invented in recent times are the proposed sleep disorders. These disorders do not have sufficient information or test results as of now. Short sleep cycle and long sleep cycle of person may not necessarily be a disorder or be pathologic, as it may depend on the particular individual. But comparison of the same person's different sleep cycles may compile to diagnose the sleep related disorders. Subwakefulness syndrome or the subvigilance syndrome is another disorder which is not classified into any of the existing categories because of its ambivalent nature. Fragmentary myoclonus is a disorder where the muscle groups are subjected to frequent myoclonus jerks. Sleep hyperhidrosis is a combination of disorders like neurologic and obstructive sleep apnea syndrome. In women, sleep disturbances often lead to problems in the menstrual cycle, menopause or pregnancy. Various other lesser known sleep disorders include hypnagogic hallucinations, narcolepsy, neurogenic tachypnea and laryngospasm which are related to sleep related breathing problems [18]. All these yet to be known sleep disorders are under study by various research groups around the world.

1.2.1 Risk Factors of Sleep Disorders

There are several germane aspects which can place an individual at a higher risk of being affected by sleep disorders. Some of the aspects are as follows [19];

1. Obesity – fat deposits may result in the blockage of blood flow in the upper airway
2. Gender – males are at a higher risk of being affected with sleep disorders
3. Overage – people aged over 40 are at a higher risk.
4. Large neck size - a large neck size in both male and female is considered to be a high risk factor.

5. Genetics – sleep disorders can be hereditary
6. Nasal obstruction – people with nasal obstruction or problem with breathing during sleep are placed at top of the pyramid of risk factors.

1.2.2 Symptoms of Sleep Disorders

There are many common symptoms which can suggest that person is suffering with sleep disorders. When symptoms are detected and treated at early stages, sleep disorders can be cured at its rudimentary phase itself. Some of the commonly found symptoms include snoring, witnessed cessation of breathing, gasping for breath during sleep, excessive sleepiness during daytime, loss of memory temporarily, loss of concentration, depression, body pain, nightmares, unnecessary movement during sleep, night terrors, sleep walking (Somnambulism), bedwetting, teeth grinding (Bruxism), etc. These are the common symptoms found to result in sleep disorders in their later stages, if remained untreated.

1.2.3 Test Method for Diagnosing Sleep Disorders

Accurate diagnosis of sleep disorders is imperative to the treatment plan and early recovery. There are four types of sleep study devices according to the Center for Medicare & Medicaid Services (CMS) and the American Academy of Sleep Medicine (AASM). Table 1.1 shows the required physiological signals for each device type. Type I test is a gold standard method for diagnosing sleep disorders and it measures almost all kinds of physiological signals with around 20 sensors and is performed by a sleep technologist in a sleep lab. For this reason, type I is referred to as a full sleep study and attended study. An In-lab test is when a patient will sleep at the sleep laboratory and a sleep technologist monitors vitals and observes through a video camera in a control room. However, it is expensive, inconvenient, time consuming and labor

intensive. Home sleep test (HST) is an unattended sleep study that is performed at home without the oversight of a sleep technologist. It captures only what is necessary for the diagnosis.

Type	Definition	Mandatory Channels
Type I	in-lab test, attended studies with full sleep staging	Type II + Chin/Limb EMG Additional channels for CPAP/BiPAP levels, CO ₂ , pH, pressure, etc
Type II	home sleep test unattended studies, minimum of 7 channels	Type III + EEG, EOG, EMG,
Type III	home sleep test unattended studies, minimum of 4 channels	2 respiratory movement/airflow 1 ECG/heart rate, 1 oxygen saturation
Type IV	home sleep test unattended studies, minimum of 3 channels	oxygen saturation, airflow

Table 4.1 Definitions of the types of sleep studies devices

1.3 Remote Monitoring of Physiological Signals for Point-Of-Care

Traditionally, health diagnosis requires the patient to be physically present in the clinics, hospitals, or laboratories. These visits may usually be repetitive because of the need for constant monitoring of health condition. During these visits, the physiological signals are obtained, stored and diagnosed to assess the improving or falling health condition. It can be highly uncomfortable for the patient to go for repetitive tests as it can be laborious, time consuming, intervening with day-today life and obviously expensive. Increasing healthcare costs and the need for patient comfort has forced the researchers to think of new methods which can have the same results as real time monitoring performed at hospitals or labs. Remote patient monitoring for point-of-care enables to monitor the patient's health condition at local or remote places and provides real time feedback information to the patient from a medical center. Remote patient monitoring is a

technology where the patient can be effectively monitored outside a hospital. The testing is performed at the patient's own level of comfort and at no particular places such as a hospital or a clinic. It is one of the recent advances in the telemedicine and a prospective cost reducing method in the field of healthcare. This method involves sending the patient's medical data such as Electroencephalogram (EEG), Electrocardiogram (ECG), Electrooculogram (EOG), and Electromyogram (EMG) to a physician from the patient's home/work place. This technology mainly serves two kinds of people who cannot visit the hospital regularly and who need constant monitoring. It can provide continuous monitoring for patients who require their vital signals to be monitored constantly. It can considerably bring down the factors leading to frequent hospitalization as constant monitoring can detect abnormalities beforehand. Remote patient monitoring can be of much use to the people suffering from sleep disorder problems. The patients need not be present in the hospital or the sleep lab, when they are required to be tested for a complete sleep cycle. Instead the patient can sleep in his/her home normally, where the recorded data is sent to the physician for diagnosis. Therefore, remote patient monitoring can reduce the cost of hospitalization and costs related to the lab tests.

1.4 Configuration of the Remote Patient Monitoring System

In general, the remote point-of-care system includes a device for testing associated with the patient, a central server, and a monitoring device for a physician. Figure 1.3 shows the data flow of the remote point-of-care system. The device for testing the patient health condition consists of sensors, amplifiers/filters, a processing unit, graphic user interface, data storage and a communication module.

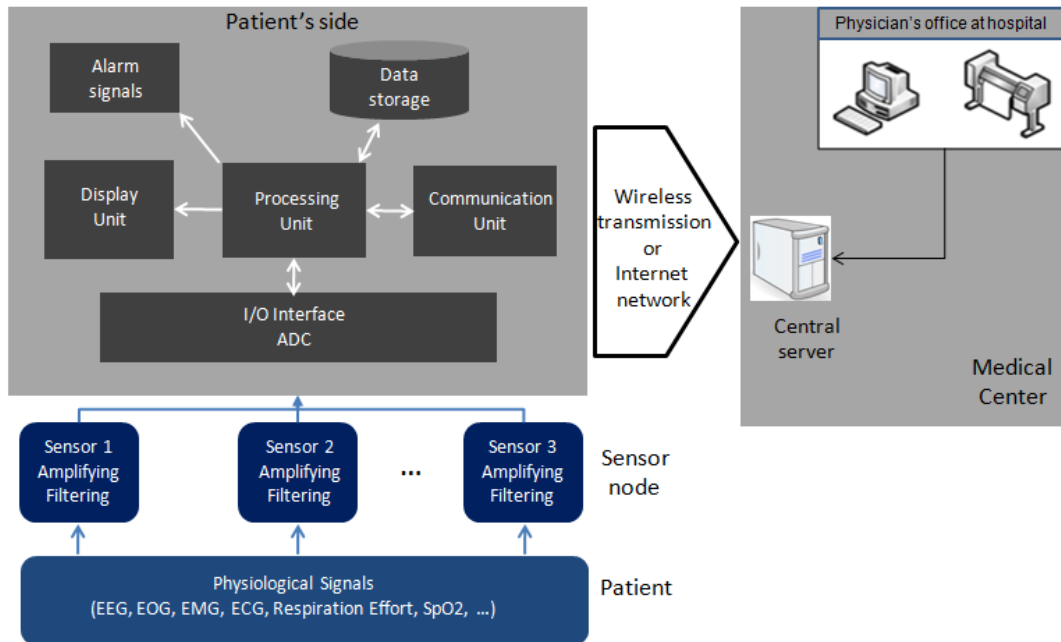


Figure 1.3 Data flow of the remote point-of-care system

The physiological signals are detected by the sensors. The signals are small in magnitude and contain undesired signals such as noises. The amplifier/filter unit modifies the raw signals to the appropriate level and quality of signals for data processing in the processor unit. The analog signals are converted to digital signals with an analog-to-digital converter. The sampling rate and resolution are decided according to the characteristic of the physiological signals. The processing unit manages the data flow in the peripheral units, a display, a communication, and a data storage unit. The display unit provides a graphic user interface through which the patient can manage the device and displays the sensed physiological signals. The data storage unit records the signals. The communication unit, either wired or wireless communication, sends the signals to the central sever which is in a service provider site or a medical center. The physician can monitor the signals in real time or diagnose disease with stored data by connecting to the central server.

1.4 Current State of Art in Wireless Health Monitoring Systems

Wireless health monitoring systems have been developing rapidly in these days. Many research groups across the world have been developing systems which have the state of the art technology in diagnosing sleep disorders and various other health ailments. The remote Point-of-Care systems are booming in the field of healthcare. The need for constant monitoring and ease of use of the systems has become an important aspect in patient care.

Research Institute - Researchers from many institutes have followed different kinds of approach in realizing wireless health monitoring systems for healthcare. Table 1.2 shows a comparison of different systems developed by research institutions. The systems have been developed with the concept of low power consumption and data coverage. The systems measure the vital signals, ECG, SpO₂, temperature and so on. UCLA developed a system with 8 analog channels and ZigBee as the communication module [20]. It adopted on board signal processing, thereby reducing the power consumption comparatively. NASA developed a 10-channel, Bluetooth enabled device [21]. Kansas State University also developed a Bluetooth enabled system with 5 analog channels [22]. Harvard University developed a 2-channel device which used ZigBee for communication [23]. Duke University developed a 12-channel device which used 802.11b as its communication method, but had higher power consumption because of its high performance control unit and the Wi-Fi [24].

Institution	UCLA	NASA	Kansas State	Harvard	Duke	TU-Berlin (Germany)
# of Input Channels	8	10	5	2	12	-
Physiological Signals	ECG SpO2 Temperature	2x ECG SpO2 Temperature Acceleration Blood Pressure	ECG SpO2	ECG	Neural signals	2x ECG SpO2 Acceleration
Wireless	Zigbee	BT	BT	Zigbee	802.11b	Zigbee
Transmission Range	9m	10m	-	9m	30 m	-
Power Supply	3V (2x AA)	3V (2x AA)	6V (4x AA)	3V (4x AA)	3.7V (1200mAh)	3.7V (850mAh) Poly lithium-ion
Power Consumption	97mW	360mW	344mW	100mW	4W	-

Table 1.5 Comparison of the wireless health monitoring systems from research institutes

ZigBee and Bluetooth are commonly used, but Duke used Wi-Fi. While the systems using ZigBee and Bluetooth consume about 100 mW and 350 mW respectively, the system using Wi-Fi consumes more power, 4 W. Even though the power consumption shown in the Table 1.2 reflects the whole system, most of the power is consumed by RF communication. ZigBee consumes less power and Wi-Fi consumes more power among ZigBee, Bluetooth and Wi-Fi. They built wireless personnel area network (WPAN) or wireless body area network (WBAN) and it has limited coverage area as the transmission and reception is only possible between short distances. Therefore, effective remote patient monitoring is not feasible with these types of communication methodologies.

Commercially available products for diagnosis of sleep disorders - Table 1.3 shows the features of the commercially available HST devices for sleep disorders. Most systems use external or internal memory device to record sleep data. In this case, real time monitoring is not

feasible. Patients should upload or hands carry the recorded data to their sleep lab the next day. Some devices use wireless communication to alleviate the inconveniences from wired connections. However, wireless communication is used for saving sleep data to a local storage devices instead of sending sleep data to the remote server or the central server because these devices build wireless personal area network or wireless body area network.

Manufactures	Product Name	Total number of channels	Storage	Wireless
Philips /Respironics [25]	Alice PDx	21channel with optional ECG and ExG	1GB SD card	No
Embla [26]	Embletta X100	12-channel with X100 proxy	128MB internal memory	No
Compumedics [27]	Somte PSG	16-channel	2GB Compact Flash	Bluetooth
Compumedics [28]	Siesta	32-amplified channel	Compact Flash	Siesta's Ethernet radio link
Cleveland Medical [28]	Sleep Scout	9-channel	SD card	2.4-2.484 GHz
ResMed [29]	ApneaLink Plus	4-channel	15MB internal memory	No
CareFusion [30]	Nox-T3	14-channel	1GB SD card	No

Table 1.6 Features of the commercially available home sleep test devices

The wireless HST devices use Bluetooth or their own wireless protocol in wireless personal area network. In addition, these devices have the fixed number of channels so that they cannot increase or decrease the number of physiological channels flexibly. Consequently, the devices cannot extend the number of channels to measure additional physiological signals. For instance, the type III device for diagnosis sleep apnea cannot be upgraded to the type II device for diagnosing sleep apnea and evaluating sleep stages by simply adding the physiological channels of EEG, EOG and EMG to the type III device. Patients should additionally purchase the type II

device to diagnose both sleep apnea and sleep stages even though they have the type III device. As a result, having a fixed number of channels per type is not a cost-effective solution.

1.5 Objectives and Organization

Based on the present state of the art in wireless health monitoring systems, in this research, it is intended to reduce the major drawbacks of the currently available health monitoring systems. Present health monitoring devices do not offer wide area coverage in terms of communication, primarily because of the use of only one type of communication methodologies. In this research, wide area coverage and the cost effectiveness of the health monitoring system are concentrated. Firstly, a combination of two communication methods, ZigBee and Wi-Fi, provides remote patient monitoring in real time. Secondly, usage of GSM/WCDMA communication facilitates wide area, continuous coverage and transmission of data over long distances, which can provide ubiquitous health monitoring. Thirdly, to implement cost-effective health monitoring system, unlike other healthcare monitoring devices, the proposed system is built with two end devices in the ZigBee network, so that the number of physiological channels is not fixed and can be varied just by adding or removing the end devices. Hence the system can be easily upgraded according the need and requirement of the patient.

With these design parameters in mind, the research in this dissertation is organized as follows. Chapter 2 describes a valuable insight about various physiological signals (ECG, EEG, EOG, and EMG) and its association to sleep disorders and cardiac diseases. Chapter 3 describes the wireless communication technologies which can be used for health monitoring. Chapter 4 describes the wireless Point-of-Care diagnosis for sleep disorders. It includes the wireless communication methods, ZigBee/Wi-Fi and GSM/WCDMA, for building the cost effective and

wide area health monitoring system. Chapter 5 explains the cardiac monitoring unit and emphasizes the application of cardiac monitoring to prevent sudden cardiac death in football players. Additionally, it elucidates a technique to reduce power consumption through the implementation of RF power control based on RSSI. Chapter 6 describes the wireless brain machine interface and the possibility of controlling a remote machine with EEG and EOG signals as an application of wireless health monitoring system. Chapter 7 states the conclusion of the work in this dissertation.

Chapter 2: Biopotentials for Sleep Disorders Diagnosis

Biopotentials are signals with an electric potential measured between two points of a human body which assists all the biochemical processes. There are various biopotentials present in the body, which can be analyzed for disease diagnosis. Each of the biopotential signals contains valuable information about a particular type of disorder. Specifically, Electrocardiogram (ECG), Electroencephalogram (EEG), Electromyogram (EMG) and Electrooculogram (EOG) are analyzed to identify and detect various disorders in a human body.

2.1 Electroencephalogram

The EEG consists of a summation of electrical activity of the neurons present in the brain. The neurons are excitable in nature and their activity produces electrical and magnetic fields. This activity can be measured by placing sensors or electrodes at various positions over the cortex or skull. Active neurons generate time-varying current at cellular level. EEG is originated from the firing activity of the neurons and the post synaptic activity after firing. The synapse is a small gap separating the neurons. Transmission between neurons takes place through the synapse. Neurotransmitters and receptors are present at the pre and post synaptic endings respectively, which help in the transmission of information. The amplitude of the EEG signal is usually in the range of a few micro-volts.

2.1.1 EEG Measurement

EEG is normally measured by placing the electrodes over the skull at defined positions according to the international 10-20 system [32]. The 10 and 20 refer to the distance between adjacent electrodes by dividing the transverse and median planes of the skull perimeters into 10% and 20% intervals. In the international 10-20 system, 19 electrodes are placed over the skull and

2 electrodes are placed on the ears as reference electrodes. The letters F, O, C, P, T in the 10-20 system of placement of electrodes stand for Frontal, Occipital, Central, Parietal and Temporal respectively. The electrodes are placed according to the location of placement and the underlying cerebral cortex. The even numbers represent the right side of the hemisphere and odd numbers represent the left side of the hemisphere. There are two basic methods by which the electrodes are placed: monopolar and bipolar. In monopolar, one side of the amplifier is connected to the reference electrode and in bipolar, amplifier is connected between the pair of electrodes. The electrical activity is acquired and amplified/filtered to record EEG waveform.

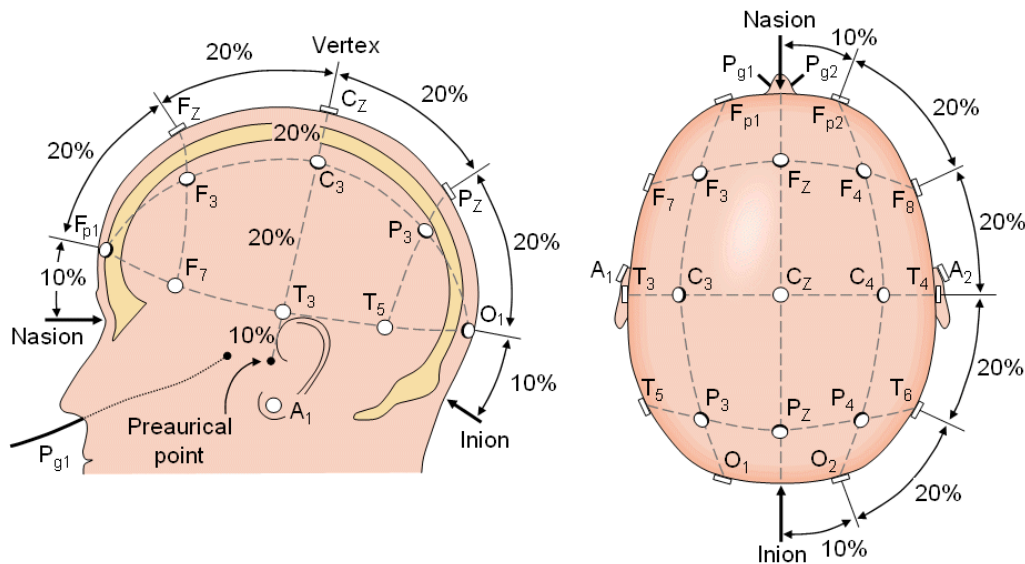


Figure 2.1 Labels for points according to the 10-20 system of electrodes placement [32]

2.1.2 Classification of EEG waveforms

EEG waveforms are classified into alpha, beta, theta and delta in frequency band. These waves are dominant depending on the electrical activity of the brain and the person's physiological conditions. Figure 2.2 shows the waveforms representing EEG waves at different frequencies.

- *Alpha waves* – These waves are generally in the frequency range of 8–13 Hz. Alpha waves are usually seen in the posterior side of the head and show higher amplitude at the dominant side of the brain. This characteristic is more predominant in right handed individuals. Alpha waves are more dominant in the EEG waveform when the person is sleeping or has his/her eyes closed. This is one of the most common waveform segments seen in adults.

- *Beta waves* – These waves are generally in the frequency range of 13-30 Hz. Beta waves are usually seen in the frontal plane of the brain and symmetrically distributed. A cortical damage in the brain causes these signals to be absent. It is dominant when person perform normal activity. These waveforms are also called as fast activity waves.

- *Theta waves* – These waves are generally in the frequency range of 4–8 Hz and are also termed as slow frequency waves. In adults, the waves are shown when person is drowsy. The waves are also normal for children up to 13 years. However, it can indicate brain dysfunction if they are seen in adults who are alert and awake.

- *Delta waves* – These are the lowest frequency waves in the frequency range of 0.5-4 Hz. These waves are highest in amplitude but slowest in terms of frequency. It can be more predominant in the frontal plane in adults and in the posterior in children. This wave is seen if person is in a moderate to deep sleep.

- *Spike and wave activity* – Number of other waveforms, which are more specific to certain conditions. Spike and wave activity indicates a seizure disorder and the frequency range of the waves are random less than 60 Hz.

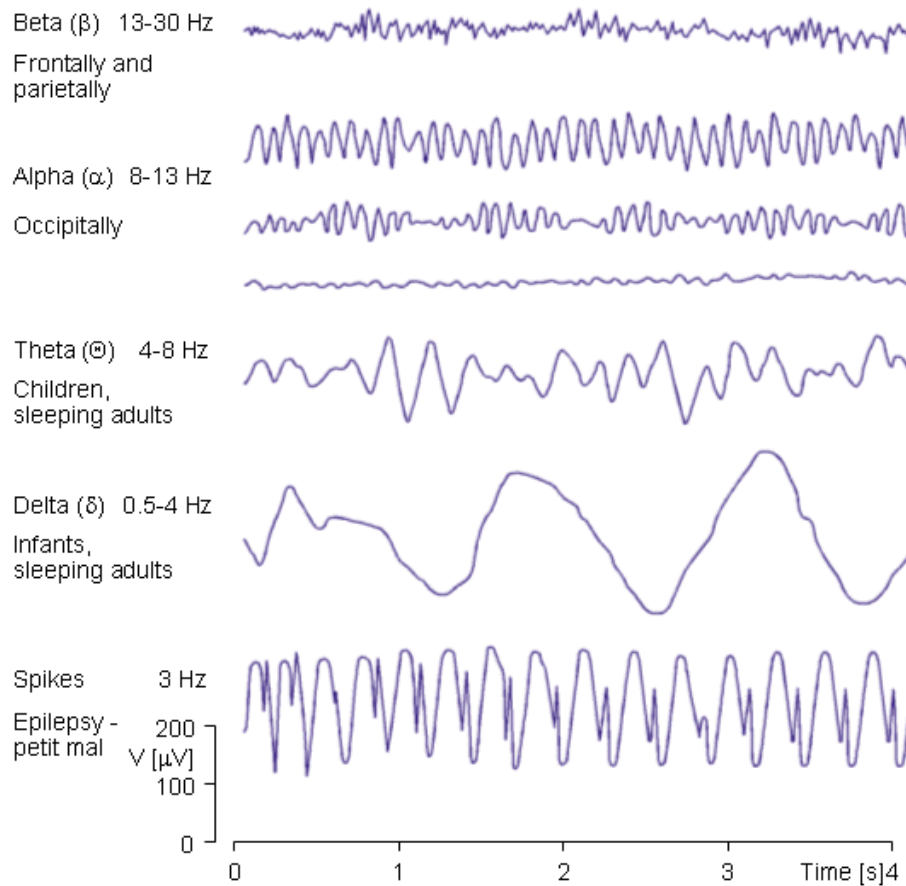


Figure 2.2 EEG waveforms at different frequencies [32]

2.2 Electrooculogram

Electrooculogram is the measurement of the resting potential of the retina. EOG monitors the eye movements by detecting the dipolar current flowing from the cornea to the retina, which also indicates the angular displacement of the eye. Applications of EOG include saccadic movements, smooth pursuit movements, convergence/divergence to record and optokinetic nystagmus [33]. The movements of the eyes are measured by placing two electrodes on the sides of the corneoretinal axis. The static electric polarization of the eye and electric potential caused by the movement of the eyes produces electrooculogram readings. The cornea of the eye is electrically

positive and posterior part is the negative potential. Figure 2.3 shows the EOG waveforms generated by horizontal movement of the eyes. Normally the electrodes are placed around the eyes with a reference electrode on the forehead. The electrodes are placed on the temple for the lateral movement and the other electrodes are placed vertically, one above and the other below the eye to measure vertical movement of the eyes.

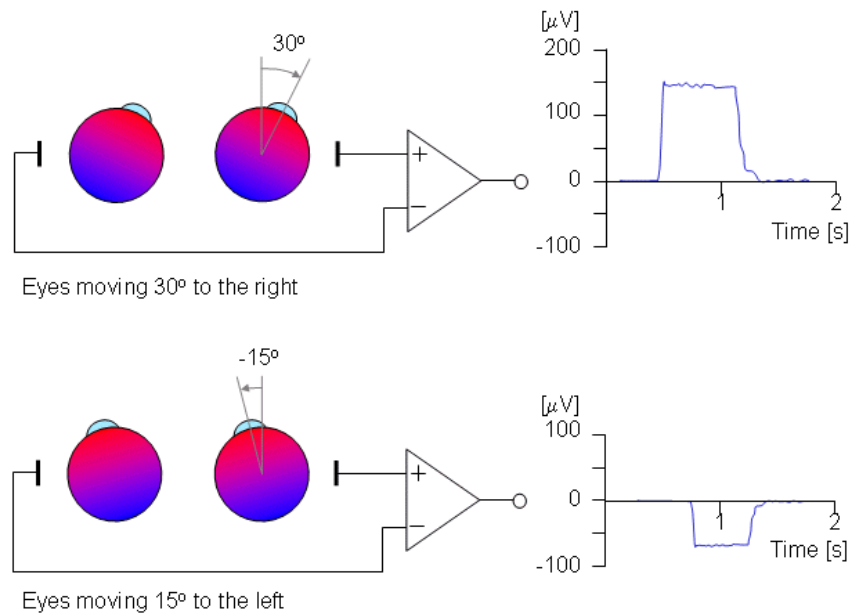


Figure 2.3 EOG waveforms generated by movement of the eyes [32]

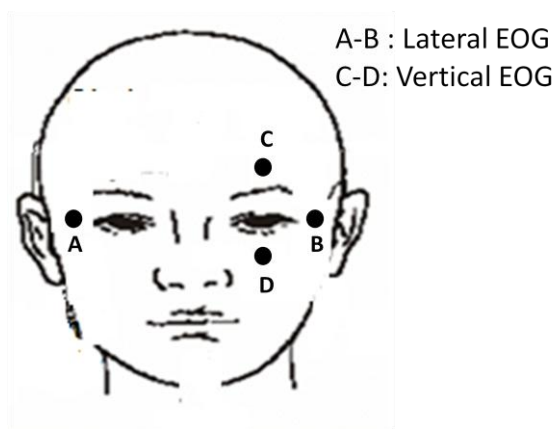


Figure 2.4 Electrodes placement for EOG measurement

2.3 Electromyogram

Electromyogram is the recording of the electrical activity of the muscles and the nerve cells that control them. The diagnostic procedure followed to record these signals is called as electromyography. The muscle fibers, prior to the production of muscle force, generates an electrical activity with currents of very low range. These currents are generated by the ion exchange across the membranes of the muscle fibers, as part of the muscle fibers to contract. Furthermore, quality of EMG signals depends on factors like distance of the electrodes from the active muscle, intensity and timing of muscle contraction, thickness of the tissue layers, contact quality between the skin and electrodes and properties of the electrodes and the amplification module. EMG can also be used to study nerve conduction between two points and can also reveal nerve-muscle dysfunction and nerve-muscle signal transmission [34]. Principle of electromyography is no different from the principles of electrocardiography. Electrical potentials are detected when the muscles contract and the signals are then processed. Generally, EMG depends on the firing action potential of the numerous motors present in the muscles. The electrodes placed on the skin over the muscle detect the electrical activity of the muscles of the underlying tissues. It is difficult to correlate the waveform with the specific muscle from which it is generated but this difficulty can be alleviated by the proper placement of electrodes. The muscle fibers which are present near the electrodes will have a greater impact on the waveforms, whereas the muscles at a longer distance will have lesser impact with respect to signal strength. This dependence of the quality of EMG on the distance of muscles and electrodes is mainly caused due to the impedance between the tissues. Therefore placing the electrodes at a long distance will provide varying and more generalized signals, and placing the electrodes at short intervals gives a signal which is more specific to the muscles over which the electrodes are

placed. However, it becomes nearly impossible to identify the specific muscles generating the signal because of the interferences from noise and motion artifacts. The electrodes are generally placed in parallel with the dominant muscles, since it minimizes signal cancellation and maximizes the biofeedback sensitivity.

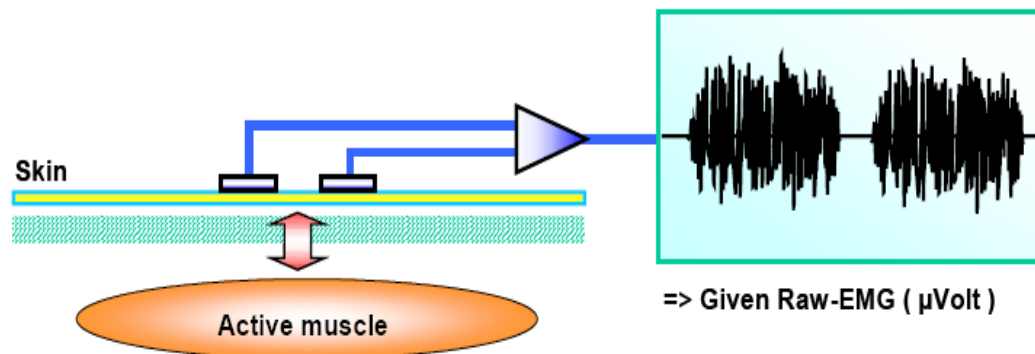


Figure 2.5 Measurement and waveforms of EMG [35]

2.4 Electrocardiogram

Electrocardiogram is the recording of the electrical activity of the heart as a vector quantity. The method by which the signals are recorded is called as electrocardiography. Electrodes are placed at lead positions at the body and the potential difference between two points are observed to derive the electrocardiogram which is treated as a vector quantity. It is used to detect abnormal rhythms of the heart muscles, heart rate variability (HRV) which provides information about the cardiovascular physiology, heart beats and position of various chambers of the heart. These electrical signals generated from the heart are of very low frequency ranging from 0.05 to 100 Hz. The electrical activities of the heart at specific instances are related to the particular field and dipole which produces it. Similarly, each type of waveform is associated with a specific function of the heart muscles. The electrical signals generated from the heart appear throughout the body

and electrodes are placed at different lead positions to determine the potential difference and measure ECG.

2.4.1 ECG Measurements

The traditional method of acquiring ECG follows the 12-lead system. Conventional wet Ag/AgCl electrodes can be used and are placed in predetermined positions called as leads. The area of skin where the electrodes are to be placed are either shaved, to remove hair or/and cleaned with alcohol swabs to provide better contact to the electrodes. Improper contact can introduce erroneous signals because of the impedance between the skin and the electrode.

- *Limb leads*: It consists of lead I, lead II and lead III. Lead I is the measurement, where the negative electrode is placed on the right arm and positive electrode is placed on the left arm. Lead II has the negative electrode on the right arm and the positive electrode on the left leg. Lead III measures with the negative electrode on the left arm and the positive electrode on the left leg. The lead vectors from these three leads form a triangle called as Einthoven's triangle. Figure 2.6(a) illustrates the positions adopted in the limb lead system.

- *Augmented limb leads*: As shown in the figure 2.6(c), aV_R , aV_L and aV_F are the augmented limb leads. These leads are unipolar leads by measuring electric potential at one lead with respect to a null point (modification of Wilson central terminal). The null point is obtained by averaging potential of the other leads. They record a change in electric potential in the frontal plane. For aV_R (augmented vector right), the positive electrode is placed on the right arm and the negative electrode is an average potential of the left leg and left arm. In aV_L (augmented vector left), the positive electrode is placed on the left arm and this signal is augmented by an average potential of right arm and left leg as the negative electrode. And in aV_F (augmented vector foot), the

positive electrode is placed on the left leg and the negative electrode is an average potential of right and left arm.

- *Precordial leads:* These leads are used to look the electrical activity of the heart at horizontal or transverse plane. The lead positions as shown in the Figure 2.6 (b) are placed over the chest wall on the intercostal spaces of the sternum. Because of its close proximity to the heart, augmentation is not necessary. The measurement between each of these positions and the Wilson central terminal gives the signal for that particular lead. Due its nature, it is also called as unipolar leads.

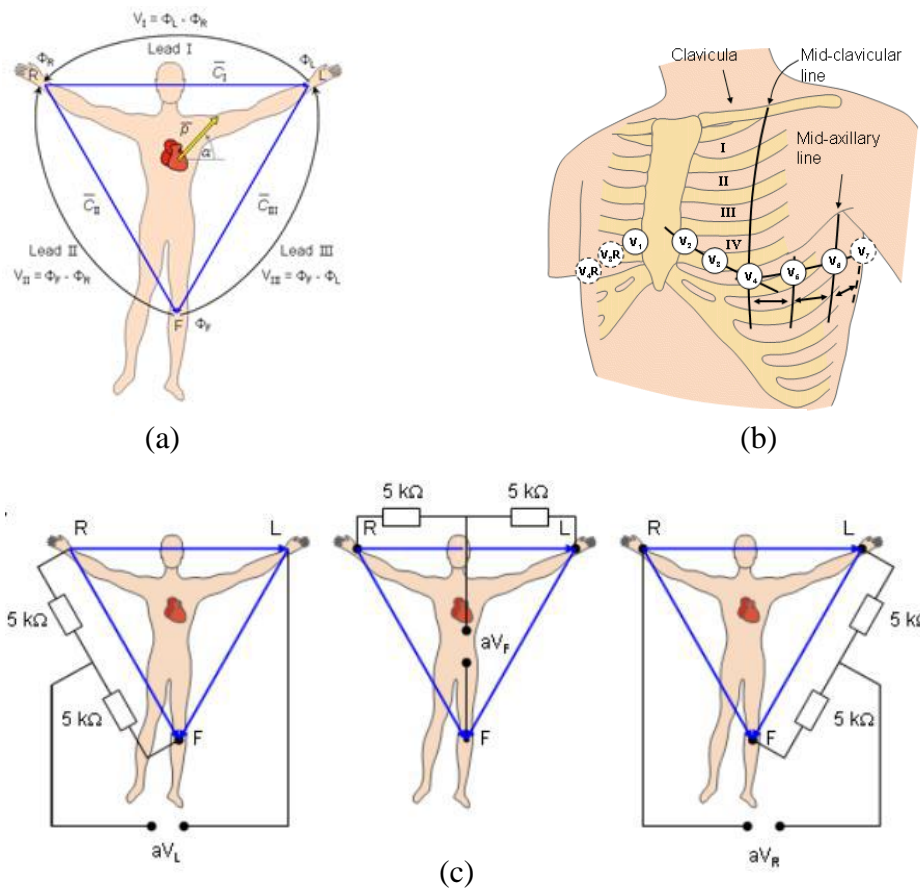


Figure 2.6 Lead system for ECG measurement; (a) limb leads, (b) precordial leads and (c) augmented limb leads [32]

2.4.2 ECG Waveform

The ECG wave is classified into P, QRS complex and T waves, where each wave has its own significance in terms the heart muscles from which it is generated or the period of generation. Accordingly, the wave has importance according to the classification and it can be used in the diagnosis of disorders. The classification of ECG waveform is as follows.

- P wave – It is the first wave snippet observed in an ECG waveform. This wave is caused when the main electrical vector is directed from the sinuatrial node to the atrioventricular node during the normal atrial depolarization.
- Q wave – It is the next visible wave after the P wave. It is a downward deflection caused by the septum depolarization.
- R wave – It is the highest amplitude wave present in an ECG waveform. It follows the Q wave and is seen as an upward deflection. It is caused because of the early ventricular depolarization.
- S wave – It is the immediate downward deflection which follows the R wave. This is caused by the late ventricular depolarization.
- QRS complex - It consists of Q, R, S wave and represents ventricular depolarization.
- T wave – This upright, rounded and asymmetric wave is caused by the repolarization of the ventricles.

These are the basic structures of an ECG waveform. Lesser known or less significant wave structures include U and J wave. U wave is a result of the repolarization of the interventricular septum and J wave usually follows the QRS complexes and looks like another R wave like a small delta wave. RR wave interval is used to determine the rate of heart beat. PR segment tells about the time taken by the electrical impulse from the sinuatrial node to reach the ventricles and

hence it used to estimate atrioventricular node function. The QRS segment represents the duration of ventricular depolarization. Similarly, the QT wave represents the time duration from depolarization to repolarization of the ventricles. Finally, the ST wave segment can give an estimate of oxygen starvation experienced by the ventricles.

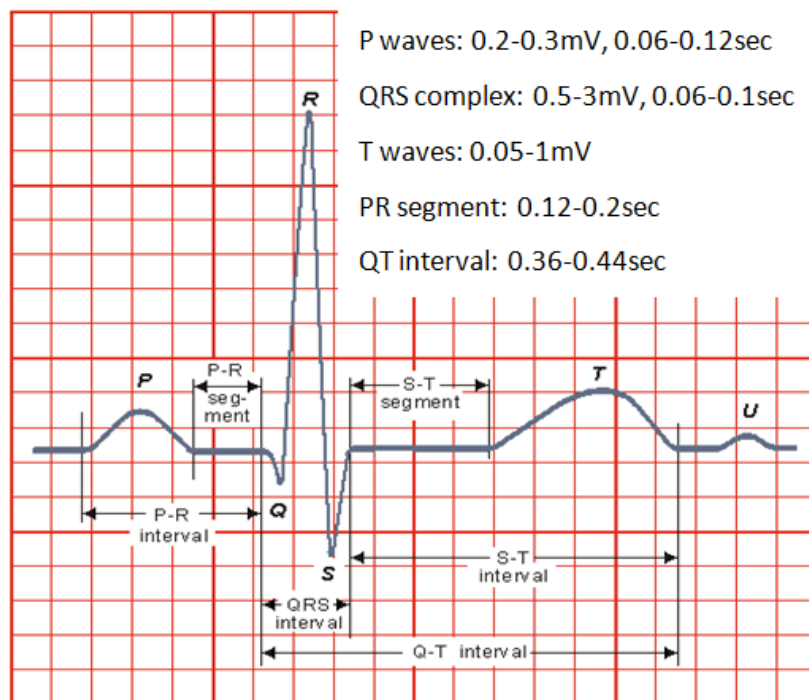


Figure 2.7 One cycle ECG waveform and its components

2.5 Scoring Sleep Stages Using Biopotentials

In 1937, Loomis, Harvey and Hobart firstly announced that the sleep stages are not steady states, but the sleep stages change with cyclic patterns during sleep. Even though they did not exactly specify each sleep stage, they revealed the correlation between the sleep stages and the physiological and behavioral changes. Their notes were modified by Dement and Kleitman in 1957. They established the criteria for scoring the sleep stages. The criteria has been proved and

modified by many researchers. In 1968, Rechtschaffen and A. Kales completed the criteria for scoring sleep stages.

2.5.1 Electrodes Placement for Scoring Sleep Stages

EEG, EOG, and EMG are usually recorded to score the sleep stages. EEG patterns show different regional information according to the placement of electrodes over the skull. However, regional information is not critical in scoring the sleep stages. If the key features, alpha, sleep spindles, K complexes, vertex sharp waves and delta waves, are associated with the sleep stages, the sleep stages could be discriminated. It is necessary to specify the electrode placement to record the optimal EEG patterns. The C3 or C4 placement is preferred because the sleep spindles, K complexes and vertex sharp waves are clearly monitored in this placement. As the placement of a reference electrode, ear lobe or mastoid placement is preferred to maximize inter-electrode distance to monitor the maximum or nearly maximum amplitude of high voltage slow waves. In addition to the C3 or C4 position, the O1 or O2 placement, the portion of the occipital lobe, is used for alpha waves activities to classify the accurate evaluation of sleep onset. EOG patterns for stage REM and wakefulness are measured with two channels. One electrode is placed a few centimeters above and slightly lateral to the outer canthus of one eye and the other electrode is placed a few centimeters below and slightly lateral to the outer canthus of the other eye. The reference electrode is placed on either the ear lobe or mastoid. These arrangements produce in-phase deflection in two EOG channels because the eye movements are binocularly synchronous during the sleep stages. The feature of in-phase deflection helps to discriminate artifacts which have out-of-phase deflection. The electrode placement for EMG is preferred on or

beneath the chin to classify stage REM or grinding tooth during sleep. Figure 2.8 shows the arrangement of the electrodes for scoring the sleep stages.

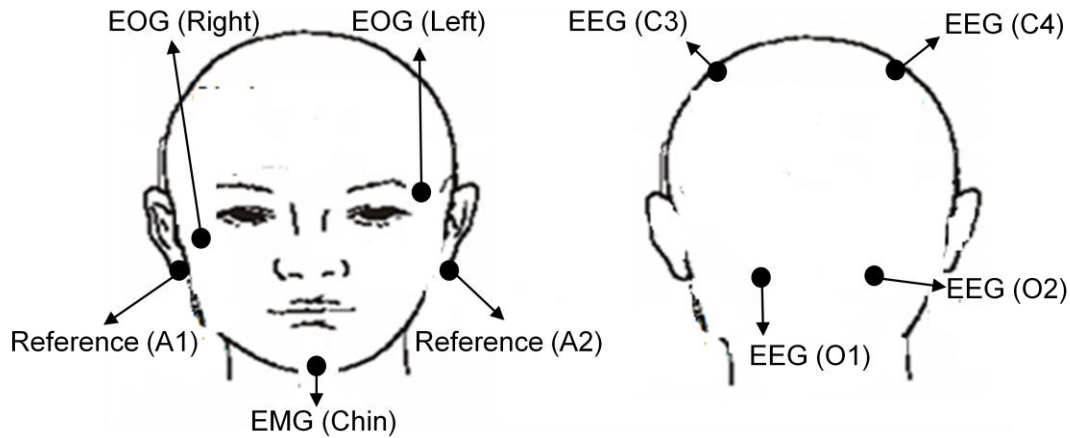


Figure 2.8 the placement of electrodes for EEG, EOG, and EMG recording

2.5.2 Scoring Criteria for Sleep Stages

Sleep stages are mainly classified as wakefulness, non-REM sleep, and REM sleep. Non-REM sleep is further into divided into four stages; stage 1, stage 2, stage 3 and stage 4. Table 2.1 summarized the sleep-wake scoring criteria [36, 37].

- *Stage W (Wakefulness)*: Stage W means the waking state. The EEG in this stage shows alpha waves and/or low voltage (10-30 μV), mixed frequency EEG. Alpha waves occupy more than 50% of the epoch. In addition, this stage may show a relatively high tonic EMG.
- *Stage 1*: Stage 1 is characterized by low voltage, mixed frequency EEG with a distinction in 2-7 Hz frequency range. The amplitude in 2-7 Hz is about 50-75 μV , and it can reach to 200 μV . Stage 1 does not show K complexes and sleep spindles. Alpha waves in the mixed frequency EEG occupy less than 50% of the epoch.

- *Stage 2*: The main feature of Stage 2 is K complexes and sleep spindles. K complexes show a negative high peak, followed by a slower positive wave. Sleep spindles have 12-14 Hz frequency band. The duration of K complexes and sleep spindles should be at least 0.5 sec and the time between K complexes and sleep spindles is less than 3 min to be scored as stage 2. This stage also shows relatively low voltage, mixed frequency EEG on background and waves with amplitude above 75 uV occupy less than 20 % of the epoch.
- *Stage 3*: Stage 3 is characterized by the brain waves with 2 Hz or slower. The waves with amplitude above 75 uV occupy at least 20 % but not more than 50 % of the epoch in stage 3. K complexes and sleep spindles may or may not be present in stage 3.
- *Stage 4*: Stage 4 shows the same waves as stage 3, with 2 Hz or slower waveforms. The classifying criteria between stage 3 and stage 4 is how much the waves with 2 Hz or slower with amplitude above 75 uV occupy over the epoch. The waves appear more than 50 % of the epoch.
- *Stage REM*: Stage REM shows the similar wave patterns of stage 1, low voltage and mixed frequency EEG. The feature of stage REM is that sawtooth wave pattern is frequently present and vertex sharp waves are not distinctive. In addition, stage REM shows the episodic rapid eye movements in EOG.

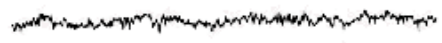
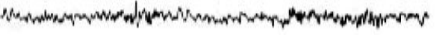
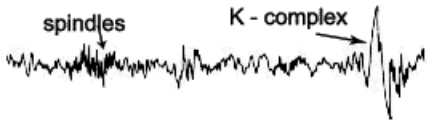

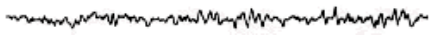
Stages	Characteristics	EEG wave patterns
Stage W	<ul style="list-style-type: none"> • Low voltage (10-30uV) and mixed frequency EEG activity • Alpha waves occupy more than 50 % of the epoch • Waking eye movement • EMG is elevated 	
Stage 1	<ul style="list-style-type: none"> • Low voltage and mixed frequency EEG activity with the highest amplitude in 2 - 7 Hz frequency range • Alpha waves occupy less than 50 % of the epoch • Slow eye movement • EMG is elevated but less than in Stage W 	
Stage 2	<ul style="list-style-type: none"> • K complexes and sleep spindles appear • Duration of K complexes and sleep spindles should be at least 0.5 sec • Waves with amplitude above 75 uV occupy less than 20 % of the epoch • EOG is silent • EMG is mildly decreased 	
Stage 3	<ul style="list-style-type: none"> • Waves with 2 Hz or slower • Waves with amplitude above 75 uV occupy 20 - 50 % of the epoch • EOG is silent • EMG is mildly decreased 	
Stage 4	<ul style="list-style-type: none"> • Waves with 2 Hz or slower • Waves with amplitude above 75 uV more than 50 % of the epoch • EOG is silent • EMG is moderately decreased 	
Stage REM	<ul style="list-style-type: none"> • Low voltage and mixed frequency EEG activity • Sawtooth wave pattern is often present • Episodic rapid eye movements • EMG is markedly decreased to absent 	

Table 2.1 Summary of Sleep-wake scoring criteria

Chapter 3: Wireless Communication

3.1 Introduction

Wireless communication has emerged as the new trend in the field of health monitoring systems. Traditionally, health information of a patient is monitored at the patient location or transferred to a medical center through wires [38]. However, these methods can restrict patient mobility and cause discomfort to the patient. The common wireless communication standards include Bluetooth, ZigBee, Wi-Fi and mobile communication. Each of these wireless standards has its respective advantages over each other based on the applications of the healthcare systems. However, all these standards are put to use in the healthcare systems according to the specific range of applications. These wireless standards are used to transmit the signals to a local or a remote server where the biopotentials can be monitored. The following parameters in wireless communication should be considered while building the wireless sensor network for the remote health monitoring.

- *Frequency* – It is the number of occurrences of a repeating event per unit time. It is measured in Hertz (Hz). Terms like Lowest Usable Frequency (LUF), Maximum Usable Frequency (MUF) and optimum frequency are used to define the usage of frequency in real world applications. FCC, in the United States, has set up limits on the frequency usage for medical communication. However, the unlicensed frequency band of 2.4 GHz is widely used for medical applications.
- *Bandwidth* – It is the difference between the highest and lowest frequency levels. It can also be interpreted as the time duration of data to reach one point from another or the width of the frequency band. Bandwidth is measured in terms of Hertz (Hz).

- *Data rate* – It is often referred in terms of bit rate. It is the number of bits transferred per unit time. Time involved here is often in seconds. The usual terms of measuring data rate are kbps, Mbps, Gbps and so on. Data rate is an important term in the health monitoring systems as the systems should not incur any data loss or improper data reception.
- *Coverage area* – It usually states the area which a signal can be transmitted. In medical applications coverage area also plays an important role to monitor the physiological signals at longer distance cost-effectively without adding a repeater.
- *Network topology* – It gives the essentials of all the elements present in a network. It also states the logical relationship and function of the nodes present in a network. Different kinds of network topologies are adopted by different wireless communication methods. The kind of network topology to be implemented is determined by the application of the system.
- *Power consumption* – It is one of the most critical factors of any wireless health monitoring system. It is defined as the unit of power a system consumes for its functioning. Because most of the health monitoring systems are powered by a battery, the proper selection of wireless communication standard should be considered because most of power is consumed by a RF transceiver and a RF amplifier.
- *Nodes* – Nodes are different points in network through which the data is usually transferred. The devices in a network can also be referred to as nodes. The number of nodes in each of the wireless communication method differs quantitatively.
- *Interference* – It is the disturbance caused to the originally transmitted signal by various sources. These sources may be other signals, reflection and refraction from wave propagation environment, signal to noise ratio (SNR) of the electronic devices, etc.

- *Broadcasting* – When the signals are transmitted from a common point to various other nodes or devices, it is called as broadcasting of signals.
- *Security* – It defines how securely the data is transmitted over a network. It is important to maintain high security in wireless communication, as personal and sensitive data may be intruded. Especially, in medical applications, intrusion of data may have a big impact on the patient's personal information.

3.2 Bluetooth

Bluetooth is a standard communication protocol named by the nomenclature as IEEE 802.15.1. It is prominently present in the mobile/cell phones as a communication medium. It is a low cost, low power consuming, small size and short ranged device. Devices like phones, PDAs, headsets, laptops and tablet computers use this technology to communicate between each other wirelessly. Bluetooth has a data rate of about 3 Mbps with version 2.0 + EDR, which is widely used. It operates at a frequency range of 2.4 GHz industrial, scientific and medical (ISM) band. This technology uses the master-slave principle and can render real time communication within 10 meters distance [39]. Both, point-point and point-multipoint communication is supported by Bluetooth. Point-multipoint system supports ad hoc communications between the devices. Combination of Bluetooth devices or the network formed by the Bluetooth devices is called as piconet [40]. A piconet may usually consist of 2 to 8 devices, where 2 devices are the minimum requirement and the network cannot exceed 8 devices. The network operation is purely automatic and is triggered when two devices are in the communication range. The master initiates the operation and the slave follows it. The master and slave devices take turns in communicating between each other. However, a slave can become a master and a master would prefer to become

slave depending on the application of the communication strategy. Similarly, two or more piconets can form a scatternet network [40]. Figure 3.1 shows the configuration of piconet and scatternet in Bluetooth network. A master of one piconet can act as a slave in the other and vice versa. This enables point-multipoint which supports ad hoc communication.

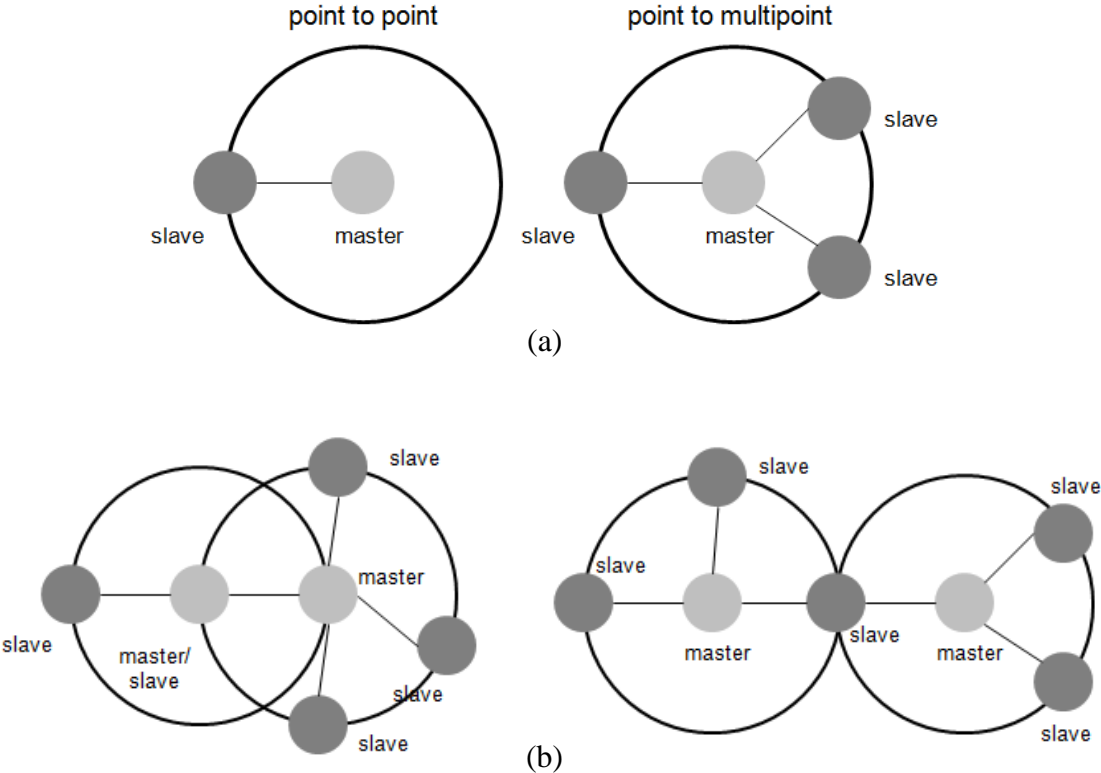


Figure 3.1 Network configuration of Bluetooth; (a) piconet and (b) scatternet

Bluetooth facilitates faster communication in its network as it is always in alert stage because of its feature of single hop. Bluetooth uses frequency hopping spread spectrum (FHSS) modulation in spread spectrum signal transmission. Bluetooth has a feature in which it can switch 79 channels at 1600 times per second [39]. Noise and other interferences are reduced in Bluetooth to great extent, because only the devices in a synchronized piconet network can hop at

the same frequency and time. Bluetooth uses 64 or 128 bit encryption according to the application, and data transmission is safe [39]. When transmission is disturbed and data loss occurs, the lost packets of data are resent automatically to prevent data losses. The Bluetooth communication started with a specification called Bluetooth v1.0 and was revamped continuously with betterments into v1.0B, v1.1, v1.2, v2.0+EDR, v2.1+EDR, v3.0+HS and v4.0. The basic Bluetooth v1.0 and v1.0B did not have interoperability between devices and the device address was mandatory for other devices to establish connection. Slightly modified, v1.1 had the possibility of adding the non-encrypted channels and also has RSSI. The backward compatible version v1.2 had a major addition to its predecessor. It included features like extended synchronous connection, host controller interface, higher transmission speed and better tolerance to resistance. After this, all the introduced versions are compatible backwards. Version v2.0+EDR is the first version to have enhanced data rate and had a practical data rate of 2.1 Mbps. It also included the combination of GFSK and PSK. Pairing was made simply through secure simple pairing (SSP) in v2.1+EDR. It had enhancements like sniff pairing and extended inquiry response. The latest version of Bluetooth is v3.0+HS. It has added AMP (Alternate MAC/PHY) for high transport and increased the theoretical data rate up to 24 Mbps.

3.3 Wi-Fi

Wi-Fi has been named in the nomenclature as IEEE 802.11. Wi-Fi alliance defines Wi-Fi as any device that can communicate in Wireless Local Area Network (WLAN) based on the IEEE 802.11 standards. Wi-Fi operates in the frequency range of 2.4/5 GHz ISM band. Wi-Fi operates in two modes: ad-hoc and infrastructure mode. The ad-hoc mode includes independent basic service set (IBSS) which is the simplest type of 802.11 network. Using the ad-hoc operating

mode, the wireless stations can communicate with each other directly and this network is stated as peer-peer network. The basic service set (BSS) is isolated and there is no connectivity to the other networks. Since this network configuration is not laborious, it is preferred for applications which require quick network formation. In the infrastructure mode, an access point is present in the BSS and it extends the network presence to other wired networks. The devices from the other network which joins this BSS must establish an association with its access point. Figure 3.2 shows the network configuration of Wi-Fi including ad-hoc, infrastructure and extended service set.

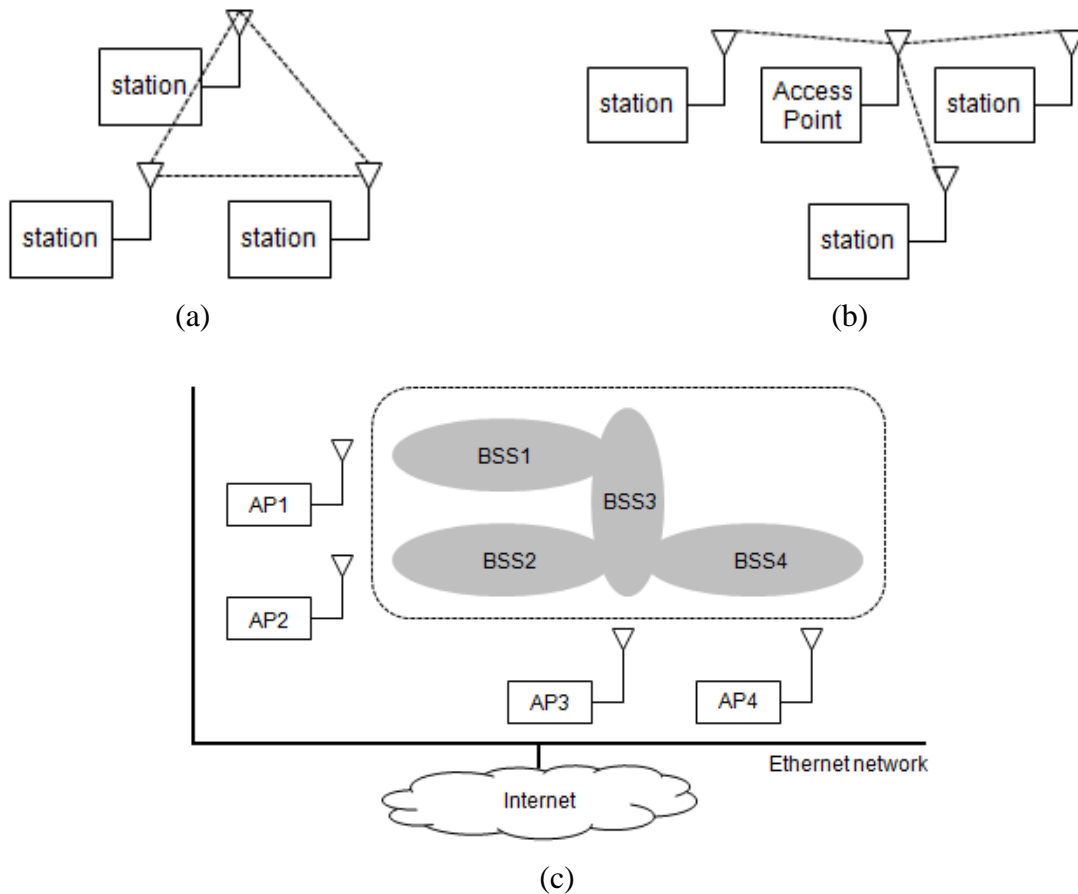


Figure 3.2 Network configuration of Wi-Fi; (a) ad-hoc, (b) infrastructure and (c) extended service set

IEEE 802.11 specification defines two layers from the five TCP layers present, the physical layer and the data link layer. The latter consists of the media access control (MAC) and logical link control (LLC) layers. The IEEE 802.11 specifications constitute several physical layers. These layers are responsible for modulation, encoding and transmission. PHY operates on a specific ISM band. Since ISM is a free band, regulations demand the usage of spread spectrum technique in PHY layers. Therefore, direct sequence spread spectrum (DSSS) is used in this band. MAC is a sub layer of the DLL (data link layer) and is positioned above the PHY layer. It has a control over the transmission of data and provides interaction with wired connections. CSMA/CA is used by the MAC layer to transmit packets of data across shared channels. This technique, unlike CSMA/CD, avoids collisions instead of detecting collision. A six octet MAC address is used by Wi-Fi and Ethernet, since the MAC layer appears as an IEEE 802 LAN to the (LLC) logical link control [39]. IEEE 802.11 has different specifications named as a, b, g and n. These networks share the same common features but in a different degree. 802.11a operates at 5.3 and 5.8 GHz and has a data rate of 54 Mbps by using orthogonal frequency division multiplexing (OFDM) modulation. 802.11b and 802.11g operate at 2.4 GHz frequency band. 802.11b has a data rate up to 11 Mbps by using DSSS modulation and 802.11g has a data rate up to 54Mbps by using OFDM. 802.11n is the latest of all the specifications for increasing the data rate. It operates at 2.4/5 GHz with the data range of up to 70 meters and the data rate of 240 Mbps. Usually, the Wi-Fi networks are unencrypted but provides a user interface in the devices through which it can be encrypted. Wi-Fi follows security standards like wired equivalent policy (WEP), Wi-Fi protected access (WPA) and Wi-Fi protected access 2 (WPA2) [41]. WEP is the first introduced security protocol which provides open and shared authentication. It uses 40 or 104 bits encryptions which are vulnerable to security threats. It had several disadvantages like no

mutual authentication, no data integrity with checksum values, no user authentication and reuse of static key. To overcome these disadvantages, WPA and WPA2 were introduced. Both these methods use temporal key integrity protocol (TKIP) to enhance the encryption key to 128 bits for each transmitted packet. A message integrity check algorithm called Michael was introduced in the WPA protocols to provide secure transmission of messages over a network. Counter cipher mode with block chaining message authentication code protocol (CCMP) was introduced with WPA2 which makes it the best security protocol available. It includes 128 bit key and 128 bit block size, thereby providing dual layer protection. This protocol was formulated to address the vulnerabilities of WPA.

3.4 ZigBee

ZigBee is based on IEEE 802.15.4 standard which specifies the physical and media access control layers for low rate Wireless Personal Area Network (LR-WPAN). ZigBee is the most cost effective and power efficient device among Bluetooth, ZigBee and Wi-Fi [42]. ZigBee focuses on applications that include low data rate, low power consumption and low cost. The wide range of applications includes consumer electronics, home automation, energy management and health monitoring [43]. The data rate of ZigBee varies from 20 – 250 kbps depending on the frequency band and the number of channels. It operates on ISM bands of 868 MHz in Europe, 915 MHz in USA and Australia, and 2.4 GHz in most of the regions worldwide [44]. The ZigBee operating at 868 MHz frequency band has a chip rate of 300 kchips/s, bit rate of 20 kbps, symbol rate of 20 ksymbols/s and follows BPSK modulation. The ZigBee at 915 MHz frequency band has a chip rate of 600 kchips/s, bit rate of 40 kbps, symbol rate of 40 ksymbols/s and follows the BPSK modulation. The ZigBee at 2.4 GHz frequency band has a chip rate of 2000 kchips/s, bit

rate of 250 kbps, symbol rate of 62.5 ksymbols/s and follows the O-QPSK modulation. The MAC layer present in ZigBee controls the network association/disassociation. ZigBee devices are classified into two: fully functional device (FFD) and reduced functional device (RFD). The difference between these two types of devices is that, a FFD can act as coordinator or router or an end device, and can communicate with any device in the network. However, a RFD can only act as an end device and it can pair only with the other FFDs in the network. ZigBee can support many nodes in its networks which includes tree, star and mesh topologies [43]. Star network is formed when the FFD establishes its network and becomes the PAN coordinator of the network. Then the other devices try to connect to the PAN coordinator. Each node in the network will have a unique identity. In tree network, the PAN coordinator performs the same function and allows more complex network formations. Mesh topology is formed by combining star and tree topologies. Figure 3.3 shows the network configuration of ZigBee.

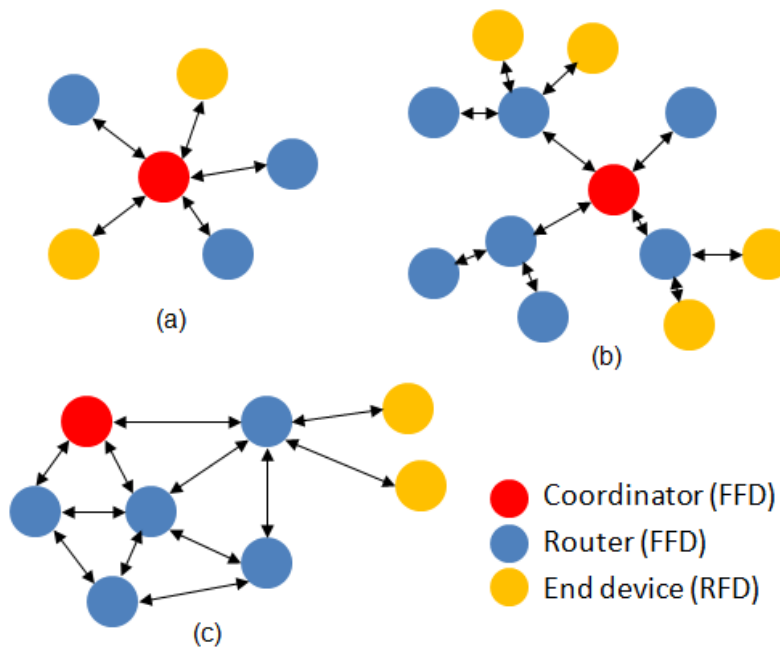


Figure 3.3 Network configuration of ZigBee; (a) star, (b) cluster-tree and (c) mesh

The current ZigBee system operates in both beacon and non-beacon modes. In the non-beacon modes, the receivers are continuously active and the device consumes more power because of this. However, in the beacon mode, beacons are sent indicating that the receiver is in a ready state. Because of this functionality, there is low duty cycle and low power consumption [43].

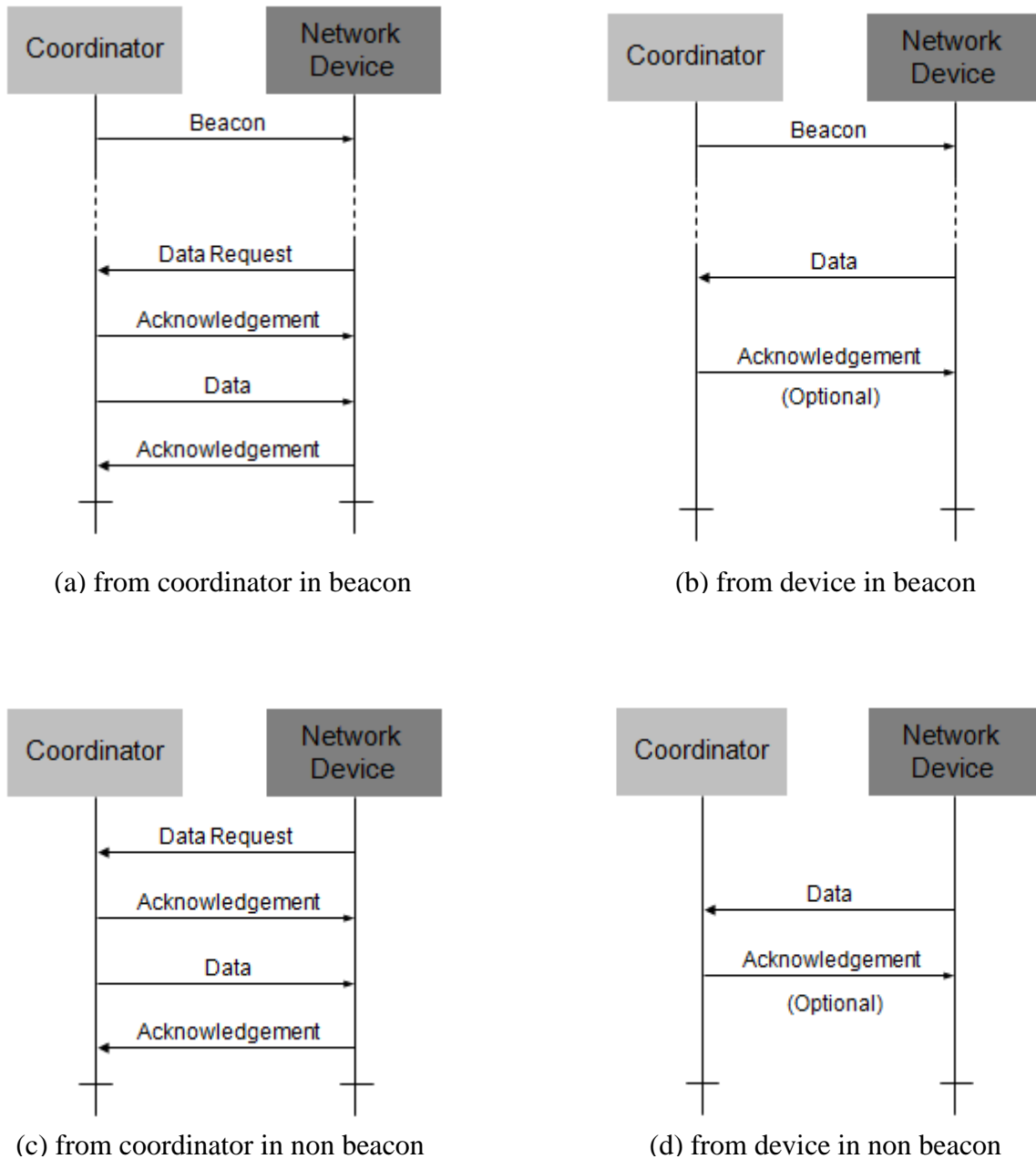


Figure 3.4 Data transmission in IEEE 802.15.4

There are three types of security protocols found in ZigBee. They are unsecured mode, access control list and secure mode. Unsecured mode is the mode where there is no security measures implemented. In access control list, as the name indicates, it controls access. It does not have any encryption but rejects the frame from unauthorized users or networks. And, the secure mode provides the access control and encryption. It uses advanced encryption standard (AES) and 128 bit encryption key. It also provides frame integrity where message integrity code (MIC) algorithm is implemented. A cryptographic key is used to protect the data from unauthenticated access.

3.5 GSM/WCDMA

The first-generation of mobile communication was developed for voice call. The data service was provided since the second-generation. Global System for Mobile Communications (GSM) was also introduced during the second generation. GSM is a digital circuit switched telephony which offers voice call, short message service (SMS). To enhance the data transfer rate, General Packet Radio Service (GPRS) and Enhanced Data rate for GSM Evolution (EDGE) was announced. GPRS allows data rate to increase to 171 kbps and EDGE supports data rate up to 384 kbps. As moving on to the third generation, the schemes for multiple accesses are changed from Time Division Multiple Access (TDMA) to Wideband Code Division Multiple Access (WCDMA) [45]. These techniques allowed data rates to reach 2 Mbps. To improve the performance of WCDMA protocols, High Speed Packet Access (HSPA) was introduced. It enables WCDMA to increase the peak data rates of up to 14 Mbps in the downlink and 5.76 Mbps in the uplink. Recently 3GPP Long Term Evolution (LTE) is launched for higher data rate and is based on GSM/EDGE and UMTS/HSPA network technologies. The LTE specification

provides downlink peak rates of 300 Mbps and uplink peak rates of 75 Mbps with Orthogonal Frequency Division Multiplexing (OFDM) and Single Carrier-Frequency Division Multiple Access (SC-FDMA) scheme.

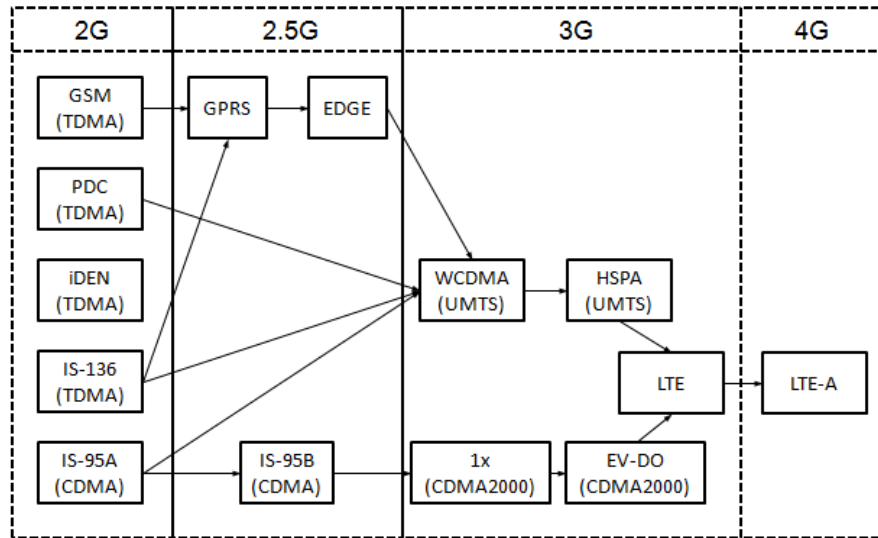


Figure 3.5 Evaluation of mobile communication

The evolution of mobile communication has increased the data transfer rate from the first-generation to the present fourth generation. Because of this evolution, it is now possible to use mobile network in wireless health monitoring systems. The physical network structure of the mobile communication is classified into base station, network and switching subsystem, core network and operations support subsystem. With the help of these subsystems, mobile network can communicate with other internet enabled devices. Data area coverage is longer, compared to the other wireless communication systems because of its ubiquity and network. Even though mobile communication consumes more power, it is feasible to have wide coverage which is one of the most important factors in health monitoring systems.

Table 3.1 summarizes the main difference among Bluetooth, Wi-Fi and ZigBee. As shown in the table 3.1, Wi-Fi has longer coverage area, high data rate, but it consumes more power. ZigBee consumes less power and shorter network join time, but comparatively, it has lower data rate than other wireless standards. Bluetooth has its parameters ranging between ZigBee and Wi-Fi.

Parameters	Bluetooth	Wi-Fi	ZigBee
Frequency band	2.4 GHz	2.4/5GHz	868/915 MHz 2.4 GHz
Max data rate	3 Mbps	54 Mbps	250 kbps
Nominal range	10 m	100 m	10 - 100 m
Tx power	0 - 10 dBm	15 - 20 dBm	0 dBm
Number of RF channels	79	14	1/10, 16
Channel bandwidth	1 MHz	22 MHz	0.3/0.6 MHz, 2 MHz
Power consumption	200 mW (National LMX9820A)	400-700 mW (Philips BGW200)	60-70 mW (Chipcon CC2420)
Spreading	FHSS	DSSS, CCK, OFDM	DSSS
Network latency	1 sec	30 ms	3 sec
Network topology	piconet/scatternet	ad-hoc/infrastructure	star/tree/mesh

Table 3.1 Comparison of the Bluetooth, Wi-Fi and ZigBee

Chapter 4: Wireless Health Monitoring Systems for Sleep Disorders

4.1 Introduction

Humans spend much more time sleeping than other activities. A good night's sleep plays a vital role in physical and mental well being by performing the recuperative function for the brain and the body. Notwithstanding the fact that, good sleep is an essential part of a person's life, an increasing number of people are experiencing sleep disorders and loss of sleep. According to the research by the National Institutes of Health (NIH), 50 to 70 million Americans suffer from sleep disorders and sleep deprivation [46]. Although sleep disorder is a highly prevalent condition like diabetes or asthma, 80 to 90 percent of the cases remain undiagnosed [47]. The short-term effects of sleep disorder are morning headaches, excessive daytime sleepiness, short-term memory loss and depression, but the cumulative long-term effects result in severe health consequences like heart attacks and strokes [48]. In addition, people suffering from sleep disorders are 7.5 times more likely to have a higher body mass index and 2.5 times more likely to have diabetes [49]. Further, undiagnosed and untreated sleep disorders have a significant direct and indirect economic impact. The costs associated with untreated sleep disorders are far higher than the costs for adequate treatment. According to the survey, approximately \$22 billion is spent on medical expenses associated with repeated doctor visits, prescriptions and medications [50]. These costs can be easily avoided with proper diagnosis. People suffering from sleep disorders are less productive because of fatigue and are at a higher risk of accidents while driving. This also leads social problems and economic burden indirectly. Therefore, timely, adequate diagnosis and treatment are required to reduce the physical risks and reduce health care costs. Causes for sleep disorders vary from nightmares to neurological problems. Sleep apnea, one of the most

common sleep disorders, is the reduction or cessation of breathing during sleep. There are three types of sleep apnea, namely, obstructive (OSA), central (CSA) and mixed sleep apnea according to the cause for the pause in breathing. 3 to 4 million individuals among those with sleep disorders suffer from OSA [51]. Insomnia, having difficulty falling asleep or maintaining sleep, is observed in about 10 percent of the American population [52]. Restless legs syndrome (RLS) from abnormal neurological conditions affects approximately 5 percent of the general population [53]. Accurate diagnosis of sleep disorders is imperative to the treatment plan and early recovery. There are four types of sleep study devices according to the Center for Medicare & Medicaid Services (CMS) and the American Academy of Sleep Medicine (AASM). As described in the introduction chapter, type I PSG is a gold standard method for diagnosing sleep disorders by recording and scoring the physiological signals. Type I PSG measures almost all kinds of physiological signals with around 20 sensors and is performed by a sleep technologist in a sleep lab. For this reason type I is referred to as a full sleep study and attended study. An In-lab test is when a patient will sleep at the sleep laboratory and a sleep technologist monitors vitals and observes through a video camera in a control room. The results of the sleep study can be distorted due to first-night effect experienced by the patient in an unfamiliar and uncomfortable sleep environment. In addition to the inconvenience of having to sleep in an unfamiliar place, these exams are expensive and there is usually a long waiting list. The cost of performing a PSG ranges from \$1,000 to \$5,000 and the waiting time from a few weeks to more than a year because of the currently insufficient capacity of sleep laboratories [54]. Recently, home sleep test (HST) devices have been developed to overcome the drawbacks of In-lab tests. HST is performed at home in the comfort of the patient's own home and there are no long waiting lists to schedule the exam. Although HST devices provide comfortable sleep environment and are

cost-effective, they also have drawbacks; lack of real-time monitoring and limited amount of physiological information. The lack of real-time monitoring not only delays the diagnosis process but is also cumbersome as the patient has to upload or hand carry the data to his/her sleep lab the next day. Moreover, the systems are usually wired and inconvenient to use. To alleviate these problems, recent HST devices use wireless communication to save the sleep data to a local storage device or directly upload to a remote server.

Most wireless HST systems adopt Bluetooth or ZigBee as a wireless communication standard while some systems use their own wireless protocols over industrial, scientific and medical (ISM) band. The system should consume less power to monitor/save sleep patterns overnight. The wireless system should also have long data coverage to build a cost-effective network and high data transfer rate to transmit several physiological signals wirelessly without data losses. Firstly, ZigBee is used as it consumes considerably lesser power than the other wireless standards. It consumes power in the range of few tens of milliwatt. ZigBee can also wake from the sleep mode and join the network in less than one millisecond which allows the number of nodes in a network to be 64 k. In addition, ZigBee can also build a wireless sensor network and is cost effective than the other wireless standards. ZigBee has 250 kbps data rate. Secondly, Bluetooth provides mediocre power consumption which is higher than ZigBee but lower than Wi-Fi. Bluetooth has a data rate of about 3 Mbps and communicates with any Bluetooth enabled devices within 10 meters range. Thirdly, Wi-Fi consumes more power than ZigBee and Bluetooth. However, it has a high data rate of up to 54 Mbps and longer distance coverage of up to a few hundred meters. However, ZigBee and Bluetooth are for wireless personal area network (WPAN) or wireless body area network (WBAN). Wireless standards, ZigBee and Bluetooth, can store data in a local server which is placed on WPAN or WBAN. However, these networks

should be extended to wide area network (WAN) to monitor the signals at a remote place. Without extending to WAN, the data cannot be monitored in real time by a physician who stays in a hospital.

The mobile communication allows the physiological signals to be transmitted and monitored from anywhere regardless of where a patient is, due to its long data coverage. The evolution of mobile communication has increased the data transfer rate from the first-generation to the fourth generation currently. While GSM provides the data rate, 9.6 kbps, the third generation, WCDMA, supports the data rate up to 2 Mbps. The evolution of the mobile communication enables the mobile communication to be applied to the wireless health monitoring system by providing sufficient data rate and long data coverage. Figure 4.1 shows the comparison of wireless standards in the view point of data coverage and data transfer rate.

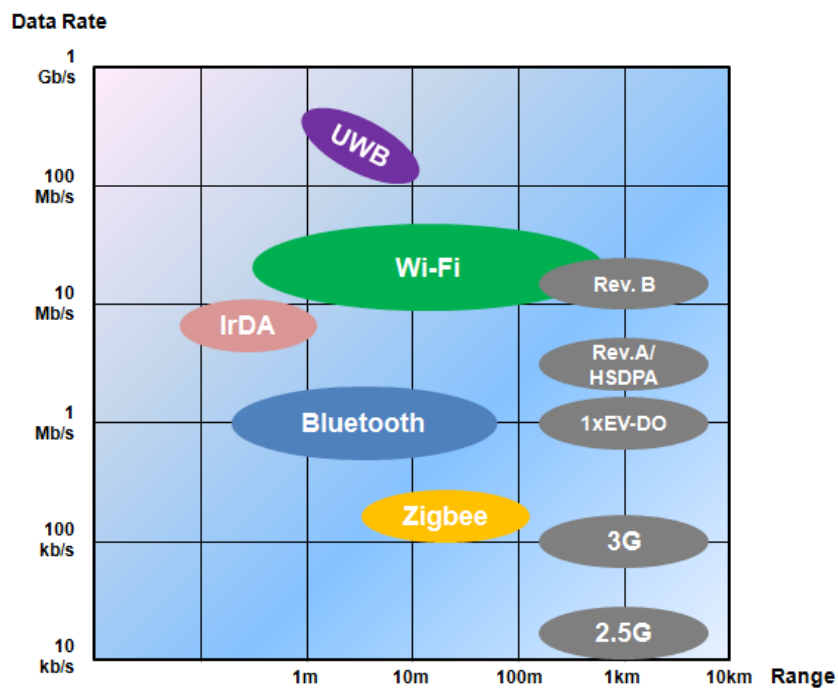


Figure 4.1 Comparison of wireless communication standards

Even though currently available HST systems use wireless communication, the systems still have some limitations. As mentioned in the previous section, because the system uses ZigBee and Bluetooth for WPAN or WBAN, the real-time monitoring of physiological signals at remote places is not feasible. In addition, the systems are standalone type; consequently the devices cannot extend the number of channels to measure additional physiological signals. For example, assuming a patient has a type III device, when the patient is required to measure EEG, EOG or EMG which is not provided by the type III devices, the patient should additionally purchase a type II device to measure these physiological signals. Type II device includes all the channels provided in the type III device, the type II device that the patient currently owns will become useless. As a result, having a fixed number of channels per type is not a cost-effective solution.

To overcome these drawbacks of the HST systems, two wireless telemedicine systems for diagnosing sleep disorders are proposed. The first system is designed with ZigBee star network and combination of two wireless communication standards, ZigBee and Wi-Fi. The system mainly consists of two wireless HST devices, a receiver and a monitoring unit. One of the HST devices has 5 input channels as a type III HST device which measures ECG, nasal airflow, chest/abdomen effort, body movement and oxygen saturation. The other HST device, as a supplementary device, has 5 channels - 2x EOG, 1x EMG and 2x EEG. The receiver unit adopts two wireless communication standards, Wi-Fi and ZigBee. The combination of two wireless standards in the receiver unit satisfies both, low power consumption and high data transfer rate of the overall system. Each HST device sends its measured signals to the receiver unit with a ZigBee star network. Each device is regarded as a standalone type III and supplementary HST device, but on the receiver unit side, the whole system is extended to a type II device by collecting and combining the signals from the type III device and the supplementary device. The

sleep data in the receiver unit are retransmitted to the monitoring unit or the remote server through the local Wi-Fi network. Figure 4.2 shows the data flow of the proposed system [85, 86].

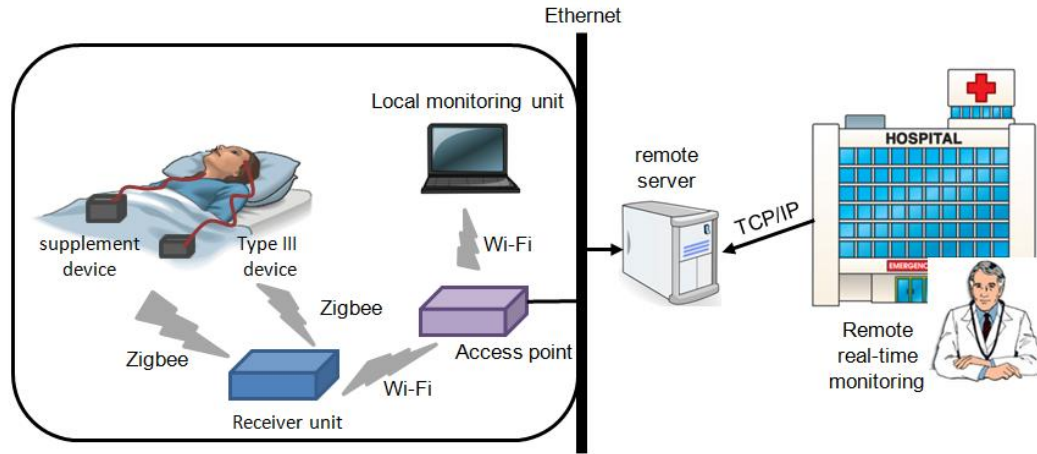


Figure 4.2 Data flow of the system to diagnose sleep disorders with ZigBee and Wi-Fi

The second system is designed with GSM/WCDMA network to reduce a patient's discomfort and monitor physiological signals at a remote place. A skull cap with equipped electronics on the top senses biopotential signals and transmits them to a remote server through the mobile networks. The device consists of an amplifier module, a power management circuit, a processor module and a GSM/WCDMA module. 5 channels of biopotential signals, 2-channel of EOG to detect right and left eyes movement, 1-channel EMG from the chin and 2-channel EEG on C3 and O2 position, are monitored to evaluate sleep stages, same as the function of the supplementary device of the first system. After transmission, based on TCP/IP (Transmission Control Protocol/Internet Protocol), the signals are processed and saved in the server. The physician connects to the server and monitors signals in real time or analyzes/diagnoses with the stored data. Figure 4.3 shows the data flow of the second system, the wireless telemedicine system with GSM/WCDMA network [88]. The deployment of the all-in-one sleep monitoring

system provides the comfort and cost reduction by removing long wire connection and installation/maintenance of dedicated sleep lab. In addition, the system based on mobile network enables the monitoring of signals in real time at any place.

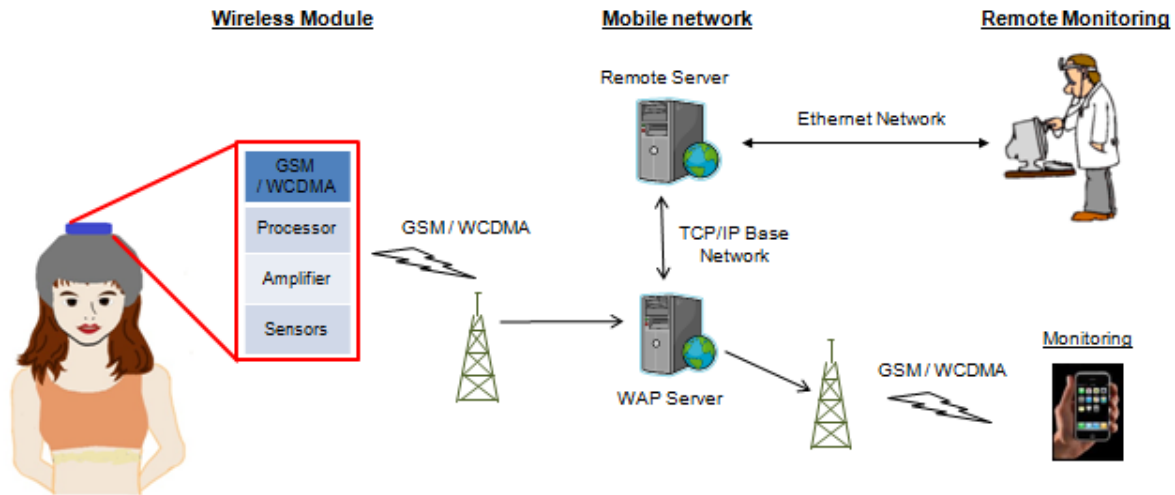


Figure 4.3 Data flow of the system to evaluate sleep stages with GSM/WCDMA

4.2 System Design and Implementation

The system with ZigBee and Wi-Fi network consists of four components; sensors, two HST devices, a receiver, and monitoring unit. Sensors detect the physiological signals. The HST devices which consist of an amplifier module, a microprocessor and a ZigBee module sense the physiological signals and send them to the receiver through ZigBee network. The receiver which consists of two RF modules, ZigBee and Wi-Fi, a microprocessor and memories re-transmits the signals to the monitoring unit through Wi-Fi network. The monitoring unit displays real time sleep data and records sleep data to the local or the remote server.

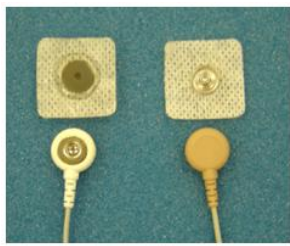
The system with GSM/WCDMA network is composed of sensors and a data acquisition/transmission unit which is placed on top of the skull cap. The sensed 5-channel

signals are sent to the remote server which has the static IP address through the mobile network. The signals are processed and monitored in the remote server with a utility program.

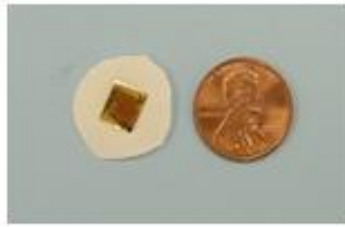
4.2.1 Sensors

Sensors are selected and characterized to measure different types of physiological signals. Biopotential signals; EEG, EOG, EMG and ECG, can be sensed with conventional wet Ag/AgCl electrodes which use the conductive gels to reduce the skin impedance or make conductive path through hairs. However, these gels can cause skin irritation. Moreover, when the gels dry out, it changes the impedance and introduces erroneous signals. As a remedy, vertically aligned gold nanowire electrodes [50] are used. As dry electrodes, the gold nanowire electrodes obviate the use of conductive gel, and minimize the impedance changes and skin irritation due to dry-out of the conductive gel. Body position is used to analyze the pattern of body movement during sleep. The gyroscope is used for body position, which is mounted on the chest belt. The amount and the direction of motions can be derived with the sensitivity of the gyroscope over yaw, pitch and roll axis. The chest respiration effort is measured by detecting the up/down movements of chest during breathing. The changes of waveforms indicate the number of movements from inspiration and expiration. The movement of chest is measured with the piezoelectric sensor which is embedded in the chest belt. Nasal airflow is to measure the rate of respiration and identify interruptions in breathing. Nasal airflow is measured by detecting pressure changes from respiration volume through the nose with a pressure sensor which is connected to the nose prongs. By measuring chest respiration effort and nasal airflow, the case of sleep apnea that has chest respiration effort without airflow can be detected. Oxygen saturation is measured and derived with a pulse oximeter. It is a relative measurement of amount of hemoglobin and the

combination of hemoglobin and oxygen. The transmittance mode of the pulse oximeter is used, in which the light emitted by LEDs is detected by a photodiode which is placed opposite to the LEDs. Arterial pulsatile waveforms are detected with the RED/IR LEDs and the photodiode, and the SpO₂ is derived with the absorption ratio of RED and IR LEDs. Figure 4.4 shows the sensors which are used to diagnose sleep disorders with the proposed systems.



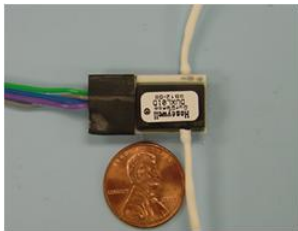
(a) Ag/AgCl electrodes



(b) gold nanowire electrodes



(c) gyroscope



(d) pressure sensor



(e) piezoelectric sensor



(f) oximeter sensor

Figure 4.4 Sensors to diagnose sleep disorders [87]

4.2.2 Amplifier Module

The raw physiological signals from the sensors are very weak, ranging from micro-volts to milli-volts, and contaminated by noises, especially 50/60 Hz power line interference. Therefore, the signals need to be amplified and filtered to improve the signal to noise ratio. The biopotential signals for sleep studies are differential signals. The body impedance and contact impedance between skin and the electrodes might vary under different skin conditions leading to impedance

mismatches. Therefore, amplifier should have high common mode rejection ratio (CMRR) and high input impedance to maintain signal integrity. The 5-channel amplifier modules for the supplementary HST device and the device with GSM/WCDMA consist of 3 stages and each amplification channel has the same configuration. Figure 4.5 shows the schematic diagram of the amplification circuit for the biopotential signals. The gain and bandwidth of each channel were tuned according to the AASM manual [55]. The instrumentation amplifier is adopted as the first stage to guarantee the high input impedance and high CMRR. The second stage, includes a RC high pass filter (HPF) designed with non-inverting operational amplifier to remove DC offset from the accumulated electric charge on the surface of the electrodes. The final stage is an active filter and a HPF. The second order Sallen-Key low pass filter is implemented. The other 5-channel amplifier for the type III HST device, for measuring different types of physiological signals, was designed according to the type of sensor used. The channels for the body position and SpO₂ have different configurations as compared to the other channels for ECG, nasal airflow and chest effort. The gyroscope for measuring body position processes data internally. Thus, the amplifier channel is not required for the gyroscope. The output of the gyroscope is directly connected to the input of the analog-to-digital converter (ADC) in the microprocessor. The first stage of the amplifier for the SpO₂ was implemented with a trans-impedance amplifier to convert the photocurrent from the oximeter sensor to voltage signals which was then amplified with a non-inverting amplifier. The amplifier channels for nasal airflow and chest effort have the same configuration as those used for the biopotential signals. The amplifier module for the device with GSM/WCDMA has the same configuration as that of the supplementary HST device because they measure the same biopotential signals, EOG, EMG and EEG. Table 4.1 summarizes the specification of each amplifier channel.

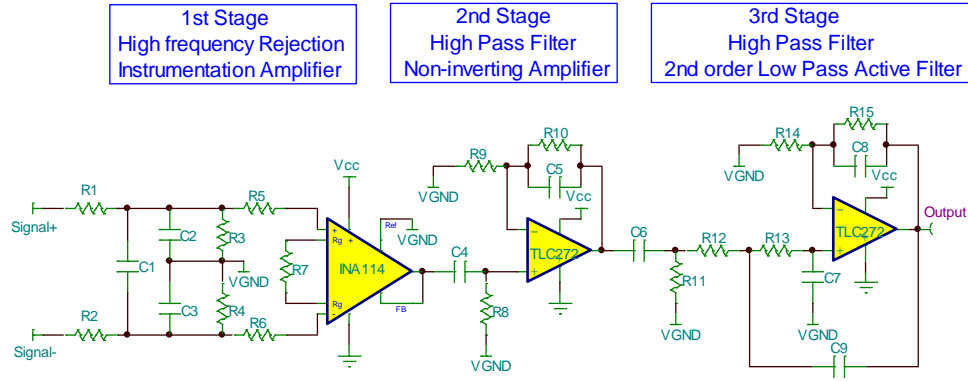


Figure 4.5 Schematic diagram of the amplification circuit for biopotential signals

Category	Specification							
Device type	Type III HST device				Supplement HST device / device with GSM/WCDMA			
Gain & Bandwidth	Ch	Purpose	Gain	BW	Ch	Purpose	Gain	BW
	1Ch	ECG	54 dB	0.3 ~ 71 Hz	1Ch	EOG	76 dB	0.3 ~ 35 Hz
	2Ch	Body Position	-	-	2Ch	EOG	76 dB	0.3 ~ 35 Hz
	3Ch	Nasal Airflow	59 dB	0.14 ~ 18 Hz	3Ch	EMG	76 dB	0.3 ~ 100 Hz
	4Ch	Chest effort	34 dB	0.13 ~ 16.3 Hz	4Ch	EEG	80 dB	0.3 ~ 35 Hz
	5Ch	SpO2	6 dB	0.15 ~ 30 Hz	5Ch	EEG	80 dB	0.3 ~ 35 Hz
Virtual ground	2.5V							

Table 4.1 Specification of the amplifiers for physiological signals

4.2.3 Data Acquisition and Wireless Unit

4.2.3.1 Devices with ZigBee and Wi-Fi

The data acquisition/wireless unit with ZigBee and Wi-Fi consists of two HST transmitters and a receiver. The HST transmitters and the receiver build the ZigBee star network in WPAN. In addition, the network is extended to WLAN with Wi-Fi module in the receiver and the network is further extended to WAN with an access point which is connected to the Ethernet network. Therefore, the real time monitoring of the physiological signals at remote places can be realized

by extending WPAN with ZigBee to WAN through WLAN with Ethernet network and Wi-Fi network respectively.

The main functions of the wireless HST transmitters are data processing, data flow management and data transmission with the ZigBee module. The analog signals from the amplifier output are digitized using the AD converter onboard the microprocessor and timer registers were used to fix the sampling rate. The register value is initially set and interrupt signals are generated whenever the value crosses zero based on the frequency of count. The interrupt signal is generated at a fixed interval and is used to trigger the AD conversion. The output of the ADC is transferred to the ZigBee module through Universal Asynchronous Receive/ Transmit (UART) interface. The data from the microprocessor are transmitted to the wireless receiver unit through ZigBee. Programs were developed to drive the ZigBee module and transmit the sleep data to the wireless receiver unit. The ZigBee module is controlled using the integrated command set. There are two different kinds of devices in a ZigBee network: A fully functional device (FFD) and reduced functional device (RFD). FFD can be a coordinator, a router or an end device. FFD can communicate with other FFD or RFD. On the other hand, RFD can act only as an end device and can communicate only with FFD in the network. ZigBee network allows only one coordinator and a number of routers and end devices. The function of an end device to two HST devices and the function of a coordinator to the wireless receiver unit were assigned while building the ZigBee star network. Upon device power up, the bootloader is loaded, following which the initialization functions are executed for the AD converter and the ZigBee module. The routine for ZigBee initialization sets up the connection between the ZigBee module and the microprocessor and configures the PAN ID and self ID of the ZigBee module. After this step, AD conversion is performed and the data are reconstituted as packets with sequential hex code

including node number, sampling rate, the number of channel and the data according to the defined communication protocol. These packets are saved in the data buffer temporarily and transmitted when receiving the data request. Finally, ZigBee interface routinely checks the wireless connection between the HST transmitters and the receiver unit, and then transmits the sleep data to the receiver unit. Figure 4.6 shows the data flow in the microcontroller of the HST transmitters.

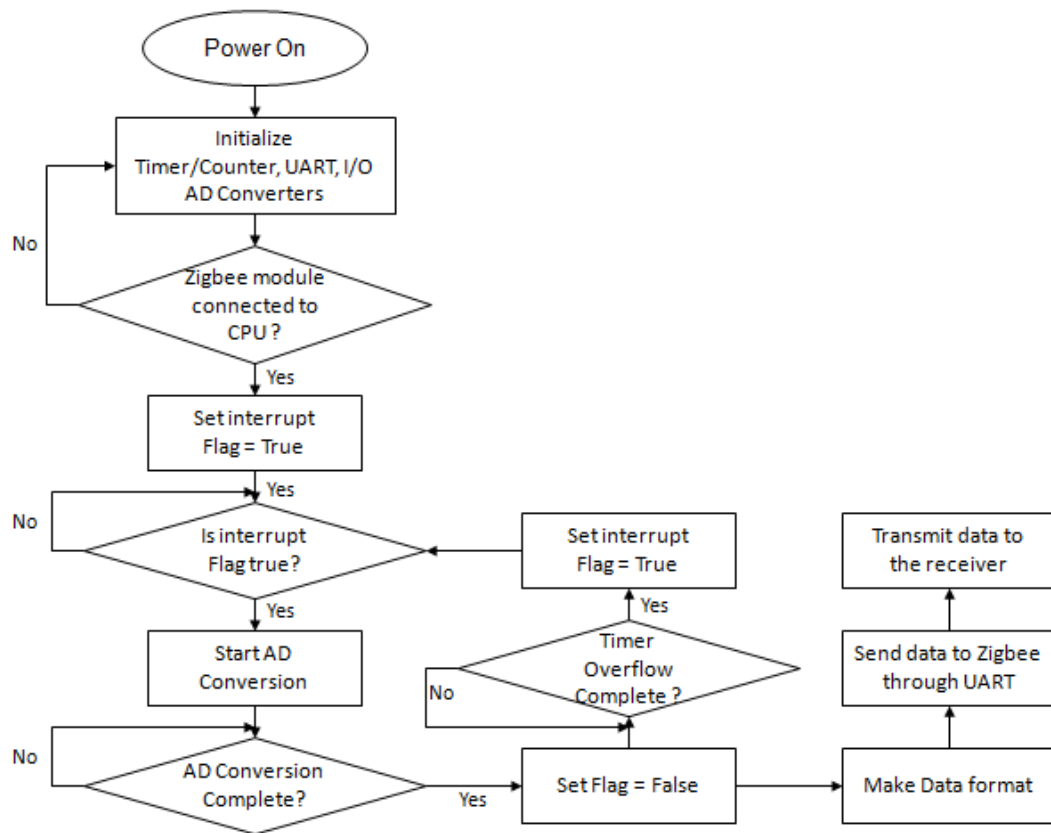


Figure 4.6 Data flow in the microcontroller of the HST transmitters

Both the wireless HST devices use a 3.7 V poly lithium battery as a power supply. 3.7 V is boosted up to 5 V by DC/DC converter to provide power to the microprocessor and the

amplifier. 5 V is regulated to 3.3 V for the ZigBee module by a low-dropout regulator (LDO).

Figure 4.7 shows the block diagram and image of the wireless HST device.

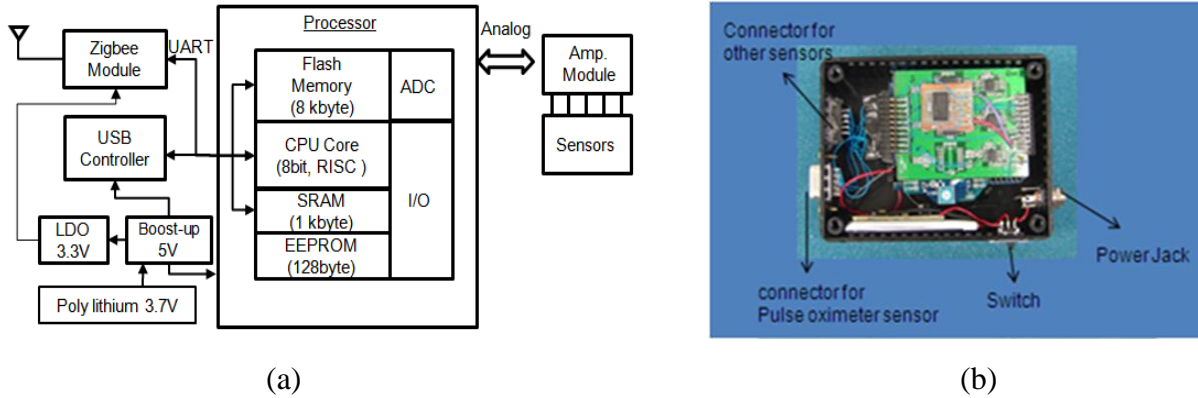


Figure 4.7 Wireless HST device: (a) block diagram and (b) image

While the function of the wireless transmitter is to build the wireless personnel area network with ZigBee, the role of the wireless receiver is to extend the ZigBee network to the wireless local area network with Wi-Fi. The sleep data needs to be monitored at remote places. Therefore, the network should be extended to use Internet. Although there are two ways that ZigBee has advantages on power consumption and WPAN/WBAN construction, the communication distance of ZigBee is at most a few hundred meters and ZigBee is not as prevalent as Wi-Fi. It will be expensive to build a local area network using ZigBee alone. Additionally, the amount of sleep data in the receiver from two transmitters is twice the amount of the sleep data in each transmitter. The receiver should handle 10 channels of data while each transmitter process 5 channels of data. Therefore, Wi-Fi facilitates extension of the number of channels by coordinating the data received from the transmitters and additional transmitters can simply be added on.

The processor board in the wireless HST receiver manages the ZigBee and Wi-Fi module and consists of a 16 MB SDRAM, a 64 MB NAND Flash memory, a 32-bit microcontroller and an Ethernet controller. The memories are needed to process and store data. SDRAM is used as the buffer for the sensor data, and the flash memory is used for the storage of programs. The Wi-Fi module and the Ethernet controller enable the receiver to connect to the Internet through wireless or wired communication. The Wi-Fi module, adopting IEEE 802.11 b/g, is connected to the microcontroller through USB 2.0 interface. USB 2.0 interface whose data transfer rate is 480 Mbps assures the full speed of the Wi-Fi module, 54 Mbps. The supplied 5 V is regulated to 3.3V for the ZigBee module, the external memory and I/O ports of the microcontroller. The other regulated voltages are 2.7V and 1.2V, is for the internal memory and operation of the microcontroller, respectively. The receiver includes the ZigBee and Wi-Fi module management and the server management based on TCP/IP. After performing devices initialization, ZigBee module management task is performed. The functions of this task are setting up the ZigBee configuration and monitoring the ZigBee connection status. After confirming the ZigBee connection between the receiver and the transmitters, the sleep data from the transmitter are saved in a ring buffer. The Wi-Fi module management task configures the Wi-Fi module to connect to the access point. After connecting to the access point, an IP address is acquired from the access point. Finally, the server management task is executed after finishing the Wi-Fi module management task. The server management task enables the receiver to access the monitoring unit based on the TCP/IP and the receiver can start sending sleep data in the ring buffer to the monitoring unit or the server every 0.5 second. Figure 4.8 shows the data flow in the wireless receiver and Figure 4.9 shows the block diagram and image of the wireless receiver.

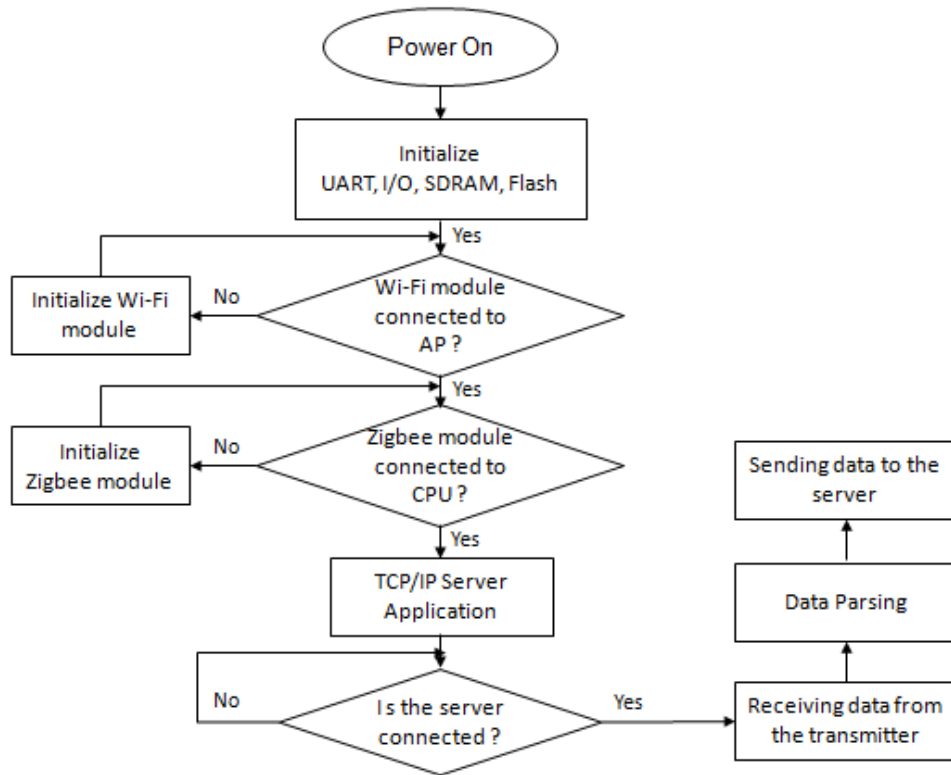
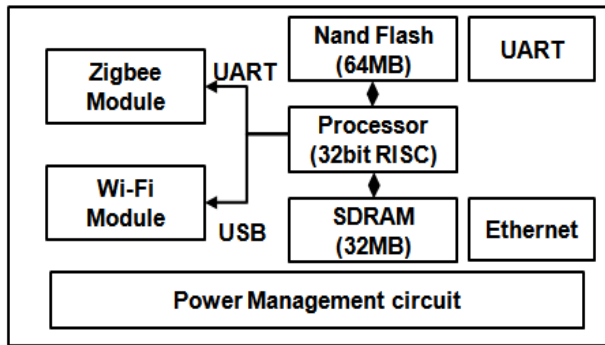


Figure 4.8 Data flow in the wireless receiver



(a)



(b)

Figure 4.9 Wireless HST receiver; (a) block diagram and (b) image

4.2.3.2 Device with GSM/WCDMA

The data acquisition/wireless device with GSM/WCDMA includes a microcontroller, a power management circuit and a GSM/WCDMA module. Figure 4.10 shows the block diagram of the system.

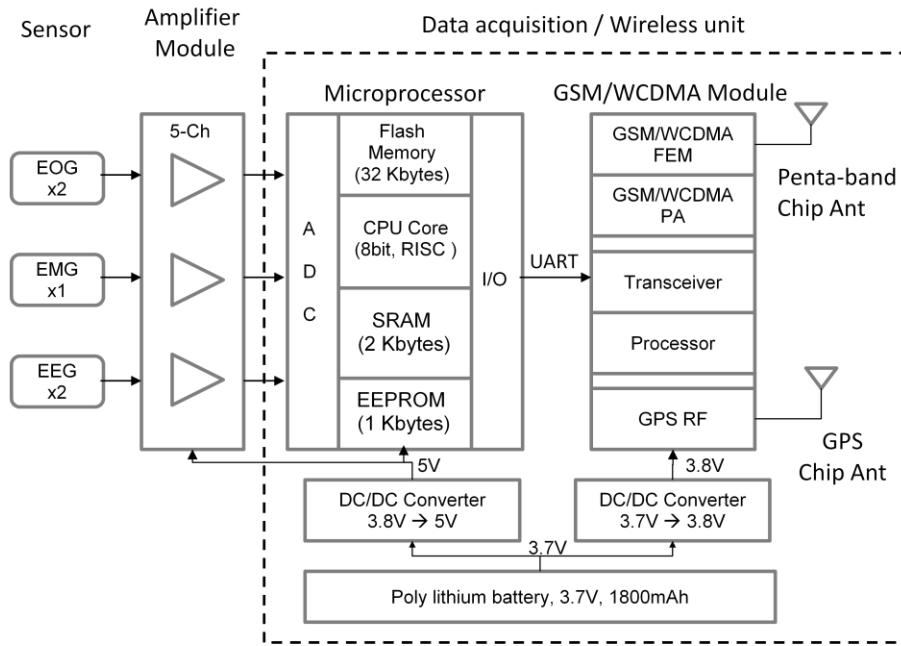


Figure 4.10 Block diagram of the data acquisition/wireless device with GSM/WCDMA

Microprocessor - The main functions of a microcontroller in the system are data acquisition and management of data flow to the GSM/WCDMA module. ATmega328P from Atmel is used as a microprocessor, which has 8-bit reduced instruction set computer (RISC) architecture, 32-kB flash memory, 2-kB SRAM, 8-channel 10-bit A/D converter and other peripherals. The operating voltage ranges from 1.8 to 5.5V and the operating voltage of the processor is set at 5V with a 16 MHz external resonator. The purpose of setting the operating voltage at 5V is to match the voltage level of the amplifier module. The signals from the amplifier module are sampled and

quantized by the A/D converter of the microprocessor. The data are saved to a buffer and then transferred to the GSM/WCDMA module through universal asynchronous receiver transmitter (UART) interface.

Power Management Circuit - A poly lithium battery with a current capacity of 1800 mAh and output of 3.7V is used as a power source. Because each block of the system operates at different voltage level, two DC/DC converters are implemented to step up to 3.8V and 5V. 3.8V is for the GSM/WCDMA module and 5V for the microprocessor and amplifier module. The DC/DC converters should not only provide operating voltage of the circuits but also deliver enough current to run the circuits. The DC/DC converter for the GSM/WCDMA module should guarantee that the input voltage of the module never drops below 3.3V even during transmission when the current consumption rises up to 2A, to prevent the module from being shut down. LTC3113 from Linear Technology is used as the DC/DC converter for the GSM/WCDMA module, which can deliver up to 3A of continuous output current and operate from input voltage above, below or equal to the output voltage. LTC1751-5 from Linear Technology is used to provide 5V to the amplifier module and the microprocessor. The DC/DC converter can produce up to 100mA at fixed 5V of output voltage. The DC/DC converter can operate only one flying capacitor and two bypass capacitors at input and output pins without an external inductor.

GSM/WCDMA Module - Mobile communication network is used instead of building local area networks to send physiological signals to the remote server. To connect the system to the mobile network, the GSM/WCDMA module, SIM5320 from SIM Com, is used. SIM5320 supports a quad-band GSM/GPRS/EDGE and dual-band UMTS/HSDPA [56]. The operating voltage of the module is set to 3.8V. The power from LTC3113 is supplied to the baseband and the RF power amplifier of the module. The ripple from the emission burst of GSM/GPRS, 2A of

current consumption, may cause voltage drop, which may lead to the shutdown of the module. Because LTC3113 delivers current up to 3A, the power supply of both the baseband and the RF amplifier are tied up to the output of LTC3113. A large capacitor (100uF) and by-pass capacitor is placed close to the input voltage pins of the module for the system stability and EMC. The turning on/off of the module is controlled by the power on/off logic in the module. The logic is pulled up internally and the logic operates at active low. The logic is pulled down to ground by an external resistor in circuit directly to turn on the module automatically when the main switch is on. The module communicates with the microprocessor over UART port. It consists of a flexible 7-wire serial interface. The module is referred as the data communication equipment (DCE) and the microprocessor as the data terminal equipment (DTE). The module supports both full modem and null modem topologies, and the null modem is used in the system. The baud rate of UART interface is set to 115,200 bit per second. The universal subscriber identity module (USIM) is implemented on the board for authentication and association with the mobile network. A transient-voltage-suppression (TVS) diode array is inserted between USIM and the GSM/WCDMA module for ESD protection. SIM5320 provides several general purpose input/output (GPIO) and the GPIO status is read or written with AT commands. One of GPIOs was used to indicate the network status with a light emitting diode (LED). The turn on/off intervals of LED represents the status of network; power on/searching network, data transmit, network registration and power off. The module supports a quad-band of GSM 850 MHz, EGSM 900 MHz, DCS 1800 MHz and PCS 1900 MHz and dual-band of WCDMA 850 MHz and 1900 MHz. A penta-band SMD antenna, Reflexus form Antenova, is used to cover all frequency bands. The average gain is -1.3 dBi for the 824-960 MHz and -1.5 dBi for 1710-2170 MHz. A microstrip line which has impedance of 50 Ohm is designed as a transmission line between the

module and the antenna. A matching circuit is placed on the transmission line and a separate DC blocking capacitor is added between the module and the antenna matching circuit. The antenna is placed on the corner of the board to achieve maximum antenna performance. The module supports both assisted GPS (A-GPS) and simultaneous GPS (S-GPS), and then provides three operating modes; mobile-assisted mode, mobile-based mode and standalone mode. A ceramic passive chip antenna, W3011A form Pulse Electronics, is used to receive the position information at GPS L1 frequency (1.575 GHz). Figure 4.11 shows the schematic of GSM/WCDMA circuit.

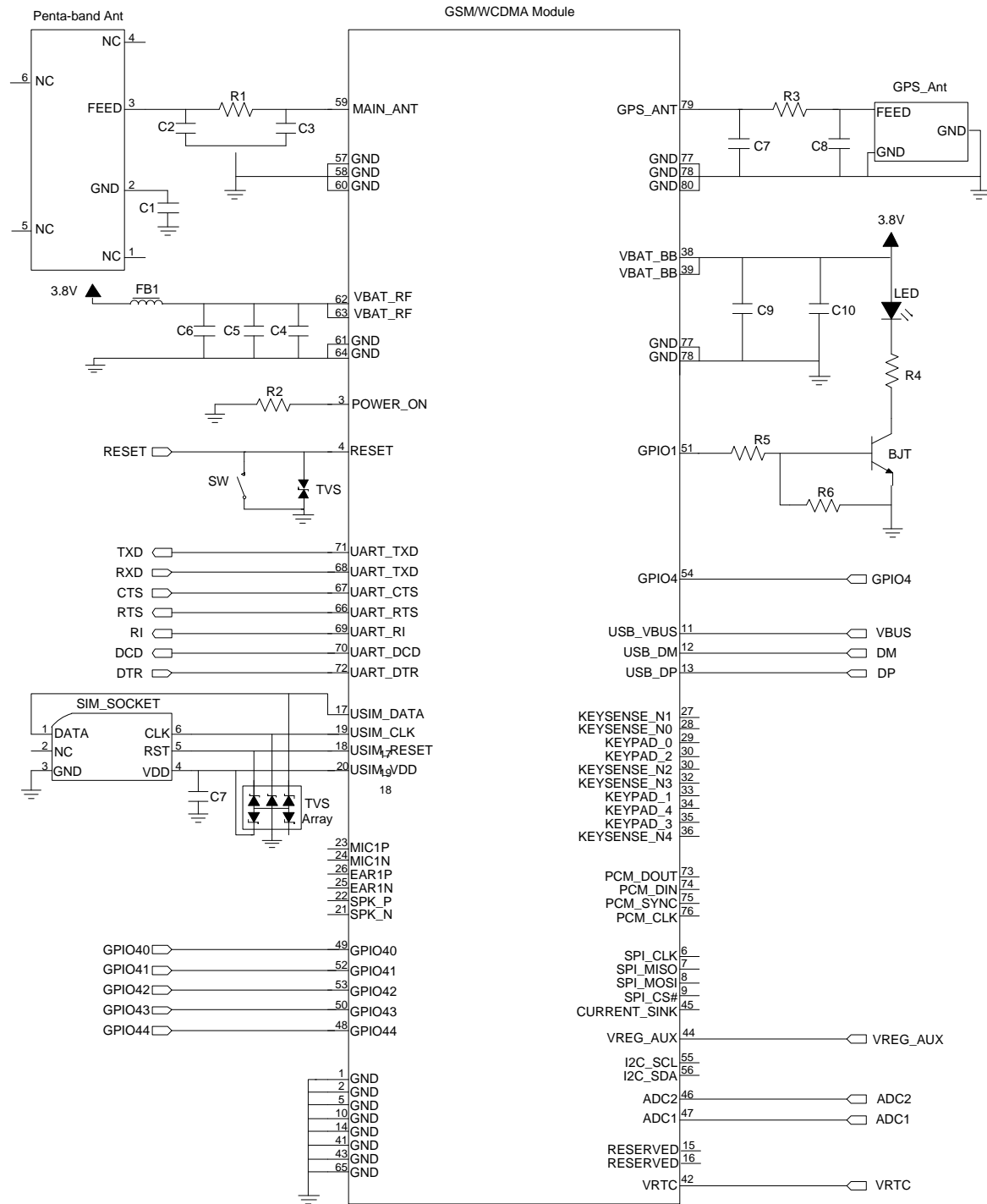


Figure 4.11 Schematic diagram of the GSM/WCDMA circuitry

The amplifier module, the processor board, the DC/DC circuit (LTC1751-5) and the battery are stacked on the back side of the GSM/WCDMA board. Figure 4.12 shows the images of top and bottom side of the system. The connection between electrodes and the amplifier module is made by snap button type of adaptors.

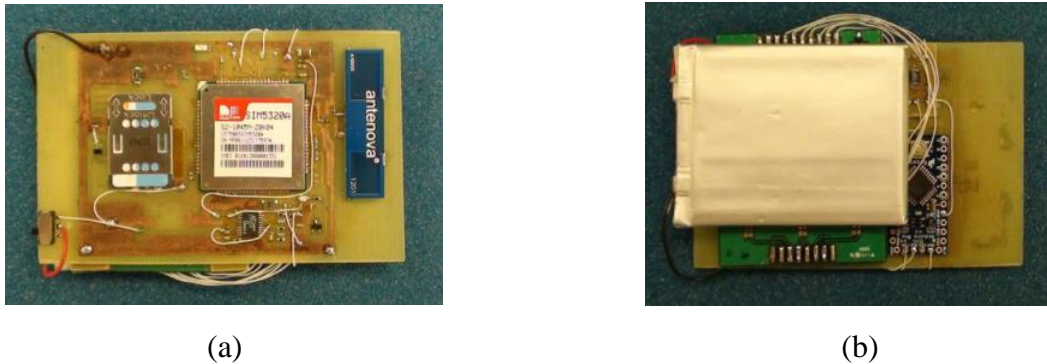


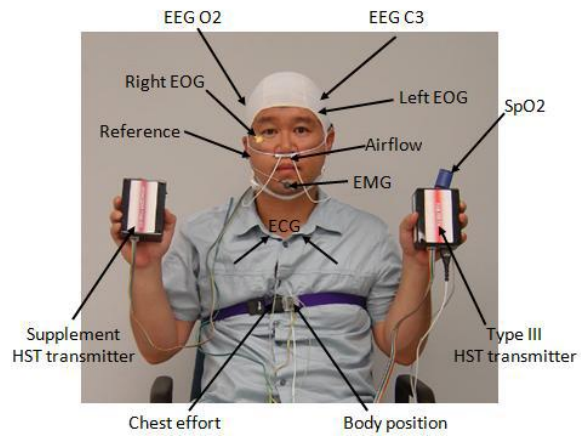
Figure 4.12 Images of the wireless HST system with GSM/WCDMA; (a) top and (b) bottom side of the system

4.3 System Evaluation

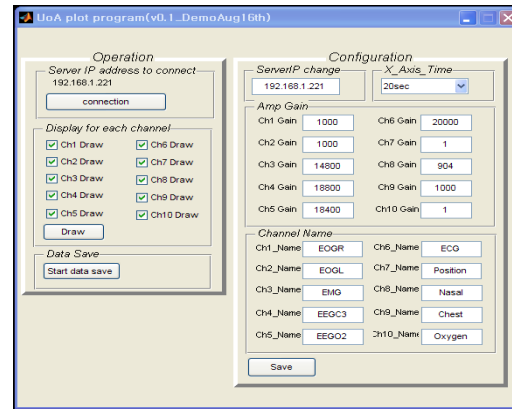
Experimental tests were performed to verify feasibility of the wireless HST system with ZigBee/Wi-Fi and with GSM/WCDMA.

Regarding to the system with ZigBee and Wi-Fi, in particular, the tests were performed to examine whether each transmitter can send the sleep data to the receiver without loss through the ZigBee star network, thereby verifying the feasibility of channel extension through wireless. The five different types of sensors were placed on the body for the wireless type III HST device. Two gold nanowire electrodes were attached to the left and right upper chest, the position of lead I ECG. A chest belt equipped with a piezoelectric sensor and a gyroscope were worn to measure the chest respiration effort and the body position. The nasal prongs including the pressure sensor

were placed in the nostrils to monitor the nasal airflow. Finally, the oximeter sensor was clipped on to the fingertip to measure SpO₂. For the wireless supplementary HST device, the gold nanowire electrodes were used to detect the three different types of the biopotential signals, EOG, EMG and EEG. The reference electrode to measure the differential biopotential signals was placed on the left ear lobe. Two electrodes were placed on the left upper and right lower side of the eyes to measure 2-channel EOG. With these positions of the electrodes, movements of the left and right eye ball produce the opposite polarities of left and right EOG. One of electrodes was placed on the chin to measure EMG and to detect grinding of teeth or mouth movement. The last two electrodes were placed on C3 and O2 position on the scalp according to the international 10-20 system. Figure 4.13 shows an image of a subject under sleep study with the proposed system and the GUI of the monitoring utility program. The 5-channel signals from the type III device and other 5-channel signals from the supplementary device were recorded and monitored in real time with the utility program at the monitoring unit/ the server under different test conditions. The test condition was established to classify the changes of physiological signals. P, QRS complex and T waves should be identified in ECG. Body position was measured as the subject moved. The chest effort and nasal airflow were monitored under no breathing, to emulate sleep apnea, fast breathing and normal breathing. In case of EOG, five different types of eye motions, blinking, left, right, up and down movement of eyeballs, were tested to emulate REM and wakeful sleep stage. EMG was produced by the movement of the chin. The EEG acquisition performance was verified by discerning between beta waves and alpha waves. The beta waves are associated with normal waking consciousness and the alpha waves with wakeful relaxation with eyes closed. By opening and closing eyes alternatively, the changes of brain waves were examined.



(a)



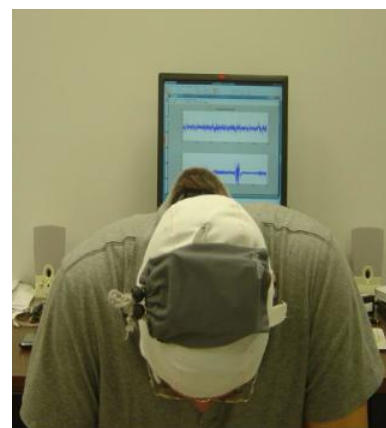
(b)

Figure 4.13 Experimental test set-up for the system with Zigbee and Wi-Fi; (a) image of a subject under experiment and (b) GUI of the monitoring utility program [86]

Regarding to the system with GSM/WCDMA, the electrodes were placed on the same positions as the supplementary HST device to monitor EOG, EEG and EMG, and test method is also same as the method involved in the supplementary HST device because the function of the system is same as that of the supplementary device with ZigBee and Wi-Fi. Figure 4.14 shows experimental test set up to evaluate the system with GSM/WCDMA.



(a) front view



(b) top view

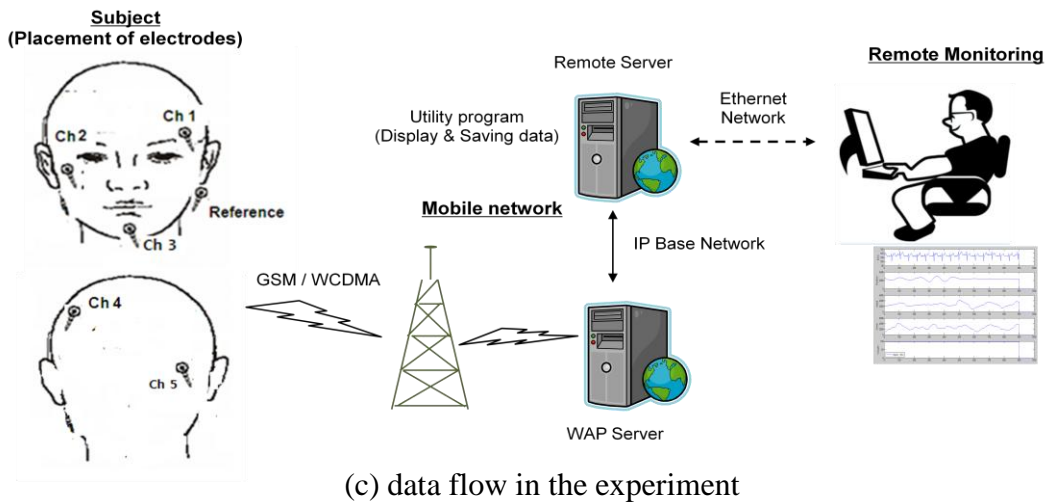


Figure 4.14 Experimental test set up for the system with GSM/CDMA [88]

Figure 4.15 shows the waveforms of each physiological signal which were measured with the type III HST device and recorded to the server. Figure 4.15(a) shows the measured lead I ECG. The ECG waves show the P wave, QRS complex and T waves clearly. Generally, the components of ECG, P wave, QRS complex, T wave, PR interval and QT interval are used to diagnose heart conditions. Furthermore, heart rate variability (HRV) is derived with the components of ECG and HRV might be used to diagnose sleep apnea. Figure 4.15(b) shows the waveforms from the gyroscope according to the three levels of body motion: no motion, slow motion and fast motion. Corresponding to the body movements, the output voltage of the gyroscope changed. The positive or negative slope of the waveforms represents the direction of rotation of the subject and the output voltage of the gyroscope reveals the velocity of the body movement. Based on the sensitivity of the sensor and the polarity of the slope, the velocity of the body movement is derived. By analyzing the waveform from the gyroscope, it can be diagnosed that how often and how much the subject moves during sleep. Chest respiration effort and nasal

airflow were also measured under three different types of breathing. Positive and negative slope of the waveforms means inhalation and exhalation, respectively. Respiration cycles can be discerned by tracking the positive and negative slopes. In addition, the frequency of the waveforms is related to the speed of breathing. Oxygen saturation is derived from the output of the oximeter sensor, amount of transmission of the IR and RED LEDs through fingertip. The monitoring utility program displays the derived SpO₂ instead of displaying absorption coefficient of the IR and RED LEDs.

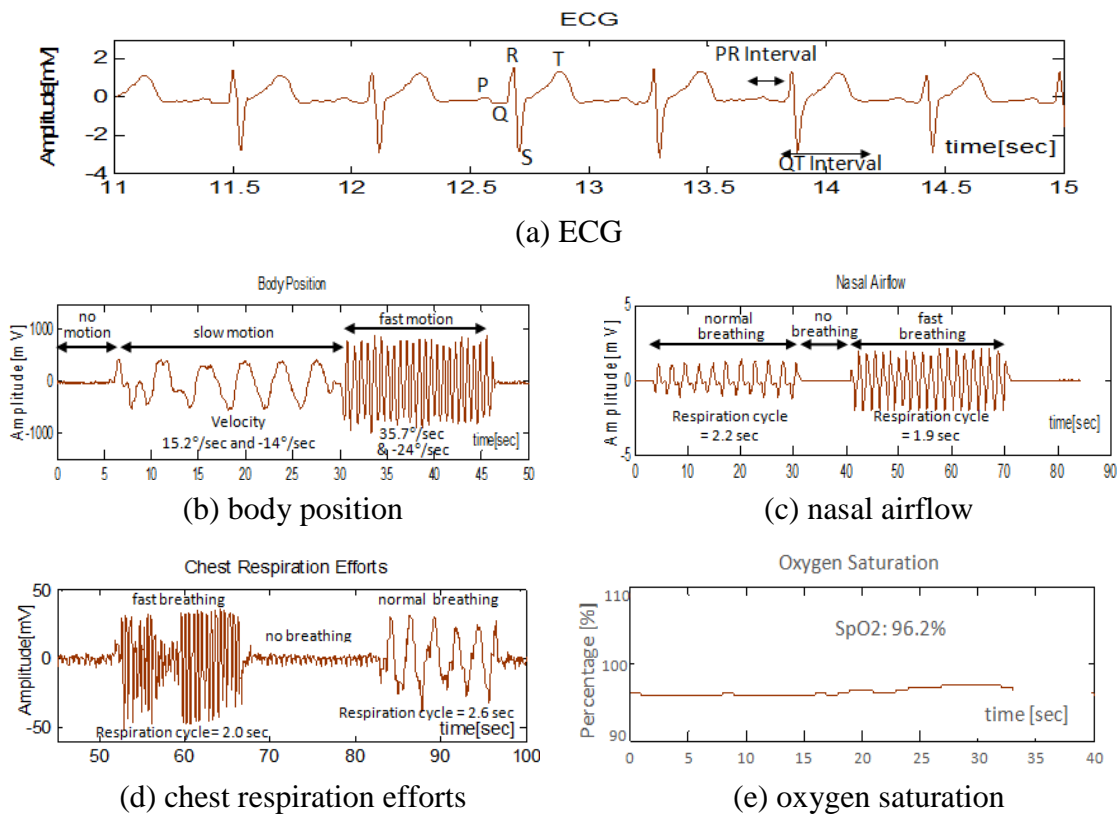


Figure 4.15 Monitored physiological signals from the wireless type III HST device

Figure 4.16 shows the recorded biopotential signals from the supplement HST device. The EOGs from left and right eyes are classified with five different movements of eyeballs. The left

and right EOGs show opposite polarity of slope due to the placement of the electrodes over the reference electrode. The blinks are represented by the sharp and high peak amplitude due to the nature of the quick eye motion while left, right, up and down movement of eyeballs are represented by wider slower waveforms. The waveforms, representing EMG, show low amplitude and flat baseline when the chin is at rest, but the waveforms are changed to high amplitude and high frequency ones during movement of chin. EEGs from C3 and O2 positions show mixed brain waves of beta and alpha waves when eyes are opened, but alpha waves are dominant when eyes are closed. EEG from position O2 shows more strong alpha waves than from position C3 even though both the channels of the amplifier are set to the same gain. It verifies that the alpha waves predominantly originate from the occipital lobe during wakeful relaxation with closed eyes.

Each HST device is operated with the receiver simultaneously by building the ZigBee star network. There was no data loss in the monitoring unit/ server due to interference between the two HST devices. Therefore, the wireless type III HST device could be upgraded to type II HST device by adding 5 channels of biopotential signals which are measured with the supplement HST device.

Figure 4.17 shows the monitored biopotential signals from the system with GSM/WCDMA. They show the similar waveforms of those of the supplement device with ZigBee/Wi-Fi under the same test conditions for each physiological signal, EOG, EMG and EEG.

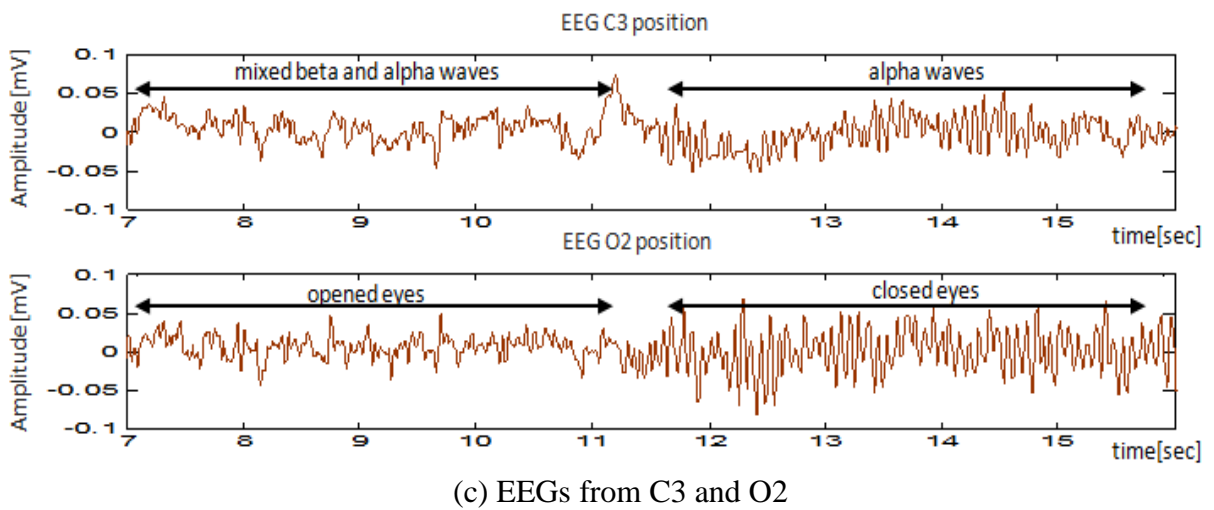
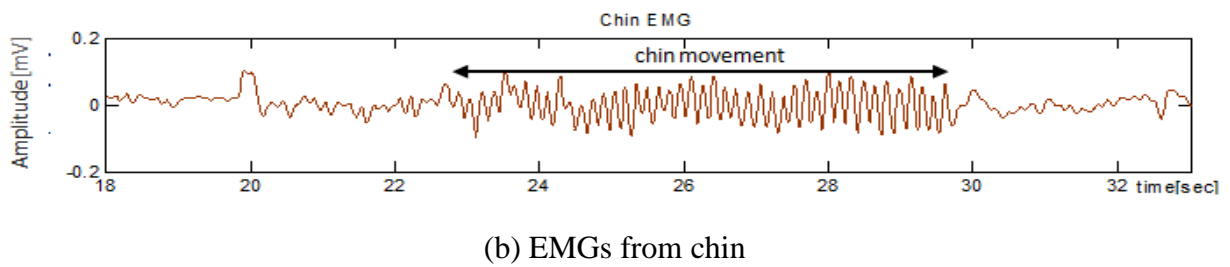
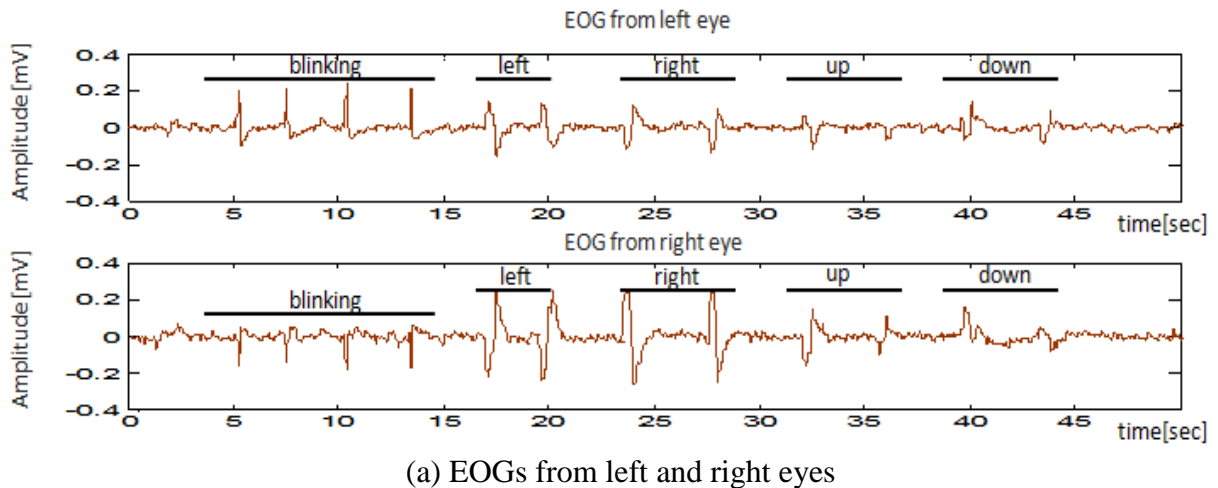
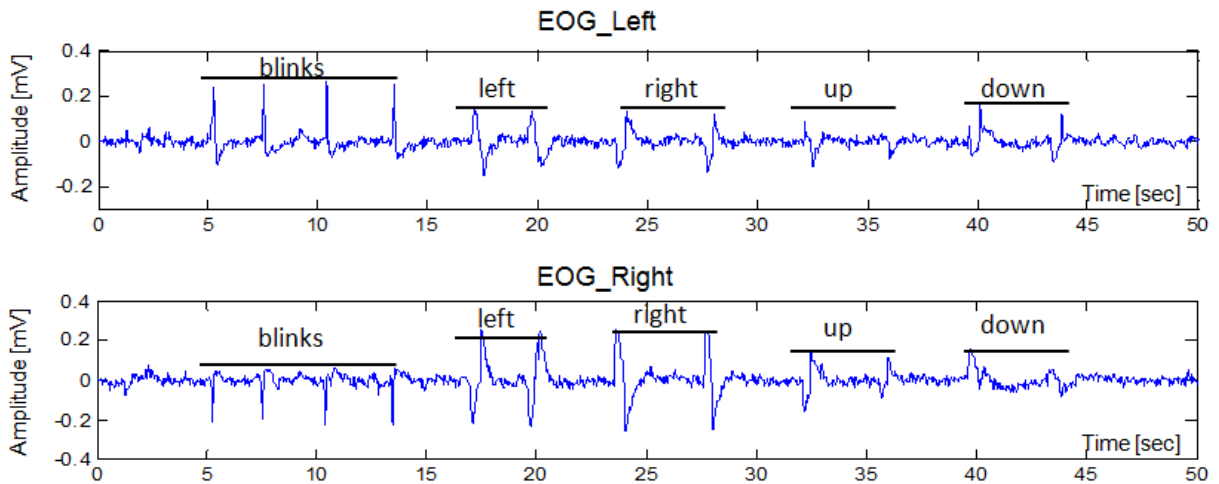
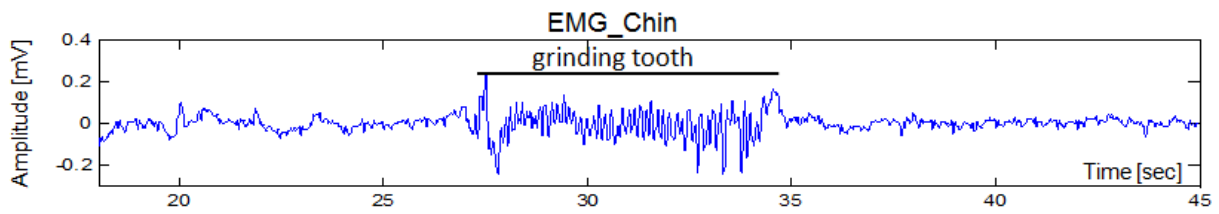


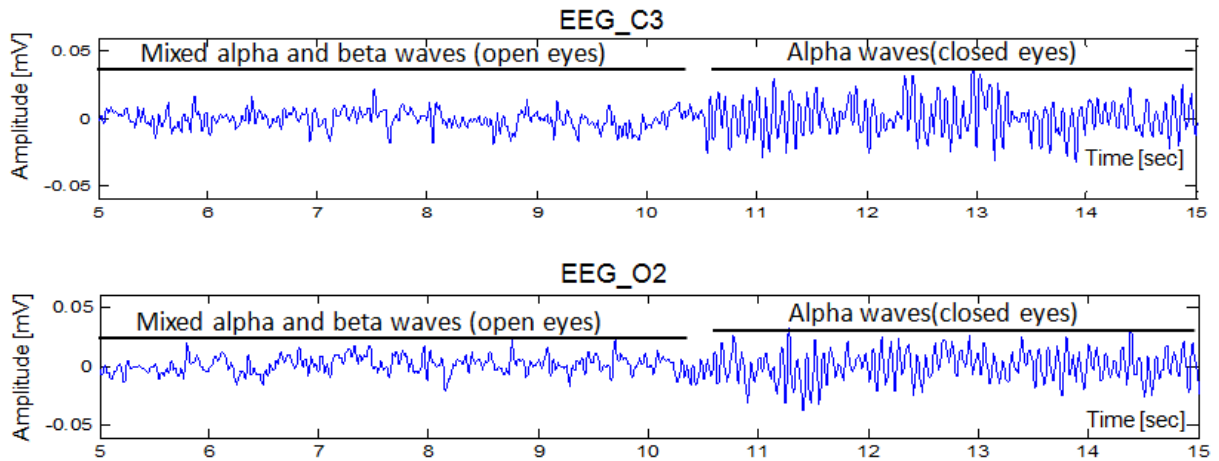
Figure 4.16 Monitored physiological signals from the wireless supplement HST device



(a) EOGs from left and right eyes



(b) EMGs from chin



(c) EEGs from C3 and O2

Figure 4.17 Monitored physiological signals from the system with GSM/WCDMA

4.4 Conclusion

The wireless HST devices and systems based on ZigBee and Wi-Fi network have been demonstrated to overcome the drawbacks of the current HST systems. The proposed system addresses the need for the cost-effective extension of the number of channels to measure supplementary physiological signals and efficient extension of network to provide remote monitoring in real time. The overall architecture of the system/network has been described. A wireless type III HST device is upgraded to a type II HST device by building a ZigBee star network with the other wireless supplementary HST device. In addition, the wireless receiver, as a coordinator in the network, receives sleep data from each HST device/transmitter with ZigBee and retransmits the data to the remote server over Wi-Fi. The combination of two wireless platforms enables WPAN of ZigBee to be extended to WLAN with the help of Wi-Fi. An experiment was performed to verify the system/network. The physiological signals under different conditions were sensed and transmitted to the receiver with the type III and supplement HST devices simultaneously. Signals were successfully monitored and recorded at the server in real time through the wireless HST receiver. In conclusion, this work reflects the development of the wireless HST system/network to achieve continuous remote monitoring and provide a cost-effective and efficient solution to diagnose sleep disorders.

In addition, another wireless HST system with GSM/WCDMA network was developed to evaluate sleep stages. The system supports monitoring/recording five different signals, EOGs from left and right eyes, EMG from the chin and EEGs from C3 and O2 positions. The processed physiological signals with the microprocessor are transferred to the GSM/WCDMA module with UART interface and transmitted to the remote server through the mobile network. By using the mobile network instead of building local area network, the system can send signals regardless of

places and the physiological signals can be monitored in real time at any place. The small platform of the system enables the system to be placed on top of the skull cap, which gives a patient free movement and comfort. An experiment was performed to verify the system. EOG, EMG and EEG which would appear during sleeping were measured, and the system classified the changes of the waveforms with different movements of eyeballs and the chin. The beta and alpha waves were monitored when eyes were opened and closed alternatively. As a result, the system can discriminate sleep stages and can be utilized for diagnosing sleep disorders.

Chapter 5: Real-time Wireless Cardiac Monitoring of Football Players on the Field

5.1 Introduction

The sudden death of an individual resulting from a sudden failure in heart function is referred to as Sudden Cardiac Death (SCD). Rigorous exercise increases the risk of SCDs in young athletes with underlying cardiovascular disorders (CVD) [57]. A recent study has shown that up to 82% of individuals who succumbed to SCD were engaged in strenuous exercise during or immediately before the incident. Nearly 58% of SCDs reported between 1980 and 2006 have been reported in basketball and football athletes. Recent studies have shown that the incidence of SCDs in young athletes in the US at the high school and college level have been underestimated in previous studies [58]. All of the data available thus far on SCDs have been through retrospective studies involving news reports, internet databases and subjective accounts. Albeit illuminating, it is important to note that these studies are inevitably under representative of the real scale of the problem.

The most prevalent causes of SCD in young athletes are CVDs and sports related injuries. Among CVD causes, the most prevalent are Hypertrophic Cardiomyopathy (HCM) (36% of cases) and coronary artery diseases (CAD) (17% of cases). Among sport injuries, Commotio Cordis and blunt trauma injuries together account for 25% of all SCDs recorded between 1985 and 2006 [58]. The current strategy for the prevention of SCDs in young athletes is to prescreen them and diagnose any cardiovascular diseases that may put them at high risk for SCDs, and promptly disqualify them from participation if diagnosed. The proven approach implemented in Italy has involved a mandatory prescreening with detailed history, physical examination and a 12 lead ECG with guidelines and criterion for identification of cardiovascular abnormalities that

may put the athlete at high risk for SCD [59]. The American Heart Association (AHA), however, does not currently recommend the inclusion of 12 lead ECG as a part of the prescreening [60-62] due to several reasons - high direct costs of the tests, lack of dedicated trained athletics personnel to perform the prescreening in place of physicians, sheer number of athletes to be screened and reported low specificity, high false positives and false negatives of ECG interpretations [63]. Although the positive diagnostic value of including a 12 lead ECG to the prescreening has been identified by both the European society of Cardiology (ESC) and the AHA [64, 65] consensus panels for recommendations on cardiovascular screening of young athletes, the cost-effectiveness of including a 12 lead ECG to the US athletic prescreening protocol is still a subject of wide debate.

Despite the evidence suggesting the effectiveness and initial success of the prescreening with ECG in Italy [59], there are four limitations to the prescreening approach that need to be addressed:

First - There is still wide debate on the differential diagnosis of HCM from the ECG changes brought on by training in many athletes with otherwise normal hearts (athlete's heart) [66, 67]. Reported differences in training induced cardiac remodeling between athletes of African origin and others have made diagnosis based on ECG findings equivocal [68]. Moreover, the remaining two prevalent causes for SCD (CADs and blunt trauma injuries) cannot be diagnosed during prescreening as CADs do not manifest as ECG abnormalities and blunt trauma injuries are non-pathological and can occur to any athlete with an otherwise healthy heart.

Second – Recommendations [69] suggest that for differentiation of HCM from athlete's heart, Brugada-like ECG abnormalities, arrhythmogenic right ventricular cardiomyopathy or dysplasia

and features like prolonged PR intervals, short PR intervals, early repolarization and inverted or biphasic T waves can be further evaluated using an exercise test to improve specificity. However, this is to be done in addition to the preliminary ECG screening at an added cost.

Third – From the perspective of secondary prevention i.e. through the adoption of strict guidelines on Sudden Cardiac Arrest (SCA) resuscitation, it is imperative that an SCA is promptly recognized, cardiopulmonary resuscitation (CPR) is started immediately and a defibrillating shock is applied as soon as possible [70]. The target resuscitation time recommended by the AHA is between 3-5 minutes, from the time the athlete's collapse was witnessed to the application of the defibrillating shock. It has been shown that survival chances may drop by 7-10% for every minute that defibrillation is delayed. In the absence of a real-time ECG, the emergency responder or rescuer has to first identify an SCA with accurate pulse or respiration assessments while the athlete may be gasping or having myoclonic jerks or seizure-like activity that may be inconsistent with SCA.

Fourth – The various mechanisms for SCD have been studied extensively at the cellular process and ionic channels level [71]. This work needs to be augmented with real-time studies on the mechanism of SCD using non-invasive techniques like ECG, which are lacking. The ECG is rarely or never available during a sudden cardiac arrest episode. Therefore, a system for the real-time monitoring of cardiac electrophysiology during exertion, which put the athletes at higher risk of SCDs, is an important step in the prevention and treatment of sudden cardiac arrest in athletes.

In this chapter, a fully wearable real-time ECG acquisition system with wireless transmission of data for the continuous monitoring of football players during training and on the field is

proposed. The case for football players was chosen because of the high incidence of SCDs in football players. Moreover, the protective gear worn by them offers several design options for both the concealment and protection of the electronic components, so as to not hinder the performance of the player in any way. Dry textile sensor electrodes are stitched into the football player's base layer compression vest. Conductive inks are used to draw traces from the electrodes and they are connected to the amplifier and wireless transmission module embedded in the player's shoulder pad.

5. 2 Research Objectives

The objective is to design and implement a system that can be used to monitor the ECG of football players in real-time during a training session or during a game [89]. The system design was formulated to optimally satisfy three criteria. *First*, the quality of signals acquired. This determines the choice of sensor electrodes for ECG, printed traces on the athletic base layer compression vest that connect the sensors to the wireless communication module and the hardware design for signal amplification and filtering for noise removal. It is important to note that the ECG signals acquired from the vest need to be of diagnostic grade so that they can be compared with ECG acquired using conventional pre-gelled Ag/AgCl electrodes.

Second, the functionality of the system, in terms of modalities of signals acquired. This addresses a trade-off between maximizing the number of sensors required to acquire all the diagnostically important vital biomedical signals, and maintaining signal accuracy and the overall usability of the system that does not interfere with the athlete's performance. In a conventional hospital setup for 12 lead ECG measurements, the Ag/AgCl electrodes can be placed at precise locations specific to the patient's anatomy. However, garments being flexible

and elastic, it is not practical to expect the same level of reproducibility as a clinical ECG in terms of electrode positioning. Therefore, in this chapter a reduced set of the 12 lead ECG namely, lead I, II, V1, V2 and V5, has been used. This reduced set of leads was chosen based on the recommendations in [69], summarized in Table 5.1. An electrode at the V1 position to gain perspective of the left atrium activity, V2 to gain perspective of the right atrium activity and an electrode spanning V5 for ventricular activity. It is well known that the full frontal ECG consisting of the Limb leads and the augmented limb leads (aV_F , aV_R and aV_L) can be algebraically derived if any two pairs among Lead I, II and III signals are known. The full frontal ECG is required to determine the QRS axis deviation.

Third, the Quality of Service (QoS) offered by the wireless communication module. This determines the extent of sensor data (in this case, ECG) loss during transmission from the football player to the receiving station due to intermittent wireless connection loss. This type of sensor data loss manifests as abnormal ECG waveforms when the actual athlete's heart function might be normal. These incidences if not identified and either excluded or corrected will lead to false positive diagnoses. Therefore, it is important to maintain good QoS within the range of the football field for all players. The system has to ensure continuous connectivity and availability of diagnostic data from all 11 players on the field, all the time.

The schematic in Figure 5.1 shows the desired overall system implementation in terms of monitoring of football players on the field.

ECG wave feature	ECG leads of interest	Criteria according to ESC [72]	Criteria according to Uberoi et al [69]
Q waves	I, II, III, aVF, aVL, V5, V6	>4mm depth (0.4mV) below isoelectric	>3mm depth (0.3mV below isoelectric) and/or >40ms in aVR, III, V1
ST depression	I, aVL, V5, V6	Further evaluation for any ST depression	>0.5mm (0.5mV) below isoelectric between J-junction and T wave onset >1 mm in any lead
T wave inversion	I,II,III, aVF, aVL, V2, V3, V4, V5, V6	Further evaluations for >2mm (0.2mV) inversion. I, II, III, aVF, aVL, V5, V6.	>1mm (0.1mV) in I, II, aVF, aVL, V3-V6 non-African origin athletes. In athletes of African origin, inversion without ST elevation in leads of interest
Atrial abnormalities	II,V1,V2	Same as Uberoi et al [69]	V1,V2 – negative portion of P wave <40ms and 1mm (0.1mV) depth, total P wave duration >120ms II – P wave amplitude >2.5mm
Right Ventricular Hypertrophy	I,II,III,aVL,aVF,V1, V2,V3,V5,V6	Same as Uberoi et al [69]	>30 years , then V1- R wave greater than 7mm (0.7mV) ,R/S ratio>1 V1,V5,V6 – sum of R wave in V1 and S wave in V5 or V6 > 10.5mm(1.05mV) <30 years, right atrial enlargement, V2,V3 – T wave inversion or II - right axis deviation >115°
Left Bundle Branch Block (LBBB), Right Bundle Branch Block (RBBB), Intraventricular Conduction Delay (IVCD)	I,II,III,aVR,aVL,aVF ,V1,V2,V3,V4,V5,V6	Same as Uberoi et al [69]	QRS > 120ms
QRS axis deviation	I,II,III,aVR,aVF,aVL	Not specified	Leftward <-30°, Rightward >115°
QT _c interval	II,V5	Any athlete <380 ms or >500ms, Males 440ms – 500ms, Females 460ms – 500ms	Males >470ms ,Females > 480ms, Any athlete < 340ms

Brugada pattern	V1,V2	Downsloping ST-segment with a ST_J/ST_{80} ratio > 1	Coved ST segment gradually descending into an inverted T wave
Pre-Excitation	II	Same as Uberoi et al [69]	Delta Waves and PR interval $< 120ms$
Ventricular extrasystoles, heart block, and supraventricular arrhythmia	I,II,V1,V2	Not specified	Atrial fibrillation/flutter, supraventricular tachycardia > 1 premature ventricular contraction in a single 12 lead recording.

Table 5.1 Summarization of 12 lead ECG prescreening parameters

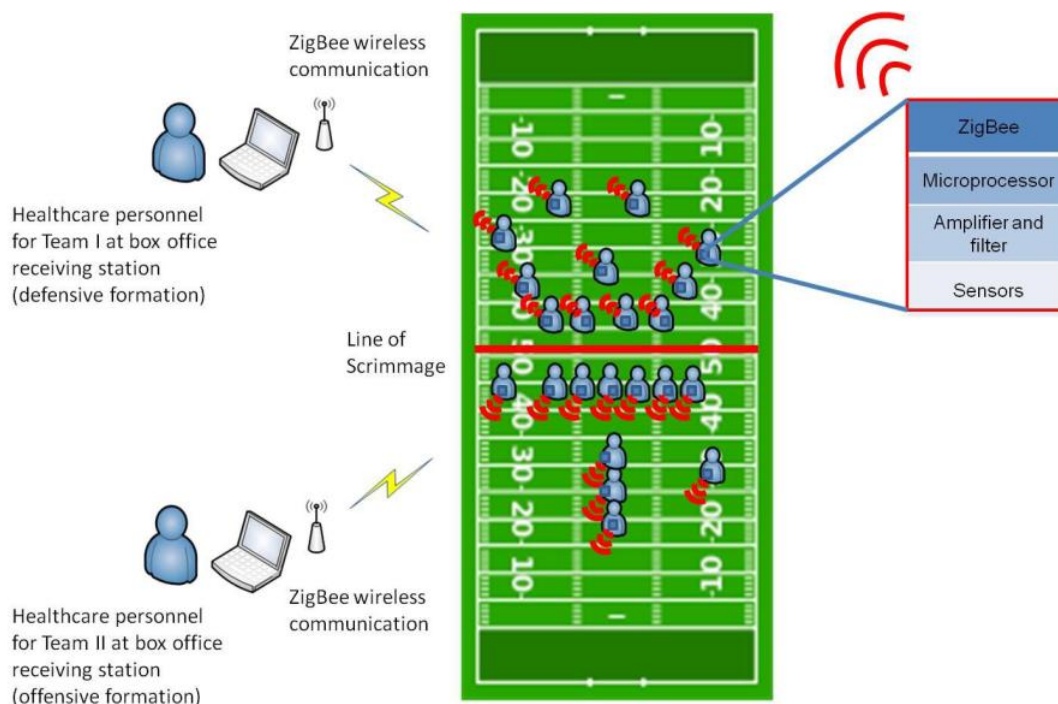


Figure 5.1 Schematic of the overall implementation of the football player monitoring system

5.3 System Implementation

The system consists of three components: – (1) The sensor platform which is the base layer compression vest with the electrode sensors and the printed connection traces worn by all

football players. (2) The wireless module that consists of the amplifier and signal conditioning circuits, a microcontroller and the ZigBee wireless radio. (3) The software at the receiving station that plots the incoming data from the football players.

5.3.1 Sensor Platform

The wearable ECG platform was fabricated as a vest with dry textile based electrodes [73]. Conductive tracks were printed on the vest fabric to connect the ECG electrodes to a centralized amplification and transmission electronics. The inks for conductive tracks were formulated with silver nanoparticles and elastic acrylic based binder to obtain a flexible nanocomposite trace compatible with the fabric [74]. The ink formulation was printed on to the fabric using screen printing technology. The transmission electronics were housed in the protective shoulder pads worn by the athlete over the vest. The connections between the amplification-transmission electronics and the conductive traces were made with metalized snap buttons. By design, the snap button allows the athlete to make connections after wearing the shoulder pad. Figure 5.2 shows the actual base layer vest used for testing and the wireless communication module mounting on the shoulder pad.

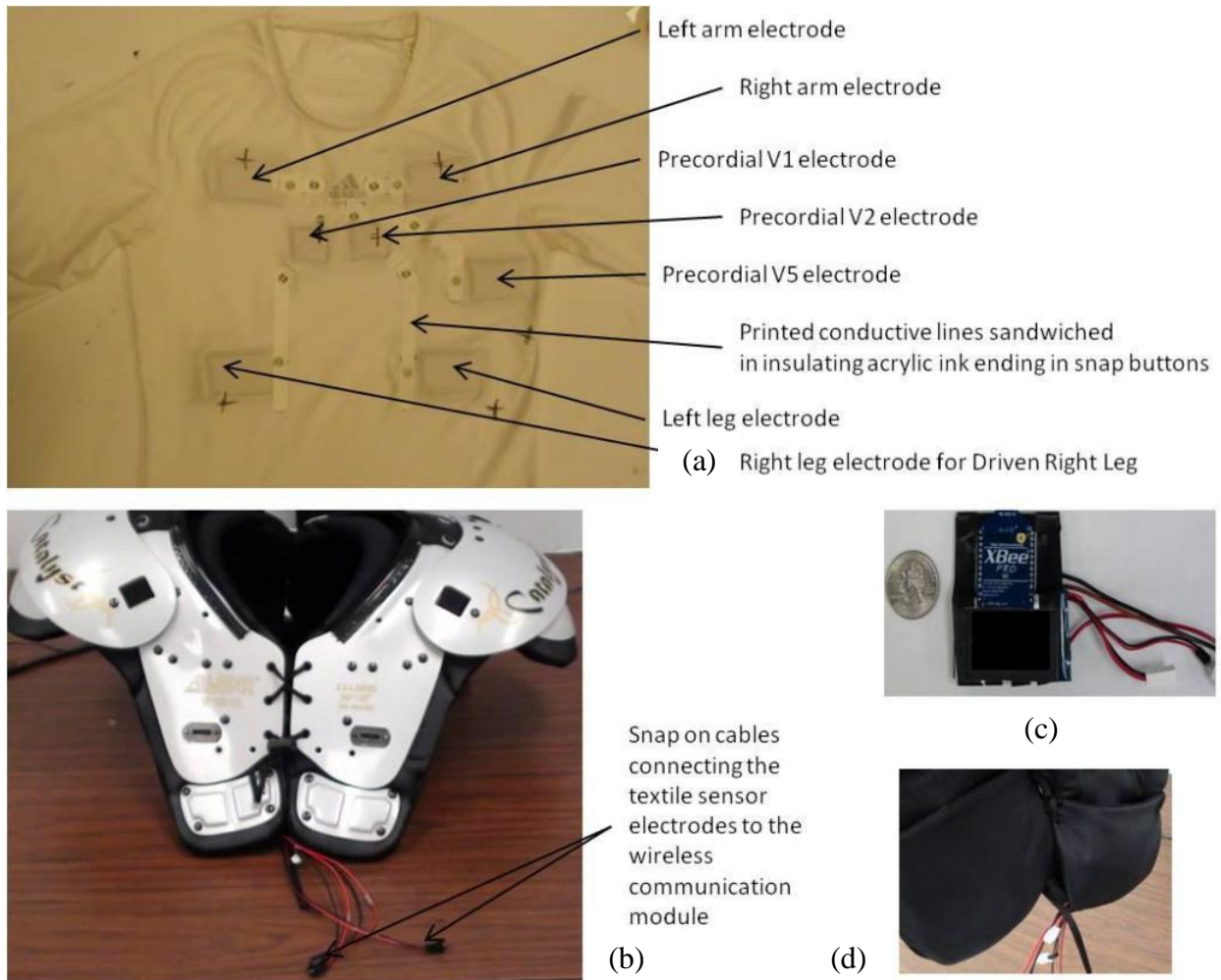


Figure 5.2 (a) Compression base layer vest with sensor electrodes and printed traces, (b) protective shoulder pad with snap on connection cables to connect sensors to wireless module, (c) wireless module with 5 channel amplifier and ZigBee module and (d) wireless communication module placed in a pocket on the interior of the shoulder pad

5.3.2 Wireless Module

The analog ECG signals acquired through the textile electrodes need to be amplified, digitized and transmitted wirelessly. The overall schematic of the wireless module is as shown below in Figure 5.3.

5.3.2.1 Amplifier and Microcontroller

As mentioned previously, five ECG signals are acquired using the wireless module. Two are bipolar limb leads and three are unipolar precordial leads (V1, V2 and V5). The bipolar limb leads, lead I and II are acquired between the Left arm and right arm electrodes, and the right arm and left leg electrodes respectively. The average potential from the three electrodes referred to as the Wilson central terminal is generated and used as a reference for the three precordial signals. The amplifier and filter used in this system had a pass band of 0.2Hz to 70Hz and a gain of 50 dB. The three stage amplifier consisting of an instrumentation amplifier, two operation amplifiers, and the Wilson central terminal generation circuit schematics are shown in Figure 5.3. The amplified signals are then digitized using the onboard Analog to Digital Converter (ADC) on the ATMEL ATMEGA328P microcontroller (Atmel Corporation, San Jose, CA).

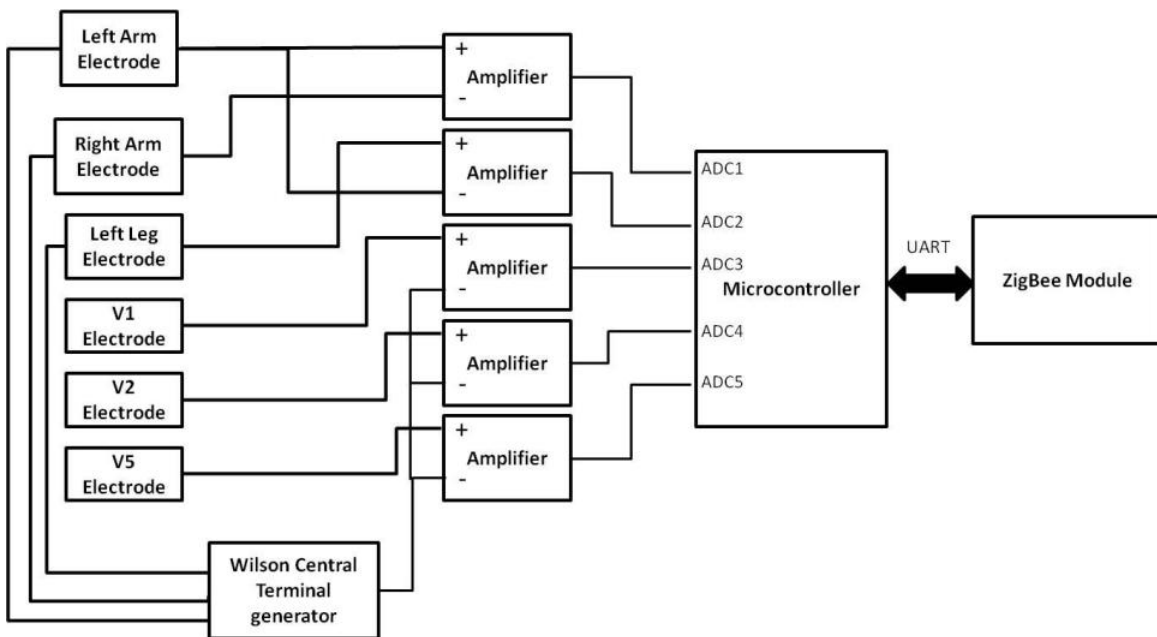


Figure 5.3 Schematic of the wireless module

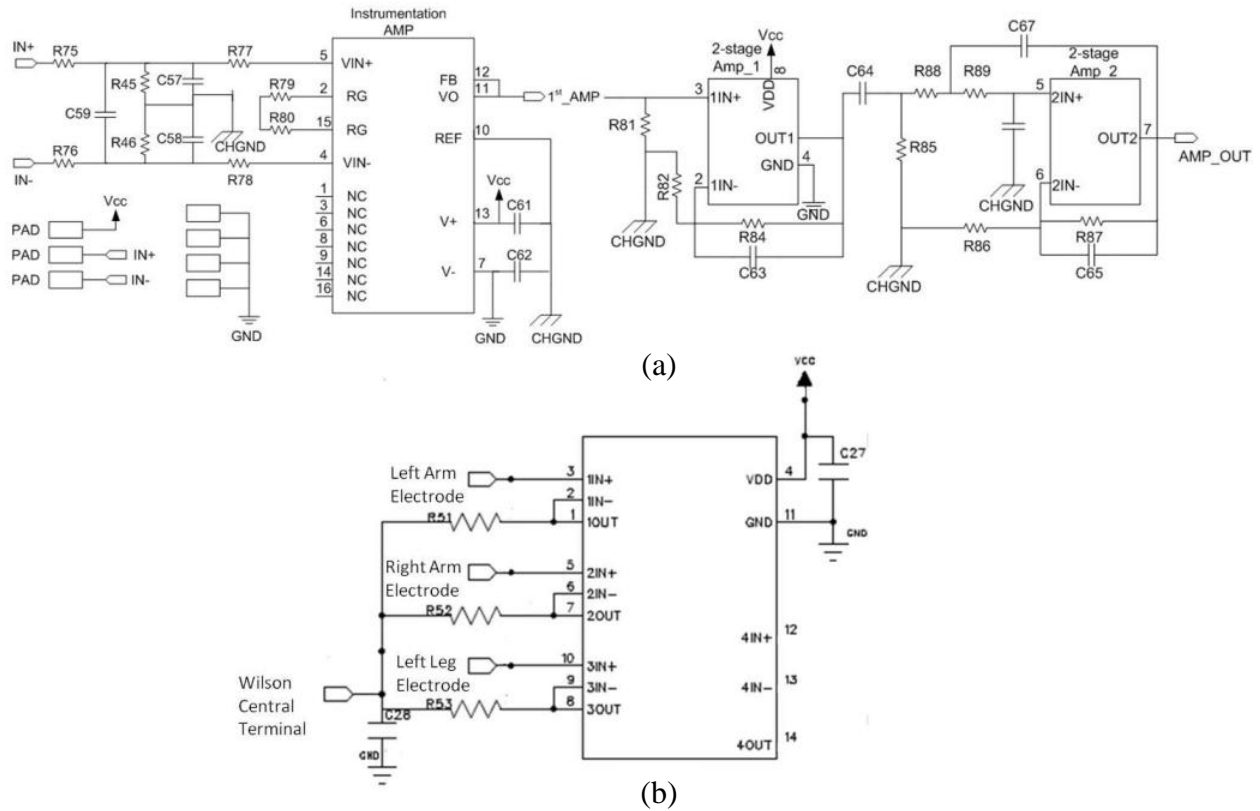


Figure 5.4 Schematic of (a) the 3 stage amplifier and (b) the WCT generation circuit

5.3.2.2 Wireless Module - ZigBee

The wireless module chosen for this implementation was 2.4 GHz XBee-PRO® (Digi international, Minnetonka, MN). This module has a range of up to 1 mile with line of sight, outdoor. Therefore, this module is more than sufficient to offer good QoS over the distance between the box office or the sideline and the football player on the field.

5.3.3 Software Implementation

The software to receive, plot and store the received ECG signals was developed using MATLAB (Mathworks, Natick, MA). In addition to the signal acquisition function an active

real-time motion artifact removal algorithm was also used to minimize the effect of motion on the baseline of the ECG signal. This algorithm is described in our previous work [79].

5.4. Adaptive RF Output Power Control

Normally, in the present communication systems for WPAN and WLAN, the output power is not varied according to the transmission distance. This requires a constant and steady power supply. Adaptive RF output power control algorithm implements a concept of controlling the RF output power with respect to the transmission distance involved in the process of communication. Thereby, reducing the power consumption when the distance between the transmitter and receiver is reduced. It is based on the received signal strength indicator (RSSI). RSSI is the measurement of power present in the signal received in the receiver.

The transmitter and receiver are initialized when the system is turned on. The analog data is converted by the processing unit in the transmitter and the data is buffered. The transmitter starts transmission when the buffer is full. After the transmission process is initiated and the data is transmitted to the receiver, the receiver goes to command mode and acquires the RSSI value. After getting the RSSI value, the receiver goes back to transparent mode, enabling two-way communication between the transmitter and the receiver. The RSSI value is fed back to the transmitter and receiver starts performing its usual function of receiving, displaying and data saving. Once the transmitter receives the RSSI value from the receiver, it goes to the command mode and changes the output power according to the received RSSI value. As soon as the output power is adopted according to the RSSI value, the transmitter once again gets back to the transparent mode to enable normal transmission of data. The regular data transmission takes place again till the distance between the transmitter and receiver changes. When there is a change

in the distance between the communicating units, the same process takes place again to determine the required output power. Figure 5.5 shows the data flow between the transmitter and the receiver.

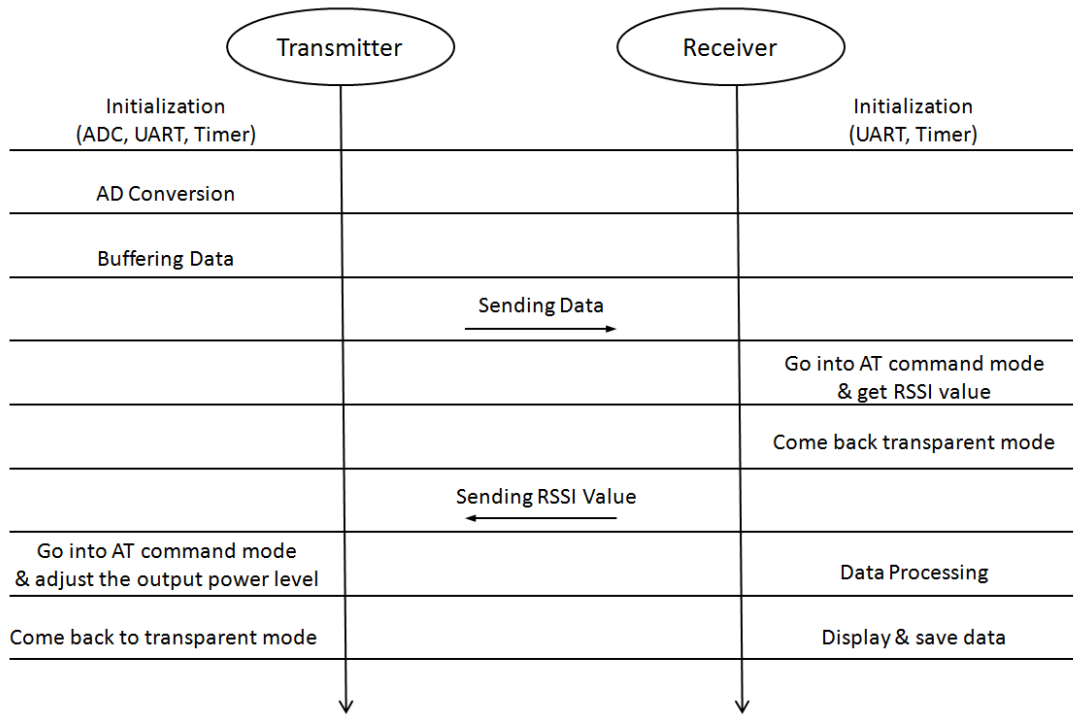
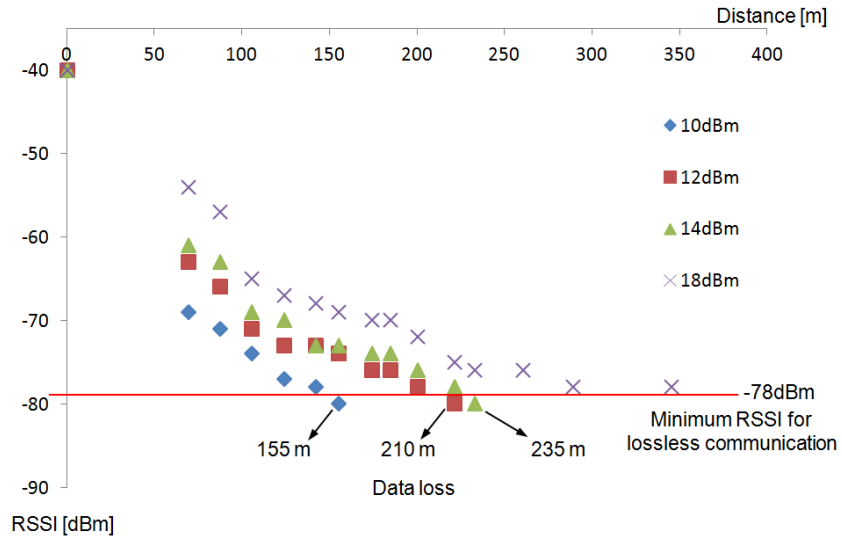


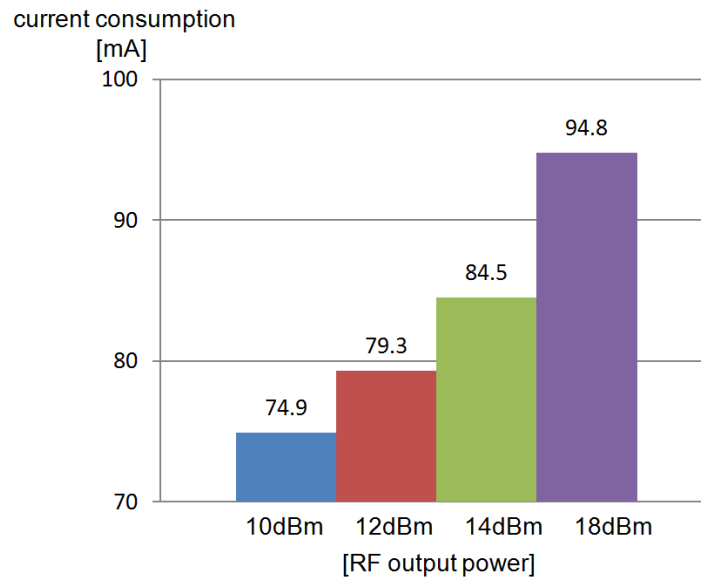
Figure 5.5 Data flow between the transmitter and the receiver with adaptive RF output power control

An experiment was carried on to verify the authenticity of the adaptive power algorithm and to measure RSSI and data loss at different output power level and at a fixed distance between the transmitter and receiver. The experiment was performed with four different RF power output levels (10dBm, 12dBm, 14dBm and 18dBm). As shown in the Figure 5.6(a), increasing the distance with constant output power reduces the value of RSSI. Results also show that, a RF output power of 18 dBm can communicate up to 350 meters and a RF output power of 10 dBm can transmit up to 150 meters. This indicates that RF output power and the communicating

distance is proportional. In addition, test results also show that the power consumption is inversely proportional to the RF output power as shown in the Figure 5.6(b).



(a)



(b)

Figure 5.6 Experimental results; (a) relation between communication distance and RSSI with different RF output power values and (b) current consumption with different RF output power values

The transmitter can transmit up to 150 m at 10 dBm rather than using 18 dBm of output power. Thereby, the power consumption can be reduced up to 21 %. Hence, based on the experimental results, it is evident that controlling the output power based on the transmission distance can considerably reduce power consumption.

5.5 Results

The data acquired through the system for a normal 25 year old subject is plotted below in Figure 5.7(a) shows the five signals namely Lead I and II, and three precordial signals V1, V2 and V5. Figure 5.7(b) shows the Lead III, aV_R, aV_L and aV_F derived from lead I and lead II. As can be observed, the acquired signals are comparable in quality to a regular clinical 12 lead ECG.

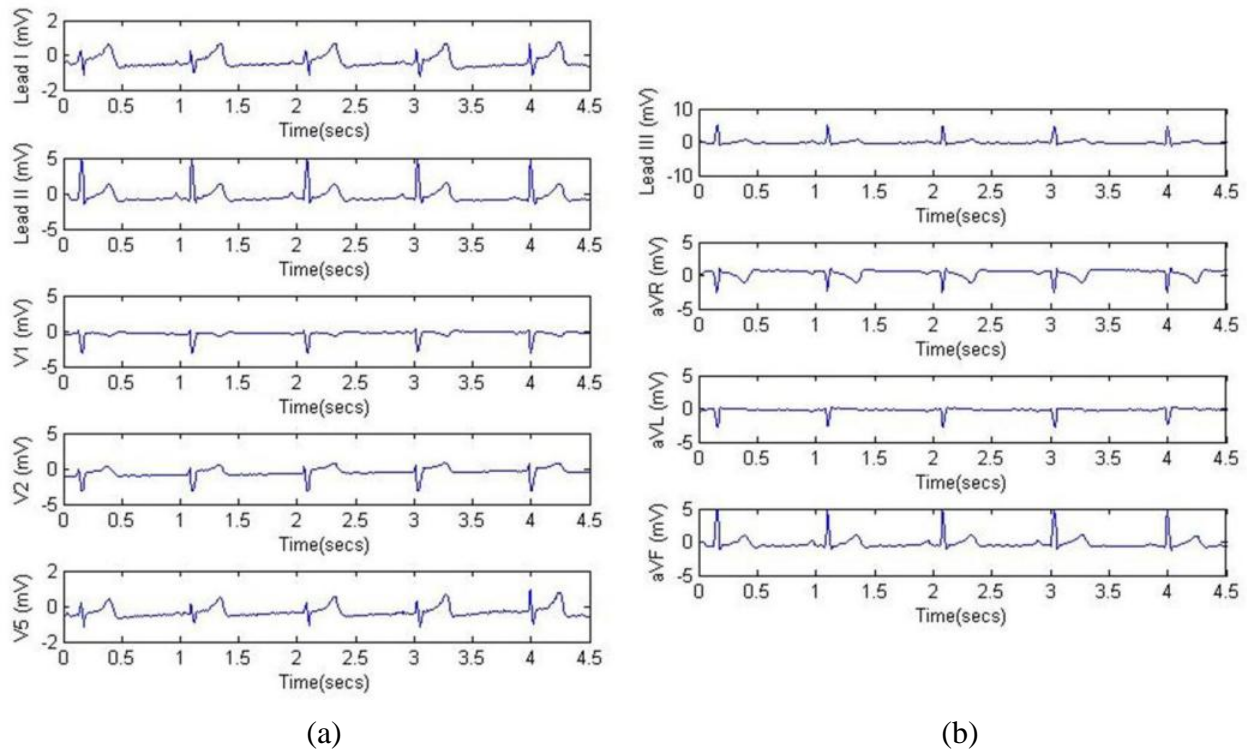


Figure 5.7 (a) ECG signals acquired using the system and (b) derived ECG signals

5.6 Discussion and Conclusions

A fully wearable real-time ECG acquisition system with wireless transmission of data for the continuous monitoring of football players during training and on the field was implemented. The system was used to acquire 5 ECG signals namely Lead I and II, and precordial leads V1, V2 and V5. The acquired data was plotted in real-time and stored for analysis. The system was further validated in outdoor environment. The current implementation ensures the acquisition of good quality ECG, without significant wander in the signal baseline, during mild activity like walking or slow jogging but fails when the wearer is engaged in rapid movement like sprinting. This is an inherent limitation in the ECG signal as it also reflects the activity of all muscle groups in the vicinity of the electrodes and not only the cardiac electrical activity. However, the signal acquired using the vest was seen to recover to its original quality within 3 seconds of slowing down from rapid movement to mild activity. Although the availability of diagnostic quality ECG may be intermittent, this system can be a great aid in both tracking the progression of any abnormalities in a football player's cardiac activity during training, as well as significantly improve the accuracy and speed of emergency cardiac care on the field.

In sports monitoring, additional measurements like joint angle, acceleration and impact will be valuable tools to assess the level of exertion and training intensity. The sensors in these cases will need to be spread throughout the athlete's body, arms and legs. The vest platform cannot accommodate these needs. In order to maintain the usability of the signal, a personal area network (PAN) of sensors will have to be implemented for each player. A schematic of this concept is depicted in Figure 5.8.

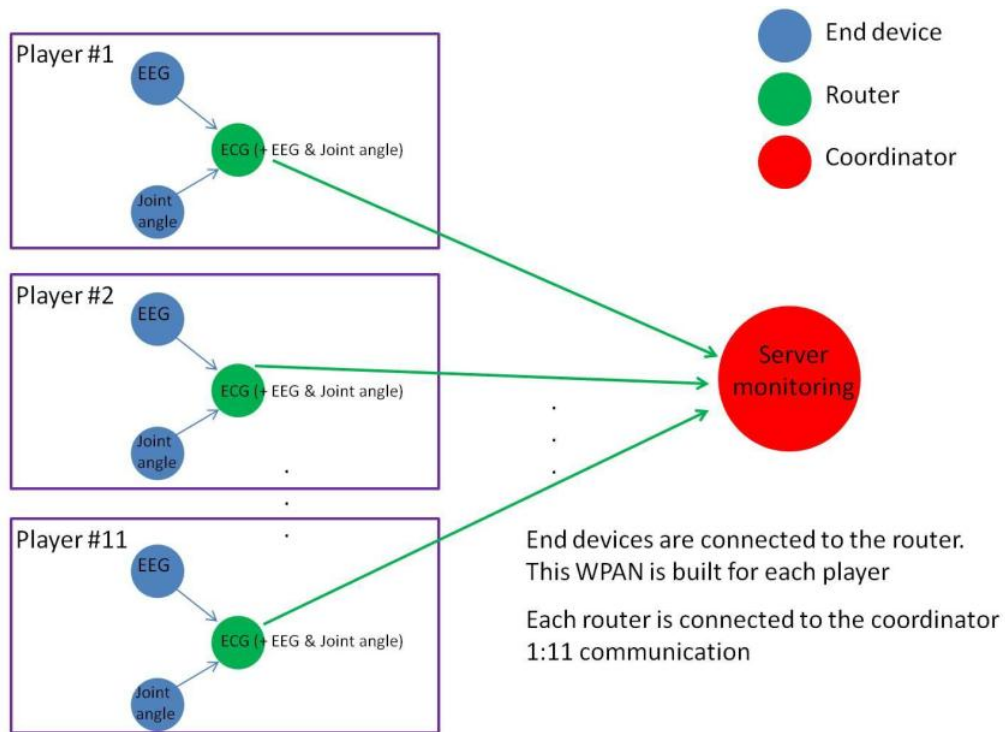


Figure 5.8 Schematic for WPAN implementation for multiple sensors spanning the full body of the athlete

Chapter 6: Application - Wireless Brain-Machine Interface Using EEG and EOG

6.1 Introduction

A brain machine interface (BMI) is a communication system that translates human's thought into signals to control devices such as a computer application or a neuroprosthesis [76]. A BMI enables the brain to communicate with the external world by deciphering the brain activity. Hence, the assistive devices or systems using a BMI improve the quality of life in disabled people. In addition, a BMI has been proposed to replace humans with robots in the performance of dangerous tasks like explosives handling/diffusing, hazardous materials handling, fire fighting etc. Earlier researches demonstrate the feasibility of BMI with the invasive method by implanting the intracranial electrodes in the motor cortex of monkeys [77-81]. While an invasive BMI can use good quality of brain signals, it is expensive and the implanting surgery may lead to undesirable side effects. A noninvasive BMI using electroencephalogram (EEG) signals are preferable for humans. EEG signals represent the electrical activity of millions of neurons in the brain. EEG has various properties and it can be used as a basis for a BMI: rhythmic brain activity, event-related potentials (ERPs), event-related desynchronization (ERD) and event-related synchronization (ERS) [82]. Different rhythmic brain activities are shown depending on the level of consciousness. The brain waves are classified according to the frequency band: Delta (0.1-3 Hz), Theta (4-7 Hz), Alpha (8-12 Hz), Beta (12-30 Hz) and Gamma (30-100 Hz). These rhythms are affected by different actions and thoughts, for example the thinking of movement attenuates or changes a typical brain rhythm. The fact that the thoughts affect the brain rhythms connote the rhythmic brain activities that can be used for the BMI. ERP represents the potential changes in EEG that occurs in response to a particular event or a stimulus. ERD and ERS are the change of

signal's power occurring in a given band, relative to a reference interval. Many researchers have been developing a BMI with two different approaches. The first is a pattern recognition approach which is based on cognitive mental tasks, and the other is an operant conditioning approach based on the self-regulation of the EEG response [83]. Pattern recognition approach detects different EEG patterns with different mental tasks. Because each different mental task activates its special EEG rhythm in different cortical areas, electrodes should be placed on the proper position to pick up the special EEG patterns. For example, the imaginary of the right hand movement activates the left motor cortex and the imagination of the left hand movement activates the right motor cortex. Meanwhile, the arithmetic tasks activate the prefrontal cortex. The operant conditioning approach is based on the self-regulation of EEG rhythms or event-related potentials. This approach differs from the pattern recognition approach. The users are not aware of any rhythms or event-related potentials happening in their brains unless they receive some kind of feedback. In general, implementation of a BMI based on EEG signals requires measurement of EEG, preprocessing, feature extraction, classification and device control. To measure EEG signals, electrodes are placed on right places, typically according to the international 10-20 system. The preprocessing process includes amplification, filtration and A/D conversion. In the feature extraction stage, certain features are extracted from the preprocessed and digitized EEG signals in frequency or time domain. The extracted features are the input of the classifier. The classifier can calculate the probabilities for the input belonging to each class. The signals are simply classified by threshold detection by the classifier. The output of the classifier is the input for the device control. The device control transforms the classification to a particular action of the device. While a number of research groups have been focusing on developing complex and multiple channels of a BMI, in point of popularization and convenience

of a BMI system, the BMI should be inexpensive and easy to use. In addition, the BMI should guarantee mobility.

The aim of this research is to develop a small wearable brain-machine interface to control a robot wirelessly [90, 91]. The BMI controls the movement of the robot by extracting the features of the EEG and EOG signals. The EEG and EOG signals are captured with gold nanowire electrodes attached to a headband [50]. The classified rhythmic brain waves are used to control the acceleration and deceleration or stopping of the robot by setting the threshold. The classified EOG signals from the left and right movements of eye balls control the left and right direction changes of the robot. Figure 6.1 shows the data flow of the wireless brain-machine interface to control the robot.

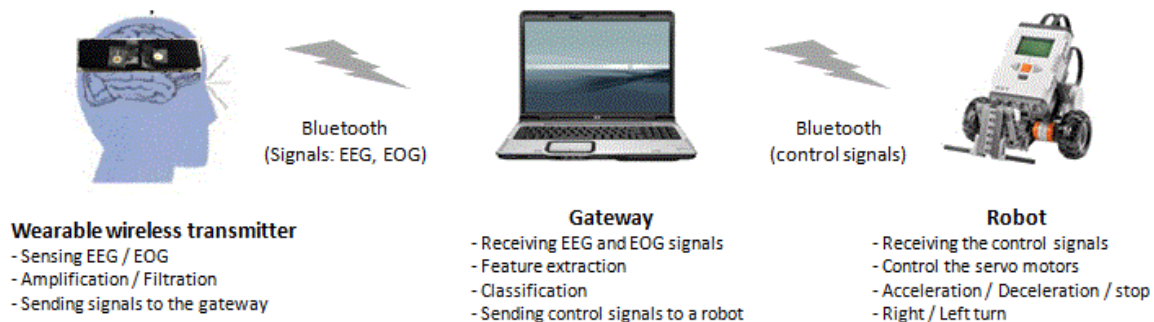


Figure 6.1 Data flow of the wireless brain machine interface

6.2 System Design

A wearable wireless sensing transmitter mainly consists of two dry electrodes and a wireless transmitter module. Figure 6.2 shows the images of the headband and the wireless transmitter module. The electrodes are attached inner side of the headband and the each electrode is electrically connected to a snap button which is stitched on the outer side of the headband. The

wireless transmitter is attached to the headband with the snap buttons. Figure 6.3 shows the block diagram of the wireless transmitter.

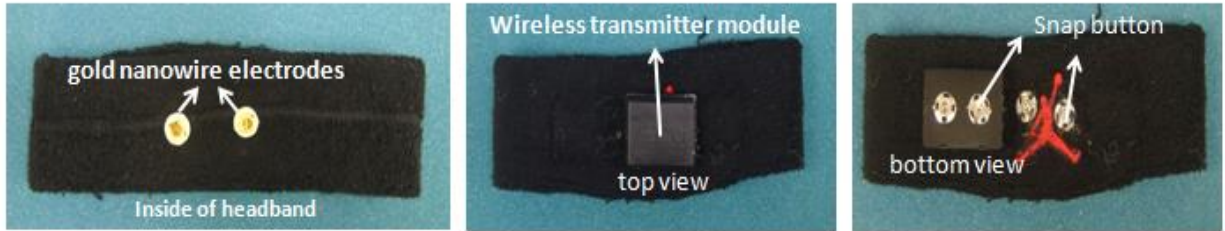


Figure 6.2 Image of the wearable wireless sensing transmitter

6.2.1 Sensor

Gold nanowire electrodes are used as the electrodes to sense the EEG signals [50]. The gold nanowire electrode does not need conductive gels which dry out and change the impedance of the electrode leading to erroneous or noisy EEG signals. In addition, the dry gold nanoelectrodes also have an unlimited shelf-life and reusable because of the inert nature of gold. Instead of placing electrodes on the hair site, the electrodes are placed on the forehead. A good contact between scalp and electrode provides good quality of EEG signals. Forehead is a convenient location for placing electrodes and it is over the frontal cortex region where cognitive signals linked to higher states of consciousness originate. In addition to detecting EEG signals, the electrodes detect EOG signals. Forehead is the suitable position to sense both rhythmic brain waves and left/right eye motions. The other eye motions, up/down motion and blinking, are regarded as noises. These undesired EOG signals from eye motions can be rejected depending on the position of electrodes. The dry electrodes are spaced 5 cm apart and aligned horizontally. The horizontal alignment of electrodes enable to acquire high amplitude EOG signals from left/right

motions, but it does not detect significant EOG signals from up/down and blink motions because of electrode placements.

6.2.2 Amplifier

EEG or EOG is a differential signal which is perceived as the difference in potential between two points. One of the electrodes act as the reference for the other. The biopotentials have small amplitude ranging from micro-volts to a few milli-volts. Because the biopotentials are vulnerable to noises from power line (50/60 Hz) and mismatch between electrodes, high common mode rejection ratio (CMRR) and small input offset voltage should be considered when designing amplifier circuit. An instrumentation amplifier with high CMRR is implemented as the first stage. Two more stages of non- inverting amplifiers are used to increase the gain further and to improve the signal quality. The instrumentation amplifier provides high input impedance as the first stage of the amplifier circuit and it prevents the distortion of EEG or EOG signals from skin contact impedance mismatch. The non-inverting amplifier stages are designed with active filters. The filters help to prevent any aliasing artifact that can be produced during the analog to digital conversion. The overall frequency band of the amplifier circuit is set to 0.3Hz to 35Hz to cover the frequency band of EEG and EOG signals.

6.2.3 Microprocessor

A microprocessor plays role in digitizing the analog signals from the amplifier and controls the Bluetooth module. The microprocessor comes with analog to digital conversion (ADC) and timer registers. Timer registers are counters which generate signals, referred as an interrupt. The upper limit of the timer register is set when the microprocessor is initialized based on the frequency of the count. Therefore, the interval can be fixed when the interrupts are generated. This interrupt

can be used as a trigger signal for ADC operation. Since the interrupt is generated periodically, the signal can be sampled with the same fixed interval. The ADC values are transferred serially to the Bluetooth module. The communication interface between the microprocessor and the Bluetooth module is Universal Asynchronous Receive/ Transmit (UART).

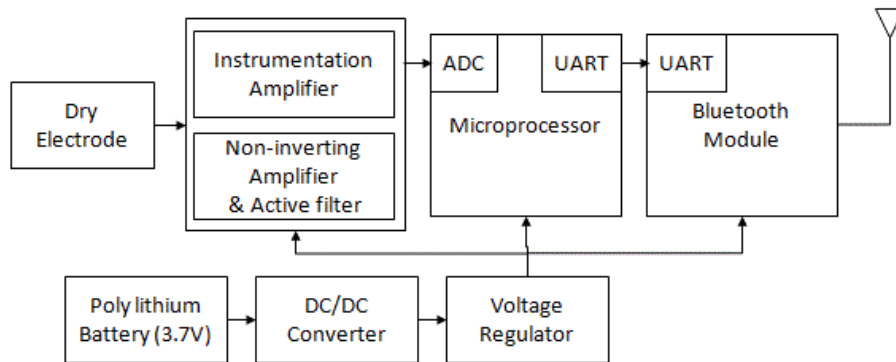


Figure 6.3 Block diagram of the wireless sensing transmitter

6.3 Feature extraction and Classification

EOG measures the resting potential of the retina according to the eye movement. In general, pairs of electrodes are placed either above and below the eye or to the left and right of the eye. If the eye is moved from the center position towards the electrode, this electrode sees the positive side of the retina and the opposite electrode sees the negative side of the retina. With this measurement method, all kinds of the eye movements are measured, left/right, up/down and blinking movement. In this BMI system, because only the left/right eye motion is used to take decision of a robot turning left or right, the other up/down and blinking motions are considered as noise. Figure 6.4 shows the measured EOG signals with our headband system according to different eye motion. As shown in the Figure 6.4, the feature of blinking is narrow and sharp amplitude of waveform. The corresponding waveforms of left and right motion are of longer

duration and somewhat dull peak of the waveforms. In common, the waveforms of up and down motion are similar to that of left/right motion, but the signals from up/down motion are not detected much with this system because of the position of electrodes.

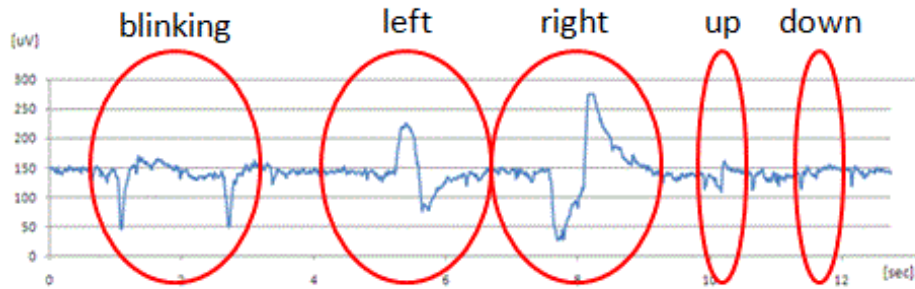


Figure 6.4 Measured EOG signals with the system

Thresholds of amplitude and time duration are used to remove the blinking and up/down motion. After removing the undesired eye motion signals, only the left and right waveforms remain. The two waveforms should be classified as left and right motion to send turning commands to the robot. The classification between two eye motions is done by investigating the polarity of waveforms. Left and right motions show different polarity. In this system, left motion shows positive polarity and right motion shows negative polarity. Figure 6.5 shows the classification processes of left/right eye motion. The left and right motion signals are filtered with 5~15 Hz bandwidth to achieve sharp waveforms to process further. After filtering, integration is performed to make the signals smooth. The floor noises are removed by setting adaptive amplitude threshold. The amplitude threshold is defined by the 75 % of peak values of waveform. The cleaned waveforms by removing noise floor are used to decide the command signals. As shown in Figure 6.5(e), finally, left eye motion coded to the pulse amplitude 1 and

followed by amplitude 5 pulse. Right eye motion is coded to the amplitude 5 pulse and followed by amplitude 1 pulse.

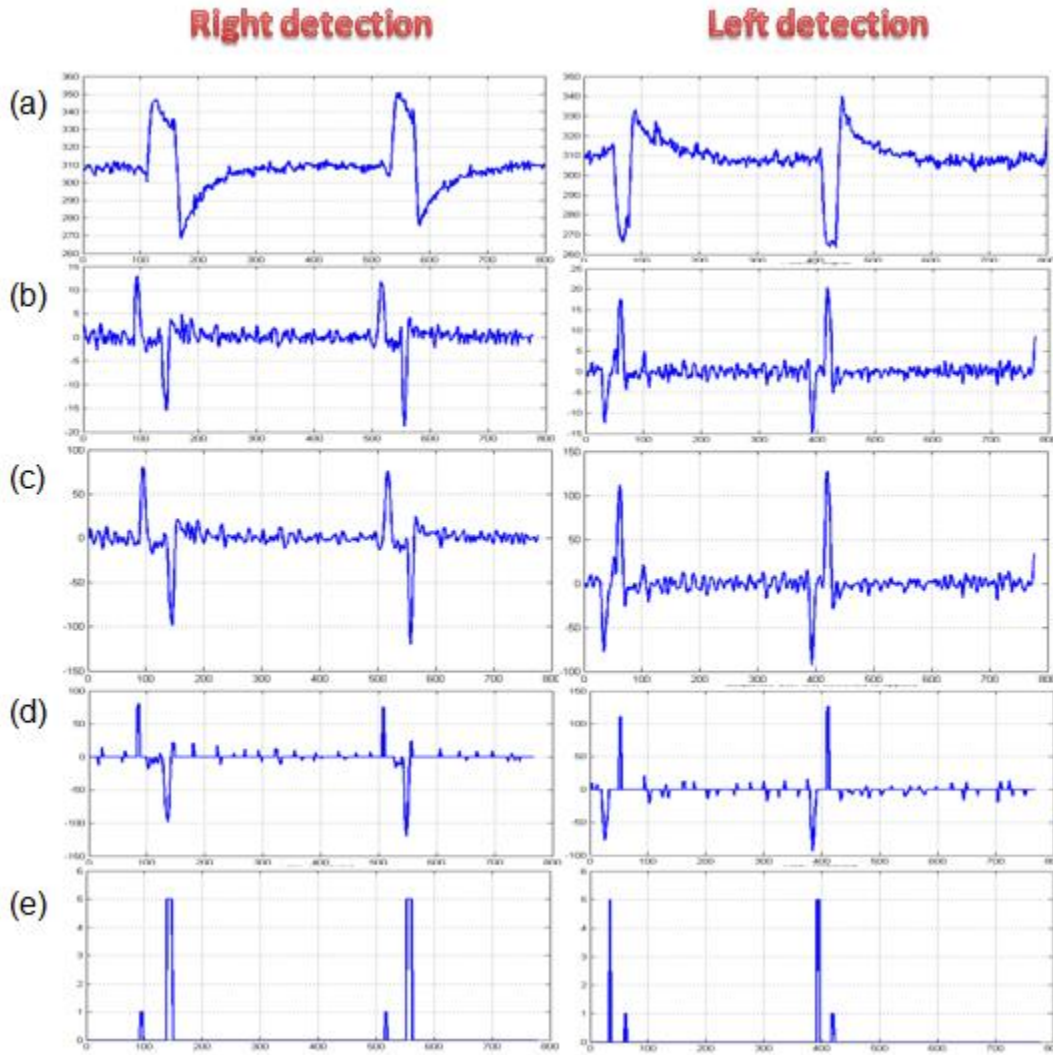


Figure 6.5 Classification process of EOG signals; (a) raw left and right EOG signals, (b) integrated signals, (c) filtered signals, (d) noise removed signals and (e) classified signals

Acceleration and deceleration of the robot are controlled by EEG signals. Among several brain waves, the alpha and beta waves are focused because they represent the mental states of attention and relaxation respectively. The received EEG signals are transformed into frequency domain

through Fast Fourier Transform (FFT) to investigate the brain waves. The each rhythmic brain wave is defined by the frequency band, and the mental states can be deduced by considering the amplitude change of the frequency band. To simplify the EEG signals and extract their frequency components, the transformed signals by FFT are further processed by an autoregressive (AR) feature extraction method. To define the attention and relaxation level, the threshold are set based on the ratio between the sum of AR power spectral density (PSD) of alpha and that of beta waves. Figure 6.6 shows the change of AR PSD when eye opened and eye closed to check if the system can detect the alpha wave and beta waves. In addition, Figure 6.6 shows the bar graph to represent the sum of AR PSD value over frequency bands. Based on the sum of AR PSD value of alpha and beta frequency band, the ratio of alpha to beta is extracted. It is used to define the threshold of attention and relaxation. However, in case that floor noises cannot be ignored, the floor noise distorts the decision of attention and relaxation mode because the sum of AR PSD over frequency band includes all the noise and signals occupied in the frequency band. Instead of taking the sum of AR PSD value, taking the peak AR PSD value over the frequency band is more tolerant in noisy condition. Figure 6.7 shows the flow chart for feature extraction and classification of the system.

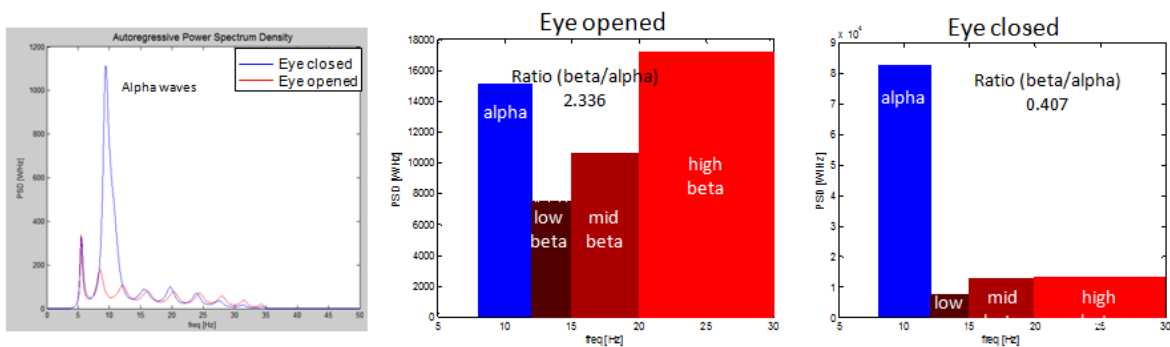


Figure 6.6 Plot of AR PSD of EEG signals

6.4 Experimental Test

In order to validate the feasibility of the BMI system, two experiments were designed. The first experiment is remote controlling the robot with this wireless BMI system. The controlling of a robot was performed by following the direction sign on the floor. The direction sign was designed with meander line style. The speed of a robot is controlled by attention and relaxation level extracted from EEG signals in the straight section and the changing direction of a robot is controlled by the left and right of eye motions in the curved section. In the second experiment, the subject was asked to be in attention or relaxation mode by an experimenter and the calculated attention level was compared with the actual mental states of a subject. By performing the second experiment, the accuracy rate of the BMI system was evaluated.

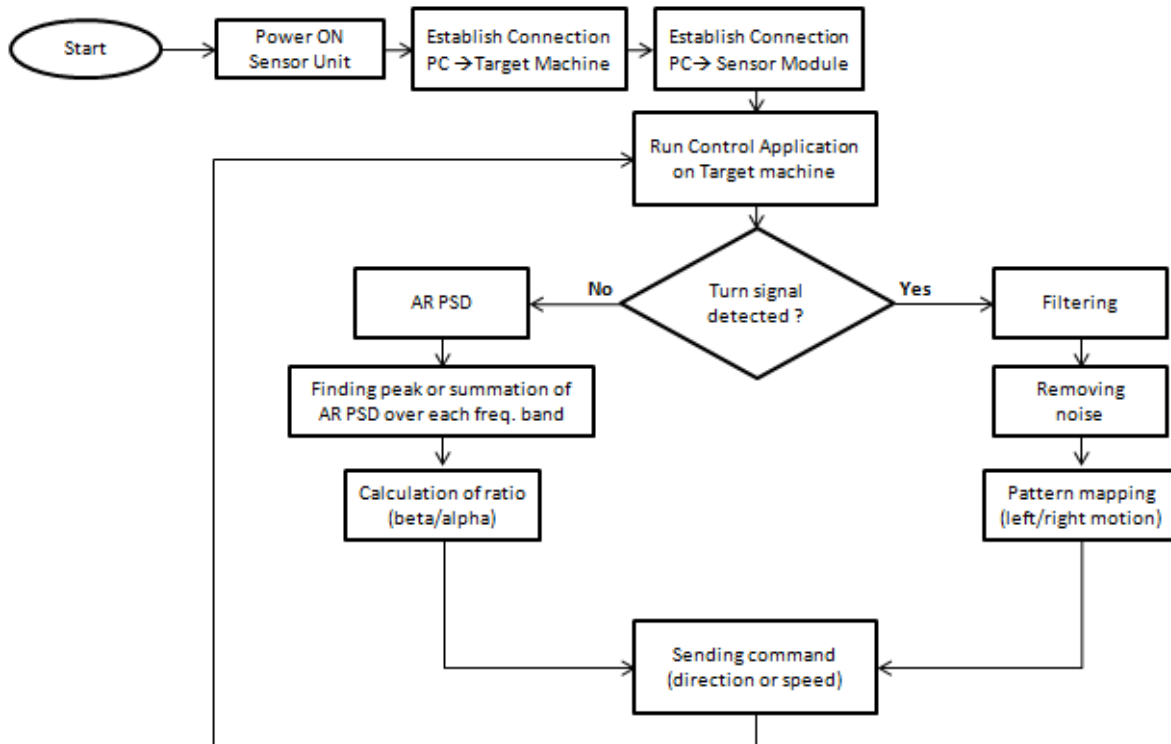


Figure 6.7 Flow chart for feature extraction and classification

6.5 Results

The data were characterized the data with two different ways. One is using the sum of the PSD value over frequency bands to determine the attention level and the other is using the peak value of the AR PSD value over frequency band. Figure 6.8 shows the results of the sum of the PSD value with different references; The power over beta frequency band is divided by total power (alpha, beta, theta and gamma), the beta power is divided by the power of alpha, theta and beta, the beta power is divided by the power of alpha and theta which are related to the relaxation and meditation and the beta power is divided by the power of alpha.

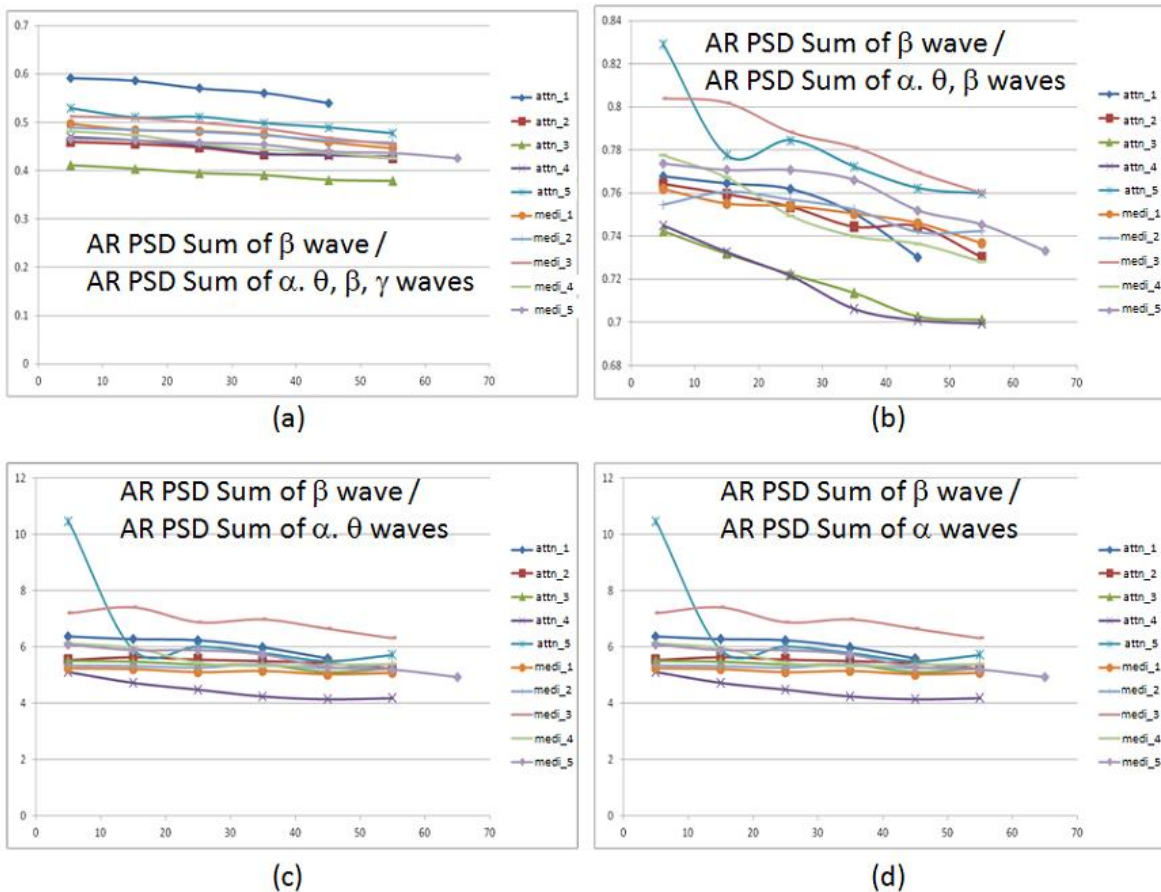


Figure 6.8 Results of attention level based on different ratio

As shown in the Figure 6.8, the calculated attention level from the sum of the power over frequency bands does not show the consistence based on the instructed attention and relaxation mode, i.e. in some case, even in spite the subject stayed in the attention mode, the attention level has lower value than in the relaxation mode. On the other hand, the peak value of PSD shows trends depending on the mental tasks. Especially, instead of using the all beta waves, beta waves are divided into low, mid and high beta waves. Even though beta waves are related to the attention state, subdivision can provide more accurate classification. Figure 6.9 shows the results of ratio the peak of the AR PSD value of low beta and alpha. In this experiment, the low beta which is related to the relaxed yet focused or integrated condition changes more than the other high or low beta wave. When the ratio of peak PSD value of low beta and alpha was used, the accuracy rate was about 95 %.

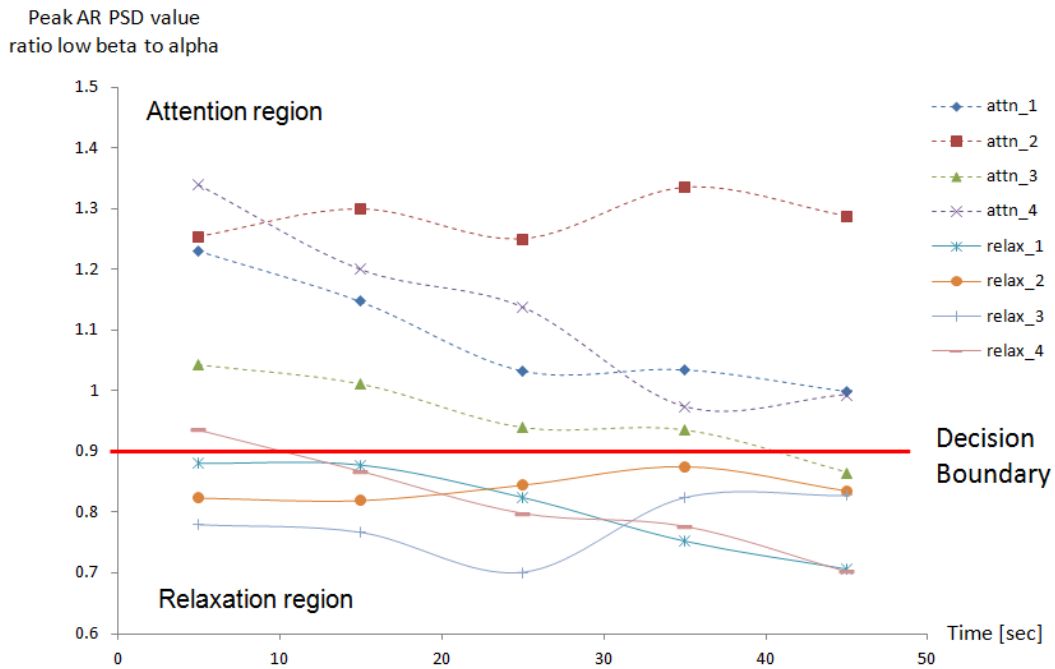


Figure 6.9 Results of ratio the peak of the AR PSD value of low beta and alpha waves

6.6 Conclusion

The wearable wireless brain machine interface was developed to reveal the level of attention or relaxation and to control the robot. To verify the system, robot was controlled based on EEG and EOG signals and the classification algorithm to define the level of attention was evaluated with the experiment. The BMI system is a wearable headband type which has electrodes and wireless transmitter module. The gold nanowire electrode and bluetooth were chosen as the electrode and the wireless communication method. The EEG and EOG signals are transmitted to the gateway (laptop). The EOG signals are extracted based on the amplitude and time duration. By using the threshold and polarity, the left and right eye motions were classified and then the gateway sends commands to make the robot turn right or left. The EEG signals are measured and transformed into frequency domain. The peak value of autoregressive PSD value of each brain wave is used to determine the level of attention. The level of attention is defined by the peak AR PSD value ratio of low beta and alpha waves. The results show that the accuracy of the determining of the attention and relaxation is 95 %. In addition, these feature extraction and classification algorithms were applied to control the robot.

Chapter 7: Conclusions

The research presented in this dissertation includes various factors to improve the present state-of-art health monitoring systems. It is focused on improving the prevailing healthcare monitoring systems by implementing novel techniques. Firstly, it establishes a relationship between the combination of two wireless communication systems and the remote health monitoring system. Secondly, results about implementing an adaptive RF output power control has been discussed. Lastly, wireless communication technologies like ZigBee, Wi-Fi, GSM/WCDMA and Bluetooth were incorporated in the health monitoring systems and their performance was studied and evaluated.

The sleep disorder system elucidates the implementation of ZigBee/Wi-Fi and GSM/WCDMA as wireless communication methods in the HST systems to achieve better coverage area and cost efficient monitoring, than the present HST systems. First, a HST device with ZigBee/Wi-Fi was implemented to overcome the drawbacks of the present monitoring systems which have the fixed number of physiological channels. The proposed and developed work in this dissertation provides methods for adding supplementary devices, extending WPAN to WLAN/WMAN and reducing power consumption. By the implementation of star network topology in a ZigBee network, the number of channels is varied without an additional device being necessary to measure the other biopotentials. Similarly, type III HST device is upgraded to a type II HST device owing to this technique. The combination of two wireless communication standards provides flexibility in data transmission and distance, as WPAN of the ZigBee network is extended to the WLAN with Wi-Fi. These incorporations provided successful results in health monitoring, which means a cost efficient and a continuous health monitoring system is

implemented. Second, another HST system to evaluate sleep stages was developed with GSM/WCDMA as a wireless communication standard. This system was built to monitor the EOG, EMG and EEG signals. The acquired biopotentials are processed, digitized and transmitted through the mobile network. Because of the redundant area coverage of the mobile network, the signals can be transmitted over long distances and can be monitored from anywhere. Moreover, the compact build of the device offers unobtrusive mounting on a skull cap. The test result proves that the device can be used to evaluate sleep stages.

The cardiac monitoring system explains about the implementation of a system for the cardiac monitoring in football players with ZigBee. The system measures 5 ECG signals and transmits them to the receiver which is then used for monitoring. Additionally, an algorithm to reduce the power consumption was implemented in this system. The RF output power control algorithm controls the transmission power of the transmitter according to the distance between the transmitter and the receiver based on the RSSI. This showed a significant reduction up to 21 % in the power consumption. This system can be used to prevent sudden cardiac death in football players.

Feature extraction/classification and robot control was implemented using EOG and EEG with the brain machine interface. A wearable headband mounted with sensors was used to acquire the EEG and EOG signals. Additionally, a classification algorithm was implemented in this system. Amplitude and time duration was used to classify EOG signals and frequency domain analysis was used to extract feature and classify EEG signals. The result showed 95% accuracy in the attention and relaxation states.

The work presented and the systems developed during this research can be improved in certain aspects: building entire body area network, removal of motion artifacts and reducing the power consumption. First, if each sensor in the body can communicate wirelessly with the receiver by building entire body area network instead of using wired connection to the transmitter which sends the gathered data from each sensor to the receiver. This would reduce the obtrusive nature of the sensors connection to the transmitting modules. Second, if the motion artifacts can be removed completely, the system will be applied to various application fields. Third, innovative methods like RF output power control reduces the power consumption. In addition, several methods like utilizing energy from the human body as an ancillary power source and implementing a technique where a system would start transmission only under abnormal health conditions can considerably reduce power consumption of a battery.

References

- [1] Daniel Foley, Sonia Ancoli-Israel, Patricia Britz and James Walsh, "Sleep disturbances and chronic disease in older adults Results of the 2003 National Sleep Foundation Sleep in America Survey," *Journal of Psychosomatic Research*, vol. 56, pp. 497-502, 2004.
- [2] California HealthCare Foundation, "Snapshot Health Care Costs 101", www.chcf.org, 2012.
- [3] The Council of State Governments, "State Official's Guide to Chronic Illness," 2003.
- [4] D. Foley, A. Monjan, E. Simonsick, R. Wallace and D. Blazer, "Incidence and remission of insomnia among elderly adults: an epidemiologic study of 6,800 persons over three years," *Sleep*, vol. 22, pp. 366-372, 1999.
- [5] S. Maggi, J. Langlois, N. Minicuci, F. Gringolotto, M. Pavan and D. Foley, "Sleep complaints in community-dwelling older persons: prevalence, associated factors, and reported causes," *Journal of the American Geriatrics Society*, vol. 46, pp. 161-168, 1998.
- [6] M. Vitiello, "Sleep disorders and aging: understanding the causes," *J Gerontol A Biol Sci Med Sci*, vol. 52, pp. 189-191, 1997.
- [7] D. Foley, A. Monjan, S. Brown, E. Simonsick, R. Wallace and D. Blazer, "Sleep complaints among elderly persons: an epidemiologic study of three communities," *Sleep*, vol. 18, pp. 425-432, 1995.
- [8] S. Ancoli-Israel, D. Kripke, M. Klauber, W. Manson, R. Fell and O. Kaplan, "Sleep disordered breathing in community dwelling elderly," *Sleep*, vol. 14, pp. 486-495, 1991.
- [9] S. Ancoli-Israel, D. Kripke, M. Llauber, W. Manson, R. Fell and O. Kaplan, "Periodic limb movements in sleep in community-dwelling elderly," *Sleep*, vol. 14, pp. 496-500, 1991.
- [10] E. Kramarow, H. Lentzner, R. Rooks, J. Weeks and S. Saydah, "Health and aging chartbook," National Center for Health Statistics, pp. 40-41, 1999.
- [11] J. Guranlnik, "Assessing the impact of comorbidity in the older population," *Ann Epidemiol*, vol. 6, pp. 376-80, 1996.
- [12] D. Lipkin, "Sleep-disordered breathing in chronic stable heart failure," *Lancet*, vol. 354, pp. 531-532, 1999.
- [13] Claudio Bassetti and Michael Aldrich, "Sleep Apnea in Acute Cerebrovascular Diseases: Final Report on 128 Patients," *Sleep*, vol. 22, no. 2, pp. 217-223, 1999.

- [14] O. Parra, A. Arboix, S. Bechich and L. Garcia-Eroles et al., "Time course of sleep-related breathing disorders in first-ever stroke or transient ischemic attack," *American Journal of Respiratory Care Medicine*, vol. 161, pp. 375-380, 2000.
- [15] H. Resnick, S. Redlin, E. Shahar, A. Gilpin and A. Newman et al., "Sleep Heart Health Study. Diabetes and sleep disturbances: findings from the Sleep Heart Health Study," *Diabetes Care*, vol. 26, no. 3, pp. 702-709, 2003.
- [16] C. Sjöström, E. Lindberg, A. Elmasry, A. Hägg, K. Svärdsudd and C. Janson, "Prevalence of sleep apnea and snoring in hypertensive men: a population based study," *Thorax*, vol. 57, pp. 602-607, 2002.
- [17] L. Donna, Hoyert and Jiaquan Xu, "Deaths: Preliminary Data for 2011," *Centers for Disease Control and Prevention, National Vital Statistics Reports*, vol. 61, no 6, 2012.
- [18] American Academy of Sleep Medicine, "International classification of sleep disorders, revised: Diagnostic and coding manual," Chicago, Illinois: American Academy of Sleep Medicine, 2001.
- [19] Susan Redline, Peter Tishler, Mark Schluchter and Joan Aylor et al., "Risk factors for Sleep-disordered Breathing in Children," *American Journal of Respiratory Care Medicine*, vol. 159, pp. 1527-1532, 1999.
- [20] Shahin Farshchi, Aleksey Pesterve, Paul H. Nuyujukian, Istvan Mody, and Jack W. Judy, "Bi-Fi: An Embedded Sensor/System Architecture for Remote Biological Monitoring," *IEEE Trans. Information Technology in Biomedicine*, vol. 11, no. 6, pp. 611-618, 2007.
- [21] C. Mundt, K. Montgomery, U. Udoh, V. Barker, G. Thonier, A. Tellier, R. Ricks, R. Darling, Y. Cagle, N. Cabrol et al., "A multiparameter wearable physiologic monitoring system for space and terrestrial applications," *IEEE Transactions Information Technology in Biomedicine*, vol. 9, no. 3, pp. 382–391, 2005.
- [22] J. Yao, R. Schmitz, and S. Warren, "A wearable point-of-care system for home use that incorporates plug-and-play and wireless standards," *IEEE Trans. Information Technology in Biomedicine*, vol. 9, no. 3, pp. 363–371, 2005.
- [23] T. Fulford-Jones, G.Wei, and M.Welsh, "A portable, low-power, wireless two-lead EKG system," in *Proc. 26th Annu. Int. Conf. IEEE Eng. Med. Biol. Soc.*, vol. 1, pp. 2141–2144, 2004.
- [24] I. Obeid, M. Nicolelis, and P. Wolf, "A multichannel telemetry system for single unit neural recordings," *J. Neurosci. Methods*, vol. 133, pp. 33–38, 2004.
- [25] "Phillips - Alice PDx"
<http://www.healthcare.philips.com/main/homehealth/sleep/alicepdx/default.wpd>
- [26] "Embla - Embletta X100"

<http://www.embla.com/index.cfm/id/57/Embletta-X100/>

- [27] "Compumedics - Somte PSG"
http://www.compumedics.com/product_detail.asp?id=15&item=product
- [28] "Compumedics - Siesta"
http://www.compumedics.com/product_detail.asp?id=4&item=product
- [29] "Cleveland Medical - Crystal Monitor"
<http://clevemed.com/sleepscout/overview.shtml>
- [30] "ResMed - ApneaLink Plus"
http://www.resmed.com/us/products/apnealink_plus/apnealink-plus.html?nc=patients
- [31] "CareFusion - Nox-T3"
<http://www.carefusion.com/medical-products/respiratory/sleep/nox-t3-portable-sleep-monitor.aspx>
- [32] Jaakko Malmivuo and Robert Plonsey, "Bioelectromagnetism - Principle and Applications of Bioelectric and Biomagnetic Fields," Oxford University Press, New York, 1995.
- [33] T. Pander, R. Czabanski, T. Przybyla, J. Jezewski, D. Pojda-Wilczek, J. Wrobel, K. Horoba and M. Bernys, "A new method of saccadic eye movement detection for optokinetic nystagmus analysis," IEEE Engineering in Medicine and Biology Society (EMBC), 2012 Annual International Conference, pp.3464-3467, 2012.
- [34] J. V. Basmajian and C. J. De Luca, "Muscles Alive; Their Function Revealed by Electromyography," Williams Wilkins, Baltimore, 1985.
- [35] Peter Konrad, "The ABD of EMG; A practical Introduction to Kinesiological Electromyography," Noraxon INC., 2005.
- [36] A. Rechtschaffen and A. Kales, "A Manual of Standardized Terminology, Techniques and Scoring System for Sleep Stages of Human Subjects," UCLA, Los Angeles, 1968.
- [37] K. Susmakova, "Human Sleep and Sleep EEG," Measurement Science Review, vol. 4, pp. 59-74, 2004.
- [38] Jianchu Yao, "Design of Standards-based Medical Components and a Plug-and-play Home Health Monitoring System," Kansas State University, Manhattan, 2005.
- [39] H. Labiod, H. Afifi, and C. De Santis, "WI-FI, BLUETOOTH, ZIGBEE AND WIMAX," Springer, Dordrecht, 2007.
- [40] J. Mander and D. Picopoulos, "Bluetooth Piconet Applications," London's Global University, London, 2005.
- [41] Matthew Gast and Matthew S. Gast, "802.11 Wireless Network: The Definitive Guide," O'Reilly, California, 2005.

- [42] Jin-Shyan Lee, Yu-Wei Su and Chung-Chou Shen, "A Comparative Study of Wireless Protocols: Bluetooth, UWB, ZigBee, and Wi-Fi," The 33rd Annual Conference of the IEEE Industrial Electronics Society, pp. 46-51, 2007.
- [43] Drew Gislason, "ZIGBEE WIRELESS NETWORKING," Elsevier's Science and Technology, Massachusetts, 2008.
- [44] Sofie Pollin, Mustafa Ergen and Sinem Coleri Ergen et al., "Performance Analysis of Slotted Carrier Sense IEEE 802.15.4 Medium Access Layer," IEEE Tran. Wireless Communications, vol. 7, no. 9, pp. 3359-3371, 2008.
- [45] Mischa Schwartz, "Mobile Wireless Communications," Cambridge University Press, Cambridge, 2005.
- [46] Bethesda, "National Sleep Disorders Research Plan, 2003," National Heart, Lung, and Blood Institute, 2003.
- [47] T. Young, L. Evans, L. Finn and M. Palta, "Estimation of the clinically diagnosed proportion of sleep apnea syndrome in middle-aged men and women," Sleep vol. 20(9), pp. 705-706, 1997.
- [48] K. Yaggi, J. Concato, N. Kernan, H. Lichtman, M. Brass and V. Mohsenin, "Obstructive sleep apnea as a risk factor for stroke and death," New England Journal of Medicine, vol. 353(19), pp. 2034-2041, 2005.
- [49] M. Gillette and S. Abbott, "Fundamentals of the circadian system," Sleep Research Society, Illinois, pp. 131-138, 2005.
- [50] Vijay K. Varadan, Sechang Oh, Hyeokjun Kwon and Phillip Hankins, "Wireless Point-of-Care Diagnosis for Sleep Disorder With Dry Nanowire Electrode," J. Nanotechnol. Eng. Med., vol. 1(031012), pp. 1-11, 2010.
- [51] T. Young, M. Palta, J. Dempsey, J. Skatrud, S. Weber, S. Badr, "The occurrence of sleep-disordered breathing among middle-aged adults," New England Journal of Medicine, vol. 328(17), pp. 1230-1235, 1993.
- [52] S. Ancoli-Israel, R. Klauber, C. Stepnowsky, E. Estline, A. Chinn, R. Fell, "Sleep-disordered breathing in African-American elderly," American Journal of Respiratory Critical Care Medicine vol. 152, pp. 1946-1949, 1995.
- [53] J. Montplaisir, D. Petit, D. Lorrain, S. Gauthier, T. Nielsen, "Sleep in Alzheimer's disease: Further considerations on the role of brainstem and forebrain cholinergic populations in sleep-wake mechanisms," Sleep vol. 18(3), pp. 145-148, 1995.
- [54] W. Flemons, J. Douglas, T. Kuna, O. Rodenstein, J. Wheatley, "Access to diagnosis and treatment of patients with suspected sleep apnea," American Journal of Respiratory Care Medicine, vol. 169(2), pp. 668-672, 2004.

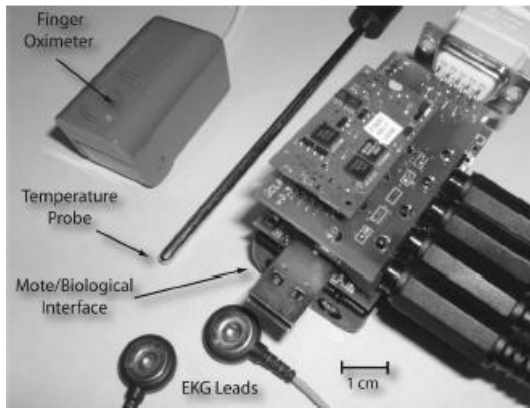
- [55] C. Iber, S. Ancoli-Israel, A. Chesson, S. Quan, "The AASM Manual for the Scoring of Sleep and Associated Events: Rules, Terminology, and Technical Specifications," Amer. Acad. Sleep Med, Westchester, IL, 2007.
- [56] SIM Com. [Online]. Available: <http://wm.sim.com/producten.aspx?id=1029>.
- [57] D. Thompson, B. Franklin and J. Balady et al., "Exercise and acute cardiovascular events placing the risks into perspective: a scientific statement from the American Heart Association Council on Nutrition, Physical Activity, and Metabolism and the Council on Clinical Cardiology," *Circulation*, vol. 115, pp. 2358-2369, 2007.
- [58] J. Maron, J. Doerer, S. Haas, M. Tierney and O. Mueller, "Sudden deaths in young competitive athletes: analysis of 1866 deaths in the United States, 1980-2006," *Circulation*, vol. 119, pp. 1085-1092, 2009.
- [59] D. Corrado, C. Basso, A. Pavei, P. Michieli, M. Schiavon and G. Thiene, "Trends in sudden cardiovascular death in young competitive athletes after implementation of a preparticipation screening program," *JAMA*, vol. 296, pp. 1593-1601, 2006.
- [60] J. Myerburg and L. Vetter, "Electrocardiograms should be included in preparticipation screening of athletes," *Circulation*, vol. 116, pp. 2616-2626, 2007.
- [61] R. Chaitman, "An electrocardiogram should not be included in routine preparticipation screening of young athletes," *Circulation*, vol. 116, pp. 2610-2614, 2007.
- [62] L. Faber and F. van Buuren, "Athlete screening for occult cardiac disease: no risk, no fun?," *J Am Coll Cardiol.*, vol. 51, pp. 1040-1041, 2008.
- [63] J. Barry and D. Maron, "National Electrocardiography Screening for Competitive Athletes: Feasible in the United States?," *Ann Intern Med.*, vol. 152(5), pp. 324-326, 2010.
- [64] D. Corrado, A. Pelliccia, H. Bjornstad, L. Vanhees, A. Biffi and M. Borjesson et al., "Cardiovascular preparticipation screening of young competitive athletes for prevention of sudden death: proposal for a common European protocol. Consensus Statement of the Study Group of Sport Cardiology of the Working Group of Cardiac Rehabilitation and Exercise Physiology and the Working Group of Myocardial and Pericardial Diseases of the European Society of Cardiology," *Eur Heart J*, vol. 26(5), pp. 516-524, 2005.
- [65] J. Maron, D. Thompson, J. Ackerman, G. Balady, S. Berger and D. Cohen et al., "Recommendations and considerations related to preparticipation screening for cardiovascular abnormalities in competitive athletes: 2007 update: a scientific statement from the American Heart Association Council on Nutrition, Physical Activity, and Metabolism: endorsed by the American College of Cardiology Foundation," *Circulation*, vol. 115(12), pp. 1643-1655, 2007.
- [66] A. Pelliccia, J. Maron, F. Culasso, M. Di Paolo, A. Spataro, A. Biffi, G. Caselli and P. Piovano, "Clinical significance of abnormal electrocardiographic patterns in trained athletes," *Circulation*, vol. 102, pp. 278-284, 2000.

- [67] A. Pelliccia, M. Di Paolo and M. Quattrini et al., "Outcomes in athletes with marked ECG repolarization abnormalities," *N Engl J Med*, vol. 358, pp. 152-161, 2008.
- [68] A. Pelliccia, "Differences in Cardiac Remodeling Associated With Race Implications for Pre-Participation Screening and the Unfavorable Situation of Black Athletes," *J Am Coll Cardiol.*, vol. 51(23). pp. 2263-2265, 2008.
- [69] A. Uberoi, R. Stein, V. Perez, J. Freeman et al., "Interpretation of Electrocardiogram of Young Athletes," *Circulation*, vol. 124, pp. 746-757, 2011.
- [70] A. Drezner, W. Courson, O. Roberts, N. Mosesso, S. Link and J. Maron, "Inter-Association Task Force Recommendations on Emergency Preparedness and Management of Sudden Cardiac Arrest in High School and College Athletic Programs: A Consensus Statement," *J Athl Train*, vol. 42(1), pp. 143-158, 2007.
- [71] M. Rubart and P. Zipes, "Mechanisms of sudden cardiac death," *J Clin Invest*, vol. 115(9), pp. 2305-2315, 2005.
- [72] D. Dorrado, A. Pelliccia and H. Heidbuchel et al., "Recommendations for interpretation of 12-lead electrocardiogram in the athlete," *Eur Heart J.*, vol. 31, pp. 243-259, 2010.
- [73] P. Rai, S. Kumar, S. Oh, H. Kwon, G. Mathur, V. Varadan and P. Agarwal, "Smart healthcare textile sensor for unhindered-pervasive health monitoring," *Proc. SPIE 8344, Nano., Bio., Info-Tech Sensors and Systems*, vol. 83440E, 2012.
- [74] P. Rai, J. Lee, G. Mathur and V. Varadan, "Carbon nanotubes polymer nanoparticles inks for healthcare textile," *Proc. SPIE 8548, Nanosystems in Engineering and Medicine*, vol. 854882, 2012.
- [75] H. Kwon, S. Oh S. Kumar and V. Varadan, "Design of electrocardiography measurement system with an algorithm to remove noise," *Proc. SPIE 7980, Nano., Bio., and Info-Tech Sensors and Systems*, vol. 79800K, 2011.
- [76] J. Wolpaw, N. Birbaumer, D. McFarland, G. Pfurtscheller and T. Vaughan, "Brain-computer interfaces for communication and control," *Clin. Neurophysiol.*, vol. 113, pp. 767-791, 2002.
- [77] J. Chapin, K. Moxon, R. Markowitz and M. Nicolelis, "Real-time control of a robot arm using simultaneously recorded neurons in the motor cortex," *Nature Neurosci.*, vol. 2, pp. 664-670, 1999.
- [78] J. Wessberg, C. Stambaugh, J. Kralik, P. Beck, M. Laubach, J. Chapin, J. Kim, S. Biggs, M. Srinivassan and M. Nicolelis, "Real-time prediction of hand trajectory by ensembles of cortical neurons in primates," *Nature*, vol. 408, pp. 361-365, 2000.
- [79] M. Serruya, N. Hatsopoulos, L. Paninski, M. Fellows and J. Donoghue, "Instant neural control of a movement signal," *Nature*, vol. 416, pp. 141-142, 2002.

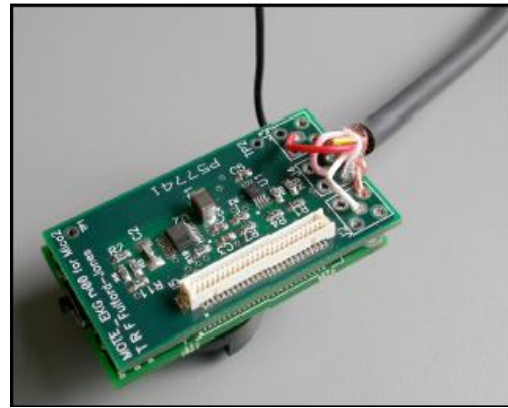
- [80] D. Taylor, S. Tillery and A. Schwartz, "Direct cortical control of 3D neuroprosthetic devices," *Science*, vol. 296, pp. 1829–1832, 2002.
- [81] M. Nicolelis, "Brain-machine interfaces to restore motor function and probe neural circuits," *Nature Rev. Neurosci.*, vol. 4, pp. 417–422, 2003.
- [82] Ali Bashashati, Mehrdad Fatourehchi, Rabab K. Ward and Gary E. Birch, "A survey of signal processing algorithms in brain-computer interfaces based on electrical brain signals," *J. Neural Eng.*, vol. 4, pp. 32-57, 2007.
- [83] Andrea Kubler, Boris Kotchoubey and Jochen Kaiser, "Brain-computer communication: Unlocking the locked in," *Psychological Bulletin*, vol. 127, pp. 358-373, 2001.
- [84] Achim Volmer and Reinhold Orglmeister, "Wireless Body Sensor Network for Low-Power Motion-Tolerant Synchronized Vital Sign Measurement," 30th Annual International IEEE EMBS Conference, pp. 3422-3425, 2008.
- [85] Sechang Oh, Hyeokjun Kwon, Robert Harbaugh and Vijay K. Varadan, "Wireless Point-of-Care Diagnosis for Sleep Disorders in WPAN and WLAN," *Smart Nanosystems in Engineering and Medicine*, vol. 2, pp. 46-54, 2013.
- [86] Sechang Oh, Hyeokjun Kwon and Vijay K. Varadan, "Wireless telemedicine systems for diagnosing sleep disorders with Zigbee star network topology," *SPIE Proceedings*, vol. 8548, DOI: 10.1117/12.946115, 2012.
- [87] Sechang Oh, Hyeokjun Kwon and Vijay K. Varadan, "Ubiquitous Health Monitoring System for Diagnosis of Sleep Apnea With Zigbee Network and Wireless LAN," *Journal of Nanotechnology in Engineering and Medicine*, vol. 2, 021008, 2011.
- [88] Sechang Oh, Hyeokjun Kwon, Prashanth S. Kumar and Vijay K. Varadan, "A Wearable Wireless Monitoring System for Sleep Disorders through GSM/WCDMA Networks," *Smart Nanosystems in Engineering and Medicine*, vol. 1, pp. 123-134, 2012.
- [89] Prashanth Shyamkumar, Sechang Oh, Pratyush Rai, Hyeokjun Kwon, Robert Harbaugh and Vijay K. Varadan, "Sudden Cardiac Death Prevention and Management through Real-time Wireless Cardiac Monitoring of Football Players on the Field," *Smart Nanosystems in Engineering and Medicine*, vol. 1, pp. 52-61, 2012.
- [90] Sechang Oh, Prashanth S. Kumar, Hyeokjun Kwon and Vijay K. Varadan, "Wireless brain-machine interface using EEG and EOG: brain wave classification and robot control," *SPIE Proceedings*, vol. 8344, DOI: 10.1117/12.918159, 2012.
- [91] Prashanth Shyamkumar, Sechang Oh, Nilanjan Banerjee and Vijay K. Varadan, "Wearable/Wireless Body Sensor Networks for Healthcare Applications," *Proceedings of Advances in Science and Technology*, vol. 85, pp. 11-16, 2012.

Appendices

A-1: Wireless Health Monitoring Systems from Research Institutes



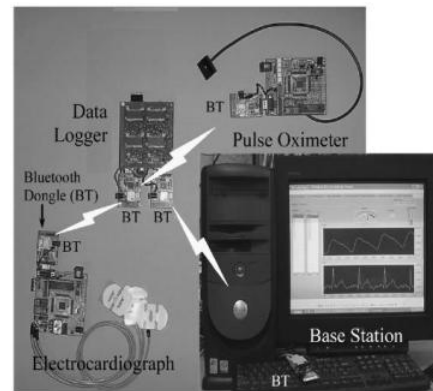
UCLA [20]



Harvard [23]



NASA [21]



Kansas State University [22]



TU-Berlin, Germany [84]

A-2: Currently Available Home Sleep Test Devices



Philips: Alice Pdx [25]



Embla: Embletta X100 [26]



Compumedics: Somte PSG [27]



Cleveland Medicine: Crystal Monitor [29]



ResMed: ApneaLink Plus [30]



CareFusion: Nox-T3 [31]



Compumedics : Siesta [28]

Appendix B: Result of case study with wireless HST system with Zigbee and Wi-Fi

- Figure B.1 to Figure B.8 shows epochs from various stages of around 60 year old, male s ubject. The test was performed at his home for 6 hours, form 10:00 PM to 4:00 AM.

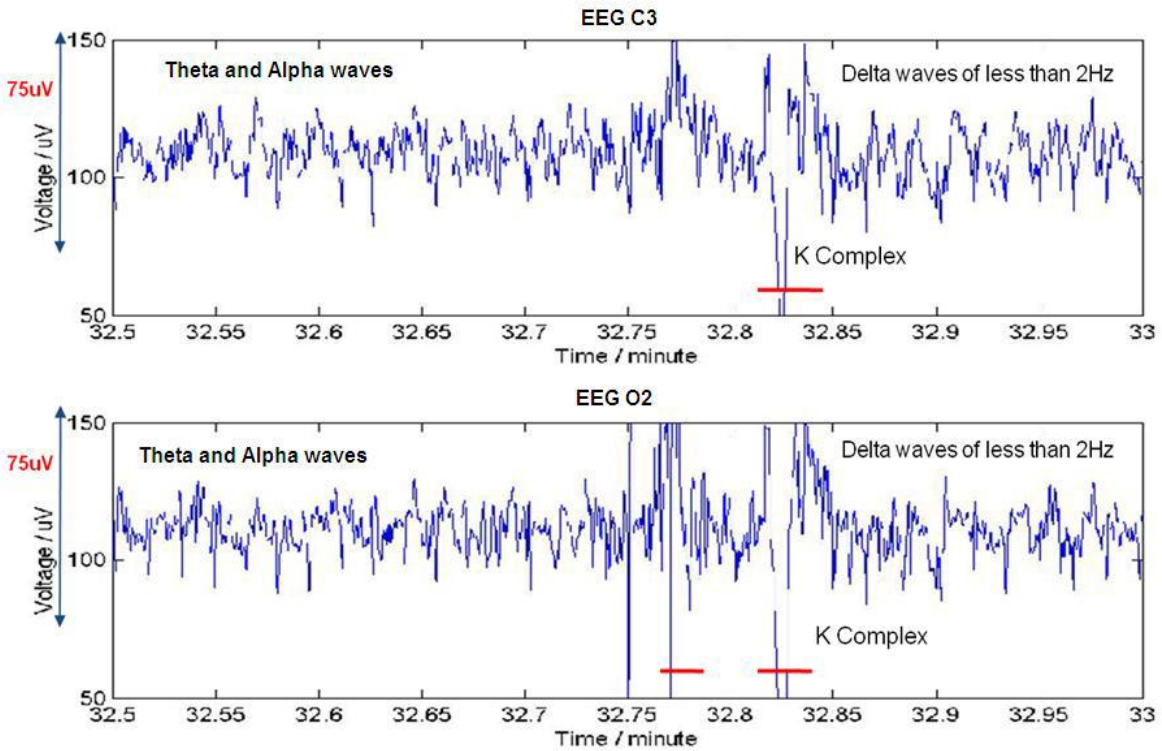


Figure B.1: This epoch illustrates the beginning of transition from Stage 1 to Stage 2. Vertex sharp waves are very prominent. In the beginning of the epoch, theta and alpha waves are dominant. In the middle of the epoch, there is a K complex. End of the epoch, delta waves less than 2 Hz are shown.

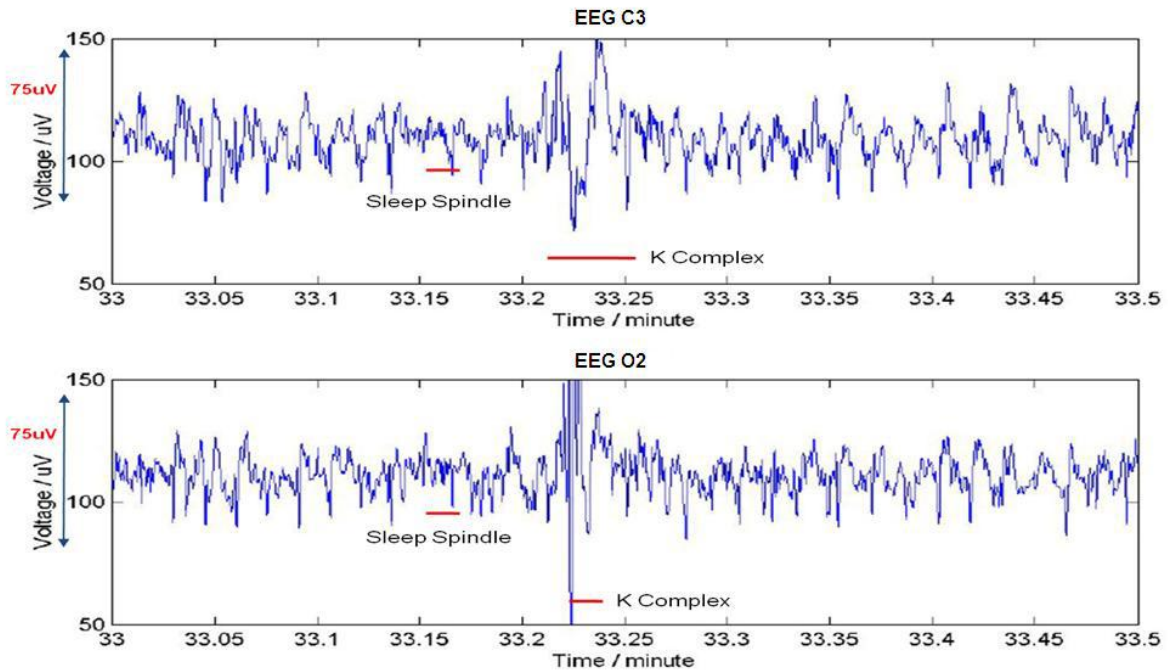


Figure B.2: This epoch illustrates the Stage 2. Vertex sharp waves, which are not a high amplitude activity of Stage 3, may be very abundant. There is a burst of activity in the 12-14 cps range (Sleep Spindle). Delta waves are shown in the entire epoch. The emergence of high amplitude, slow wave activity is usually accompanied by an overall increase in back ground amplitude.

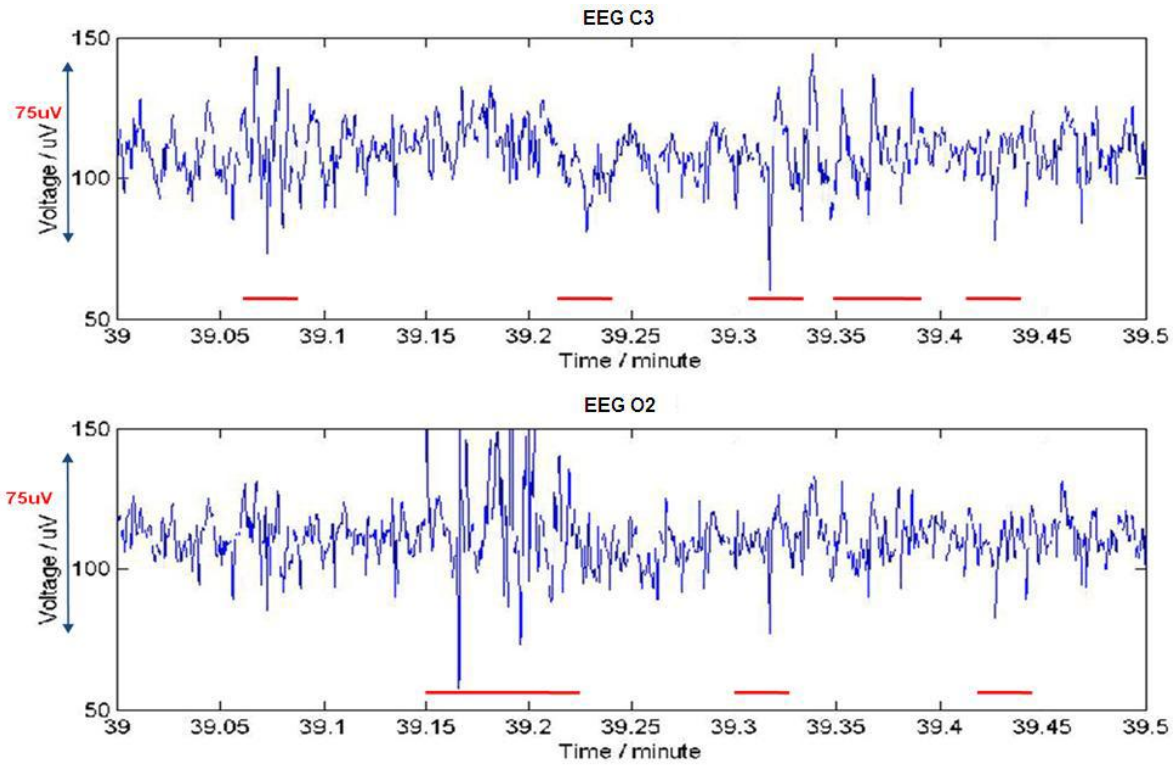


Figure B.3: This epoch illustrates the Stage 3. Acceptable high amplitude, slow wave activity occupies between 20% and 50%.

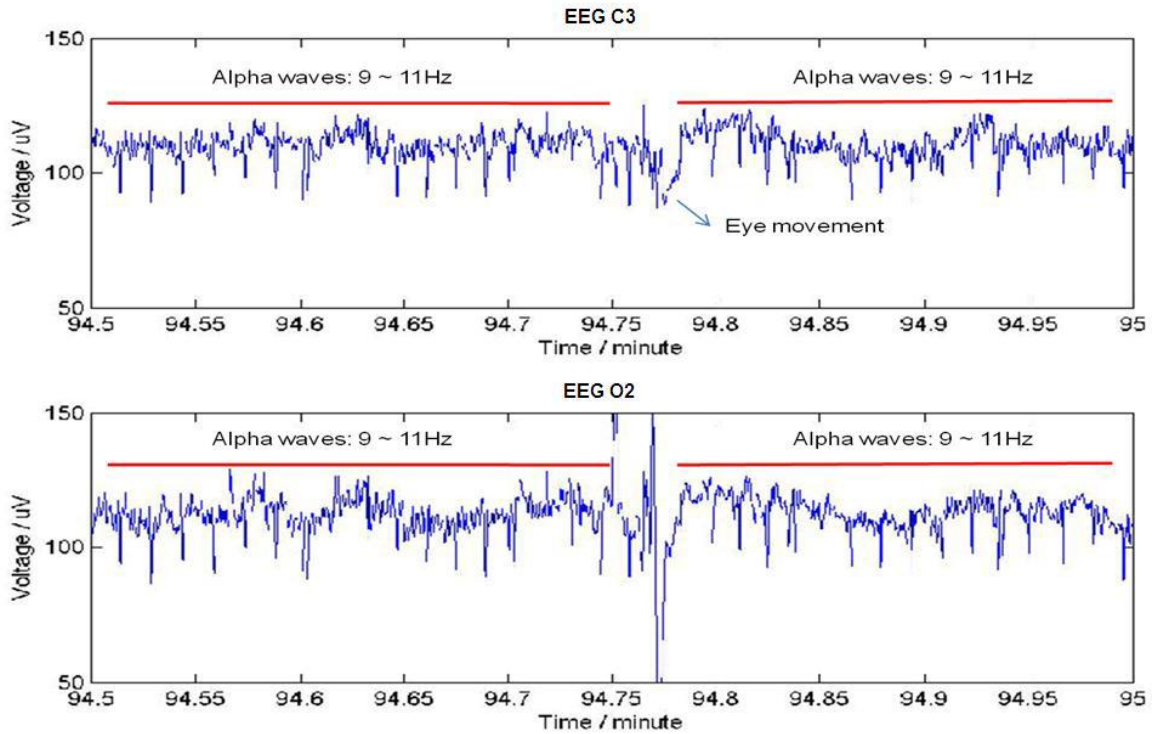


Figure B-4: The record is clearly Stage W in that more than half the epoch is occupied by alpha activities. In the middle of the epoch, there is a high and wide range of signal which comes from eye movement

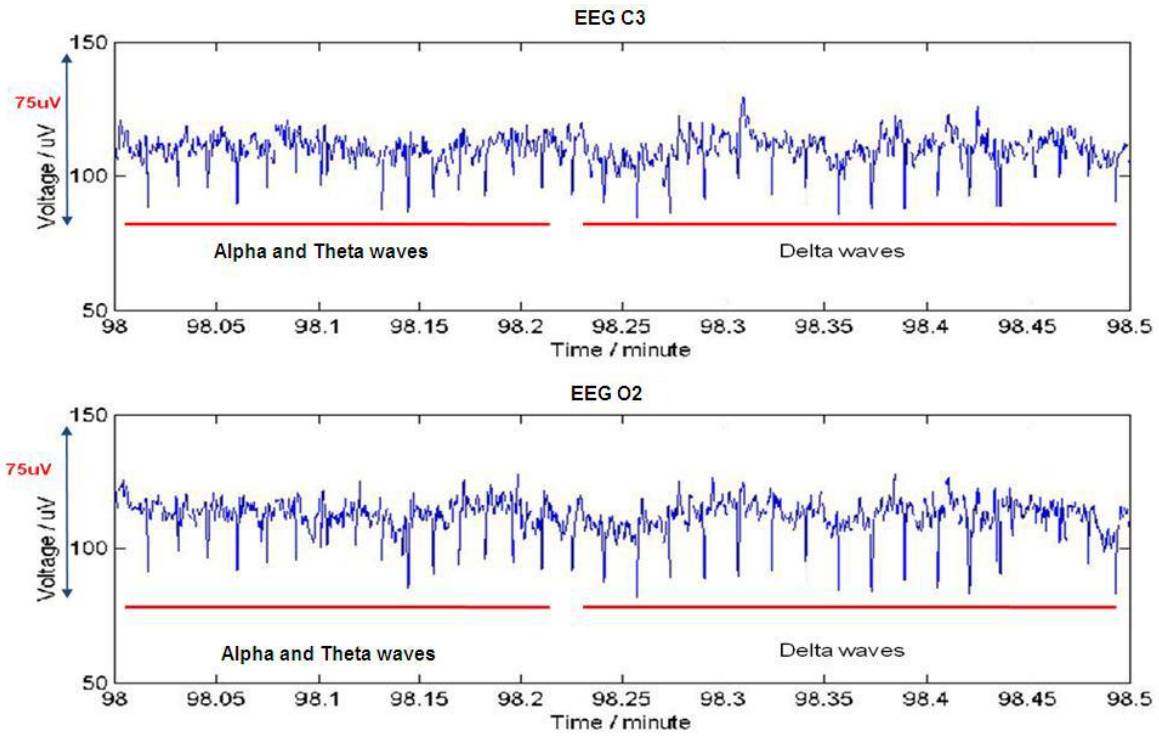


Figure B.5: This epoch illustrates the transition from Stage 1 to Stage 2. In the beginning of the epoch, theta and alpha waves are dominant. Theta waves (4-7 Hz) indicate dozing off. From middle of the epoch, delta waves are appeared less than 2 Hz are shown. It indicates the object sleeps into Stage 2.

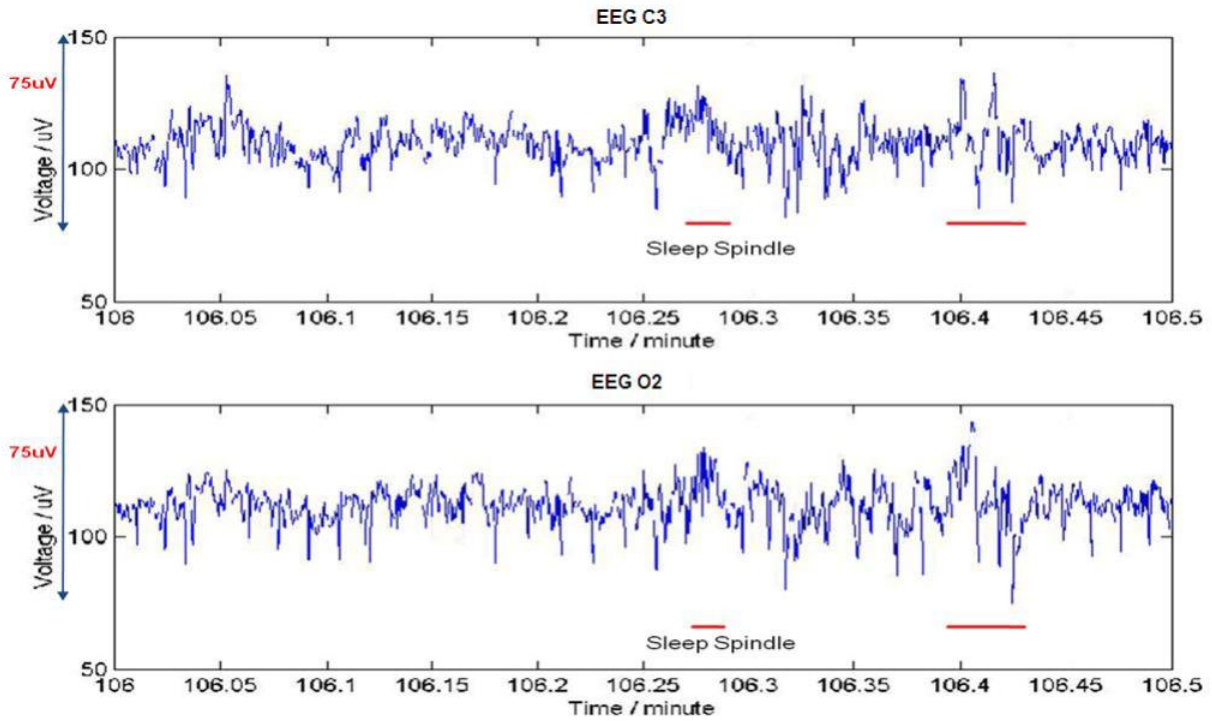


Figure B.6: This epoch illustrates the Stage 2. In the beginning of the epoch, slow waves are shown. There is a burst of activity in the 12-14 cps range (Sleep Spindle). High amplitude waves are also shown. Its occupation is less than 20 %.

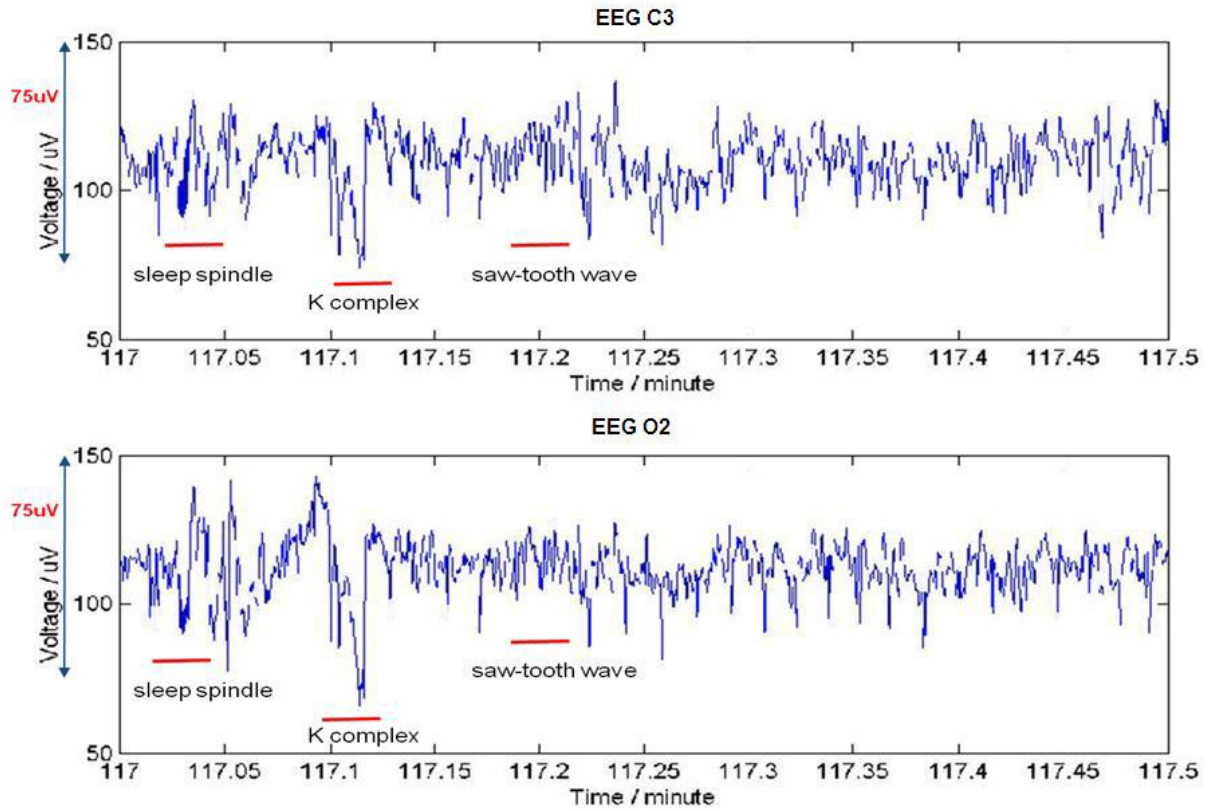


Figure B.7: This epoch illustrates a transition between Stage 2 and Stage REM. In the beginning of the epoch, there is sleep spindle followed by a K complex. Following the K complex are saw-tooth waves which herald the appearance of REM. The last half of epoch shows relatively low voltage, mixed frequency.

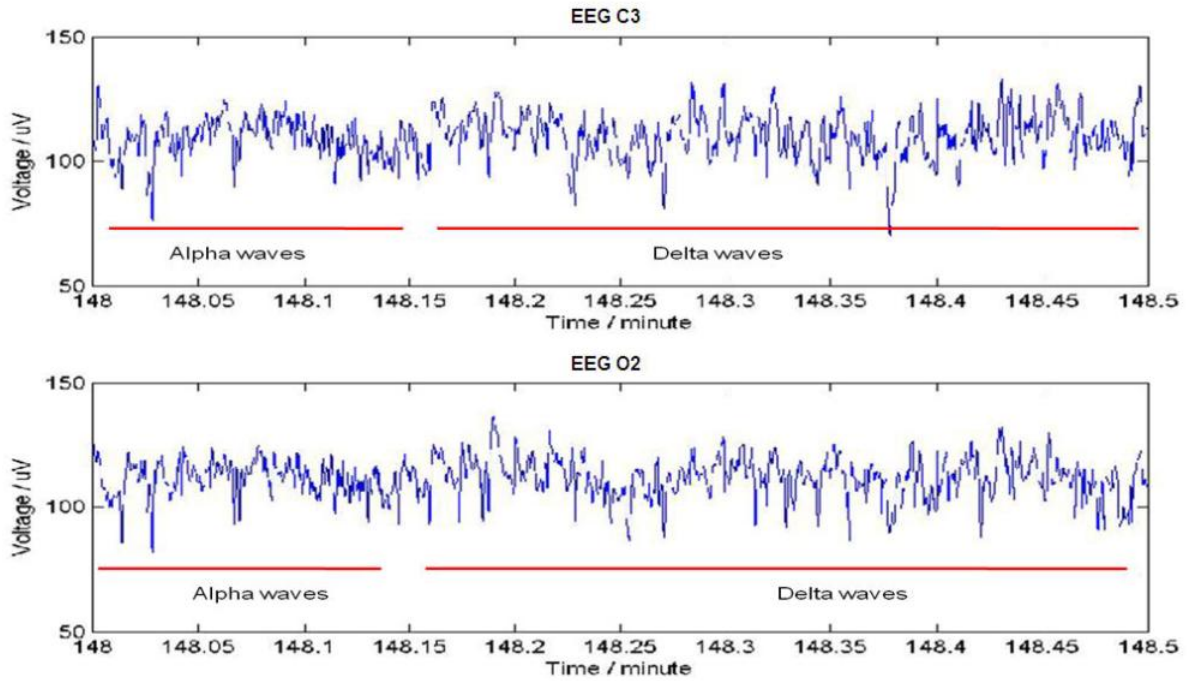


Figure B.8: The beginning of a third of epoch shows the alpha waves, and the rest two third of the epoch show the delta waves. The epoch shows the transition from Stage 1 to Stage 2

Appendix C: Program used to determine the attention level from alpha and beta waves

```
clear all;
close all;
clc;

gain = 18400;fs = 100;ts = 1/fs;resolution = 1024;max_v = 4.8;mV = 1000;uV
=1000000;

attn = load('attn_1.txt');

attn = attn*resolution/max_v/1000;
attn = attn*max_v/resolution/gain;
attn = attn*uV;

raw_time_attn = 0:ts:((length(attn)-1)/fs);
peak_freq_attn = zeros(10,10);peak_powerspec_attn = zeros(10,10);
min_freq_attn = zeros(10,10); min_powerspec_attn = zeros(10,10);

[c,d] = butter(10,[1 49]/50);
raw_attn_filt = filter(c,d,attn);

attn_pos_thres = 20; attn_neg_thres = -19;
EOG_window = 10;

j = 1;
for i= EOG_window+1:length(raw_attn_filt)-EOG_window
    if raw_attn_filt(i) >= attn_pos_thres | raw_attn_filt(i) <=
attn_neg_thres
        EOG_index(j) = i;
        j = j+1;
    end
end

for i= 1:length(EOG_index)
    raw_attn_filt(EOG_index(i)-10:EOG_index(i)+10) = 0;
end

j = 1;
for i = 1:length(raw_attn_filt)
    if raw_attn_filt(i)> 0 | raw_attn_filt(i) < 0
        attn_filt(j) = raw_attn_filt(i);
        j = j+1;
    end
end

time_attn = 0:ts:((length(attn_filt)-1)/fs);

[powerspec_attn, freq_attn] = ar_psd_burg(attn_filt,20,4096,100);
fft_attn = abs(fft(attn_filt,4096));
```

```

i = 1; j = 1; n = 1; t = 1; window_sec = 1;
window = window_sec*fs;

i = 1:window:length(raw_attn_filt);
if length(raw_attn_filt) < (i(end)+window-1)
    section = i(end)-1;
else
    section = i(end)+window-1;
end

for i = 1:window:section
    windowed_attn_filt = raw_attn_filt(i:i+window-1);
    for j = 1:length(windowed_attn_filt)
        if windowed_attn_filt(j) > 0
            attn_filt(n) = windowed_attn_filt(j);
            n = n+1;
        end
    end
end

[powerspec_attn, freq_attn] = ar_psd_burg(attn_filt,20,4096,100);
fft_attn_power = abs(fft(attn_filt,4096)).*abs(fft(attn_filt,4096));
fft_attn = abs(fft(attn_filt,4096));

%%%%%%%%%%%% Calculate peak value of PSD %%%%%%%%%%
kkk = 1;nnn = 1;
for ttt = 2:(length(powerspec_attn)-1)
    if powerspec_attn(ttt)-powerspec_attn(ttt-1)>0 & powerspec_attn(ttt)-
powerspec_attn(ttt+1)>0
        temp_peak_freq_attn(kkk) = freq_attn(ttt);
        temp_peak_powerspec_attn(kkk) = powerspec_attn(ttt);
        kkk = kkk+1;
    end
end

peak_freq_attn(t, 1:length(temp_peak_freq_attn)) = temp_peak_freq_attn;
peak_powerspec_attn(t,1:length(temp_peak_powerspec_attn)) =
temp_peak_powerspec_attn;

%%%%%%%%%%%%%%%%%%%%%%%%%%%%%%%%%%%%%%%%%%%%%%%%%%%%%%%%%%%%%%%%%%%%%%%%

figure(i);
plot(freq_attn, powerspec_attn, 'r'); xlabel('freq [Hz]');ylabel('PSD
[W/Hz]');
ylim([0 500]);
hold on;

freq_theta = freq_attn(164:328);
freq_alpha = freq_attn(328:491);

```

```

freq_low_beta = freq_attn(491:615);
freq_mid_beta = freq_attn(615:817);
freq_high_beta = freq_attn(817:1228);
freq_gamma = freq_attn(1228:end);

plot(freq_theta,80*ones(1,length(freq_theta)),'g','LineWidth',2);
plot(freq_alpha,75*ones(1,length(freq_alpha)),'c','LineWidth',2);
plot(freq_low_beta,70*ones(1,length(freq_low_beta)),'b','LineWidth',2);
plot(freq_mid_beta,65*ones(1,length(freq_mid_beta)),'r','LineWidth',2);
plot(freq_high_beta,60*ones(1,length(freq_high_beta)),'k','LineWidth',2);
plot(freq_gamma, 55*ones(1,length(freq_gamma)),'m','Linewidth',2);

plot(peak_freq_attn(t,:), peak_powerspec_attn(t,:), '*r');

title('Autoregressive Power Spectrum Density','fontsize', 13)
hold off;

ii = 1; kk = 1; jj = 1; ll = 1; mm = 1; nn = 1;pp = 1;
%% Calculating Sum of PSD according to frequency band
attn_alpha_sum = 0;attn_low_beta_sum = 0; attn_mid_beta_sum = 0;
attn_high_beta_sum = 0;attn_theta_sum = 0;attn_gamma_sum=0;
for ii = 1:length(freq_attn)
    if freq_attn(ii) >= 8 & freq_attn(ii) < 12
        attn_alpha_sum = attn_alpha_sum+powerspec_attn(ii);
        attn_alpha_index(kk) = ii;
        kk = kk+1;
    end
    if freq_attn(ii) >= 12 & freq_attn(ii) < 15
        attn_low_beta_sum = attn_low_beta_sum+powerspec_attn(ii);
        attn_low_beta_index(jj) = ii;
        jj = jj+1;
    end
    if freq_attn(ii) >= 15 & freq_attn(ii) < 20
        attn_mid_beta_sum = attn_mid_beta_sum+powerspec_attn(ii);
        attn_mid_beta_index(ll) = ii;
        ll = ll+1;
    end
    if freq_attn(ii) >= 20 & freq_attn(ii) <= 30
        attn_high_beta_sum = attn_high_beta_sum+powerspec_attn(ii);
        attn_high_beta_index(mm) = ii;
        mm = mm+1;
    end
    if freq_attn(ii) >= 4 & freq_attn(ii) < 8
        attn_theta_sum = attn_theta_sum+powerspec_attn(ii);
        attn_theta_index(nn) = ii;
        nn = nn+1;
    end
    if freq_attn(ii) >= 30 & freq_attn(ii) <=50
        attn_gamma_sum = attn_gamma_sum+powerspec_attn(ii);
        attn_gamma_index(pp) = ii;
        pp = pp+1;
    end
end

```

```

end
theta(t) = attn_theta_sum;
alpha(t) = attn_alpha_sum;
low_beta(t) = attn_low_beta_sum;
mid_beta(t) = attn_mid_beta_sum;
high_beta(t) = attn_high_beta_sum;
beta(t) = attn_low_beta_sum+attn_mid_beta_sum+attn_high_beta_sum;
gamma(t) = attn_gamma_sum;

theta(t) = attn_theta_sum;
alpha(t) = attn_alpha_sum;
low_beta(t) = attn_low_beta_sum;
mid_beta(t) = attn_mid_beta_sum;
high_beta(t) = attn_high_beta_sum;
beta(t) = attn_low_beta_sum+attn_mid_beta_sum+attn_high_beta_sum;
gamma(t) = attn_gamma_sum;

%% attn ratio calculation
beta_attn_ratio_1(t) = beta(t)/(theta(t)+alpha(t)+beta(t)+gamma(t));
beta_attn_ratio_2(t) = beta(t)/(theta(t)+alpha(t)+beta(t));
beta_attn_ratio_3(t) = beta(t)/(theta(t)+alpha(t));
beta_attn_ratio_4(t) = beta(t)/alpha(t);

gamma_attn_ratio_1(t) = gamma(t)/(theta(t)+alpha(t)+beta(t)+gamma(t));
gamma_attn_ratio_2(t) = gamma(t)/(theta(t)+alpha(t)+beta(t));
gamma_attn_ratio_3(t) = gamma(t)/(theta(t)+alpha(t));
gamma_attn_ratio_4(t) = gamma(t)/alpha(t);

total_attn_ratio_1(t) = (gamma(t)+beta(t))/(theta(t)+alpha(t));
total_attn_ratio_2(t) =
(gamma(t)+beta(t))/(theta(t)+alpha(t)+beta(t)+gamma(t));
total_attn_ratio_3(t) = (gamma(t)+beta(t))/alpha(t);
%% meditatioin ratio calculation
alpha_medi_ratio_1(t) = alpha(t)/(theta(t)+alpha(t)+beta(t)+gamma(t));
alpha_medi_ratio_2(t) = alpha(t)/(alpha(t)+beta(t)+gamma(t));
alpha_medi_ratio_3(t) = alpha(t)/(beta(t)+gamma(t));
alpha_medi_ratio_4(t) = alpha(t)/beta(t);

theta_medi_ratio_1(t) = theta(t)/(theta(t)+alpha(t)+beta(t)+gamma(t));
theta_medi_ratio_2(t) = theta(t)/(alpha(t)+beta(t)+gamma(t));
theta_medi_ratio_3(t) = theta(t)/(beta(t)+gamma(t));
theta_medi_ratio_4(t) = theta(t)/beta(t);

total_medi_ratio_1(t) = (alpha(t)+theta(t))/(beta(t)+gamma(t));
total_medi_ratio_2(t) =
(alpha(t)+theta(t))/(theta(t)+alpha(t)+beta(t)+gamma(t));
total_medi_ratio_3(t) = (alpha(t)+theta(t))/beta(t);

low_beta_ratio(t) = low_beta(t)/alpha(t);
mid_beta_ratio(t) = mid_beta(t)/alpha(t);
high_beta_ratio(t) = high_beta(t)/alpha(t);
%%

```

```

    t=t+1;

end

A_peak_freq_attn = peak_freq_attn';
A_peak_powerspec_attn = peak_powerspec_attn';

[row col] = size(A_peak_freq_attn);

for n = 1:row
    for m = 1:col
        AB_peak_freq_psd(n,2*m-1) = A_peak_freq_attn(n,m);
        AB_peak_freq_psd(n,2*m) = A_peak_powerspec_attn(n,m);
    end
end

% Autoregressive Power Spectrum Density Estimation Function
% Function accepts as inputs
% "signal_in" is the time domain signal to be analyzed
% "order" is the order of the AR model to be determined
% "nz" is the zero padding length required to make the signal length a power
% of 2
% "fs" is the sampling frequency
% Function returns as outputs
% "psd_ar" Power spectrum density values and "f_n" the corresponding
% frequency vector.

function [psd_ar,f_n] = ar_psd_burg(signal_in,order,nz,fs)
fsh = fs/2;
nzh = nz/2;
f_n = ([1:nzh]/nzh)*fsh;
f_n = f_n';
az = 0*[1:nz];
[c,e] = arburg(signal_in,order); % arburg computes AR parameters
az(1:(order+1)) = c;
fft_az = abs(fft(az));
den = fft_az.*fft_az;
psd = e./den;
psd_ar = (psd(1:nz/2))';

```